

THESIS  
Ep735s  
1996  
c.2

A SPATIAL VARIABILITY AND CHRONOSEQUENCE STUDY OF  
SOILS DEVELOPING ON BASALT FLOWS IN  
THE POTRILLO VOLCANIC FIELD,  
SOUTHERN NEW MEXICO

Martha Cary Eppes

Department of Earth and Environmental Sciences  
New Mexico Tech  
Socorro, New Mexico

Submitted in partial fulfillment of the requirements for the degree of  
Master of Science in Geology

**NMIMT**  
Library  
SOCORRO, NM

October 1996

AP 17 '97  
36754837

UNIVERSITY  
LIBRARY  
SOCORRO, NM

## ABSTRACT

Investigations of soils on well dated basalt flows in the Potrillo volcanic field, southern New Mexico demonstrate that spatial variability is minimal in soils on topographic high points and that these soils yield an accurate chronofunction of carbonate accumulation. Soils were described on four basalt flow surfaces which had been dated at ~19 ka, ~94 ka, ~184 ka, and ~260 ka using  $^{40}\text{Ar}/^{39}\text{Ar}$  and  $^3\text{He}$  surface dating methods.

Topographic relief on basalt flow surfaces in the Potrillo volcanic field is reduced through time as depressions are filled with basalt rubble and eolian dust. Soil development on surfaces varies between soils formed over original topographic high areas on flows (O.T.H. soils) and original topographic low areas (O.T.L. soils). Spatial variability of O.T.H. soils is minimal, and these soils are considered preferable for chronosequence studies. Spatial variability of O.T.L. soils is a function of the rate of infilling of depressions by virtue of the size and shape of depressions in which soils have developed. Chloride concentrations provide evidence that water flux was initially high in all depressions. Over time, however, depressions have filled with eolian material, decreasing the water flux in developing soils. Also, small depressions fill more quickly and become stable sooner than large broad depressions. Consequently, on a single isochronous basalt surface, there are a number of geomorphic surfaces of

varying age with varying amounts of soil development. The high rates of water flux through these depressions suggests that they may play an important role in aquifer recharge in this area of New Mexico.

The chronosequence study reveals a strong exponential relationship between carbonate content and surface age in O.T.H. soils. Higher rates of carbonate accumulation in older soils are apparently caused by plugging of underlying basalts with silt and carbonates. Buried soils in the O.T.L. profiles provide evidence that changes in climate or regional dust have occurred flux since ~90 ka. Despite potential changes in climate and dust composition and flux, the profile mass of  $\text{CaCO}_3$  appears to be a relatively accurate measure of the age of O.T.H. soils on basalt surfaces in the Potrillo volcanic field.

## ACKNOWLEDGMENTS

I would like to acknowledge the XRF laboratory of New Mexico Tech, the New Mexico Geochronological Research Laboratory, and Los Alamos Laboratories for their contributions to this project. I would like to thank my committee members, Bill McIntosh and Peter Mozley, as well as Les McFadden, Jane Poths, and Libby Anthony for their valuable support and input for this project. I would also like to acknowledge a few young men who may not necessarily have provided the most sound scientific advice, but who contributed to this work in the Potrillos in many liters of blood and sweat: Dennis McMahon, Matthew Smith, and especially, Doug Zink, who did more than his share and then some. Thanks guys. Finally, I would like to acknowledge my advisor, Bruce Harrison. His ideas, encouragement, and friendship were an invaluable part of this thesis and my career as a graduate student at New Mexico Tech. I wish him great success in the future.

## TABLE OF CONTENTS

ACKNOWLEDGMENTS .....	ii
TABLE OF CONTENTS .....	iii
LIST OF FIGURES .....	iv
LIST OF TABLES .....	vi
LIST OF APPENDICES .....	viii
INTRODUCTION .....	ix
PART 1: Spatial Variability of Soils Developing on Basalt Flows in the	
Potrillo Volcanic Field, Southern New Mexico: Prelude to a Chronosequence	
Study .....	1
Abstract .....	2
Introduction .....	4
The Potrillo Volcanic Field .....	7
Geologic Setting .....	7
Ages of Basalts .....	10
Geomorphology of Basalt Flows .....	11
Field and Laboratory Methods .....	13
Calculation of Profile Mass of Carbonate .....	14
Total Element Analysis: E-I Coefficients .....	15
Results and Discussion .....	22
Variability Between O.T.L. and O.T.H. Soils .....	22
Morphology Differences Between O.T.L. and O.T.H. Soils .....	22
Soil Chemistry Differences Between O.T.L. and O.T.H. Soils .....	24
Soils Developing on Topographic Highs: A Preference for Soil Chronosequence	
Study .....	27
Variability of O.T.L. Soils: A Function of the Size and Shape of Depressions in	
which Soils are Developing .....	28
Leaching Characteristics of O.T.L. Soils .....	28
Effects of Infilling Depressions with Different Sizes and Shapes on Water Flux in	
Soil Profiles: Depositionally Induced Aridity .....	32
Effects of Infilling Depressions with Different Sizes and Shapes on Water Flux in	
Soil Profiles: Depositionally Induced Stability .....	37
Implications for Aquifer Recharge .....	41
Conclusions .....	45

PART 2: Examination of a Soil Chronosequence in Light of a Prior Spatial Variability Study: Soils Developing on Well Dated Basalt Flows in the Potrillo Volcanic Field, Southern New Mexico.....	47
Abstract.....	48
Introduction.....	49
The Potrillo Volcanic Field.....	50
Geologic Setting.....	50
Spatial Variability of Soils .....	54
Field and Laboratory Methods.....	56
Calculation of Profile Mass of Carbonate .....	57
Results and Discussion.....	61
Rates of Carbonate Accumulation in the Potrillo Volcanic Field .....	61
Intrinsic Thresholds.....	61
A Changing Dust Flux or Composition .....	65
Textural Differences Between Surfaces .....	66
Carbonate Accumulation Rates: Correlations with other Chronosequence Studies.....	67
Predicting Basalt Ages in the Potrillo Volcanic Field Using Carbonate Chronofunctions .....	69
Conclusions.....	71
REFERENCES.....	72
APPENDICES .....	75

# LIST OF FIGURES

## Part 1

Figure 1: Location of study area, basalt flows, and sample sites in the Potrillo volcanic field.....	8
Figure 2: Photograph of AD basalt flow (~20 ka) in the Potrillo volcanic field...	12
Figure 3: Photographs of O.T.H. and O.T.L. soils in the Potrillo volcanic field....	12
Figure 4: Graph of profile sum of $\text{CaCO}_3$ for both O.T.H. and O.T.L. soils developing on basalt flows of varying ages in the Potrillo volcanic field. Boxes represent analytical error for single points and $1\sigma$ error for multiple points.....	25
Figure 5: Graph of profile sum of conductivity for both O.T.H. and O.T.L. soils developing on basalt flows of varying ages in the Potrillo volcanic field. Boxes represent analytical error for single points and $1\sigma$ error for multiple points.....	26
Figure 6: Graph of profile normalized soil-water chloride concentrations vs. surface age for O.T.L. soils. Boxes represent analytical error for single points and $1\sigma$ error for multiple points.....	30
Figure 7: Overall profile E-I coefficients for AD5, AF2, and LBM4.....	31
Figure 8: Graph of depression surface area vs normalized profile soil-water chloride concentrations.....	33
Figure 9: Soil water chloride depth profiles for the AF1 and AF2 soils.....	34
Figure 10: Effects of catchment area and thickness of eolian mantle on water flux through O.T.L. soils.....	36
Figure 11: Differences in the depth of eolian mantle accumulated in depressions with different surface areas and shapes. Rate of dust accumulation is assumed constant at $0.05 \text{ m}^3$ over a period of 50,000 years. Catchment area for all depressions is equal.....	39
Figure 12: Three geomorphic surfaces on an isochronous basalt flow. The timing of the stability of the surface is a function of the size and shape of the depression in which eolian material is accumulating. Topographic highs become stable essentially at the time of basalt deposition.....	40
Figure 13: A graph of the maximum amount of precipitation affecting the bottom of depressions with similar surface areas but different shapes. Graph assumes 100% runoff with a constant dust accumulation rate of $0.05 \text{ m}^3/\text{yr}$ . As the area of the bottom of the depression approaches the surface area of the depression itself, effective precipitation approaches the average precipitation of the region.....	42

## Part 2

- Figure 1: Location of study area, basalt flows, and sample sites in the Potrillo volcanic field.....51
- Figure 2: Chronofunctions of the log of carbonate content (profile mass and normalized profile weight percent of  $\text{CaCO}_3$ ). Boxes represent analytical error for single points and  $1\sigma$  error for multiple points.....62
- Figure 3: Graphs of profile mass of  $\text{CaCO}_3$  and normalized profile weight percent of  $\text{CaCO}_3$  in the  $<2$  mm portion of sample vs surface age for soils developing on basalt flows of different ages in the Potrillo volcanic field. Boxes represent analytical error for single points and  $1\sigma$  error for multiple points.....63



## LIST OF TABLES

### Part 1

Table 1: $^{40}\text{Ar}/^{39}\text{Ar}$ and $^3\text{He}$ dates obtained for the AD, AF, LBM, and LBMX flows in the Potrillo volcanic field.....	10
Table 2: Soil Field Descriptions.....	18
Table 3: Soil Analyses.....	20

### Part 2

Table 1: Summary of $^{40}\text{Ar}/^{39}\text{Ar}$ and $^3\text{He}$ age data for the AD, AF, LBM, and LBMX surfaces in the Potrillo volcanic field.....	52
Table 2: Soil Field Descriptions.....	59

## LIST OF APPENDICES

APPENDIX A: $^{40}\text{Ar}/^{39}\text{Ar}$ Age Spectra for 6 Samples from the LBM and LBMX flows.....	76
APPENDIX B: Analytical Methods and Data for 6 Samples from the LBM and LBMX flows.....	83
APPENDIX C: Vegetation.....	87
APPENDIX D: Profile Normalized Values of pH, Clay, Silt, and Sand.....	89
APPENDIX E: Total Element Analysis: Major Element Sample Weight Percent	94
APPENDIX F: Total Element Analysis: E-I Coefficients.....	95

## INTRODUCTION

Soil chronosequences have been widely studied, and are often used for correlating and dating geomorphic surfaces. However, many of these soil chronosequence studies lack good age control and an understanding of spatial variability within the chronosequence. The purpose of this thesis was to develop a chronosequence study in which both of these problems were adequately addressed before soil-time trends were examined. Given that accurate ages had previously been obtained using  $^{40}\text{Ar}/^{39}\text{Ar}$  and  $^3\text{He}$  surface dating methods for a number of Quaternary basalts in the area, the Potrillo volcanic field in southern New Mexico was chosen for this chronosequence study. Nineteen soils were described, and laboratory analyses, including bulk density, pH, conductivity, particle size analysis, weight percent  $\text{CaCO}_3$  in the  $<2$  mm portion, and soil water chloride, were performed. Parts 1 and 2 of the thesis are meant to stand alone as publishable manuscripts for professional journals. Part 1 discusses spatial variability of soils developing on basalt surfaces in the Potrillo volcanic field. Part 2 discusses trends of soil properties with time in the Potrillos. Appendices include data, figures, and discussions that were not incorporated elsewhere in the thesis.

*Part 1*

SPATIAL VARIABILITY OF SOILS DEVELOPING ON BASALT  
FLOWS IN THE POTRILLO VOLCANIC FIELD,  
SOUTHERN NEW MEXICO:  
PRELUDE TO A CHRONOSEQUENCE STUDY.

Martha Cary Eppes

Department of Earth and Environmental Science  
New Mexico Tech

1996

## ABSTRACT

Spatial variability of soils developing on well dated basalt flows in the Potrillo volcanic field, southern New Mexico was examined in order to determine which soils are least variable and therefore preferable for use for a later soil chronosequence study. Surfaces were dated using  $^{40}\text{Ar}/^{39}\text{Ar}$  and cosmogenic  $^3\text{He}$  methods, and their ages range from ~20 ka to ~260 ka. Basalt flow surface relief in the Potrillos is reduced with time as depressions are filled with basalt rubble and eolian dust. Soil development on the surfaces varies according to whether the soil is forming over a high or low point in the original flow topography. Soils developing over original topographic lows (O.T.L. soils) are developing primarily in eolian dust, have greater overall amounts of carbonate and soluble salts, and overall greater variability than soils developing on original topographic highs (O.T.H. soils). Given their minimal variability, it is concluded that O.T.H. soils should be employed for a soil chronosequence study of these surfaces.

Chloride concentrations suggest that the greater variability of O.T.L. soils is attributable to variability of water flux through those soils. Depressions fill at different rates depending on their size, shape, and catchment area, and this rate of infilling affects the hydrologic characteristics of that depression. Small, narrow, depressions fill quickly, reducing the

catchment area for runoff and increasing the thickness of eolian material that is being leached. Large depressions fill at a slower rate, and not only have larger catchment areas resulting in greater runoff, but also thinner eolian mantles. Consequently, leaching is greater in these soils.

Furthermore, depressions which fill quickly also become stable sooner than those which continue to be affected by processes of leaching and aggradation. Therefore, on a single isochronous basalt surface, there are a number of geomorphic surfaces of varying age with varying amounts of soil development. The high rates of water flux through these depressions suggests that they may play an important role in aquifer recharge in this area of New Mexico.

## INTRODUCTION

Soils are simple and effective tools for dating and correlating geomorphic surfaces. However, the use of chronofunctions derived from chronosequence studies to accurately describe soil development has been limited due to a number of shortcomings (Switzer et al., 1989, Shaetzl et al., 1994). Contributions to the inaccuracy of chronofunctions include poor dating of geomorphic surfaces, too few soils on each surface, and spatial variability of soils on supposedly isochronous surfaces (Bockheim, 1980, Harrison et al., 1990, Harrison and Yaalon, 1992). With the development of more accurate dating techniques, the accuracy of surface ages is increasing. Though many workers have recognized the spatial variability of soils as a significant cause of inaccuracy in chronofunctions, few studies have actually addressed the nature of spatial variability within the soil landscape. Variability of soils can be divided into random variability and systematic variability, where systematic variability is variability which can be explained by geomorphic processes (Wieland and Drees, 1993). If systematic, as opposed to random variability can be distinguished on soil surfaces, accuracy of chronofunctions can be increased (Harrison et al., 1990). Unfortunately, it is difficult if not impossible, logistically, to sample enough soils on a single surface so that these two types of spatial variability can be statistically differentiated

(Wieland and Drees, 1983, Switzer et al., 1988, Harrison et al., 1990).

However, if spatial variability in a particular locale was understood *before* the soil chronosequence was studied, it would become possible to sample surfaces in such a way that spatial variability is minimized.

Chronofunctions derived from these soils would be more accurate than those derived from a random population. This paper is part one of a two part chronosequence study in which spatial variability of soils is investigated in order to determine which soils would be most useful for the chronosequence study.

It is often a costly, time-consuming, and sometimes impossible task to obtain reliable dates for Quaternary surfaces. Therefore, the primary criterion in choosing a location for this study was to find a set of surfaces for which good age control was already established. The Potrillo Volcanic field in southern New Mexico was chosen for this investigation because the basalt flows in this field are well dated. Recent advances in radioisotope technology have increased the accuracy and precision with which young basalt flows can be dated. Both  $^{40}\text{Ar}/^{39}\text{Ar}$  and cosmogenic  $^3\text{He}$  dating methods have been proven to give accurate dates of these types of surfaces (McDougall, 1988, Cerling, 1990, Anthony and Poeths, 1992).

Furthermore, the Potrillo volcanic field is located in the vicinity of another large soil-geomorphic study, the Desert Project (Gile et al., 1981), with which data may be compared.



Previous geomorphic and soils work on basalt flows in both the Cima and the Pinacate volcanic fields in California (Wells et al., 1985, Slate et al., 1991) showed that the surface topography of basalt flows evolves dramatically with time. Young basalt surfaces are extremely irregular with high relief. The topography of flows is due primarily to the collapse of lava tubes in the basalt which forms abundant depressions ranging in size from meters to hundreds of meters in circumference. Flow surfaces around these depressions can be either fractured or smooth. In the Cima volcanic field, as topographic lows fill with basalt rubble and eolian dust, the ratio of eolian mantle to exposed bedrock increases with increasing age up to approximately 250 ka (Wells et al., 1985). On flows ranging in age from ~250-750 ka accumulation is no longer an active process, and topography of the original basalt flow is no longer evident. On flows older than ~750 ka, processes of erosion become dominant and bedrock surfaces are reexposed. A similar evolution of topography occurs in the Potrillo volcanic field. It is evident that soils developing on topographic lows would develop in much greater amounts of eolian material and would vary dramatically from those soils developing over topographic highs.

As a prelude to a chronosequence study in the Potrillos, it is the purpose of this paper to: 1) further evaluate the evolution of basalt flow topography with time, 2) identify the causes of systematic variability of

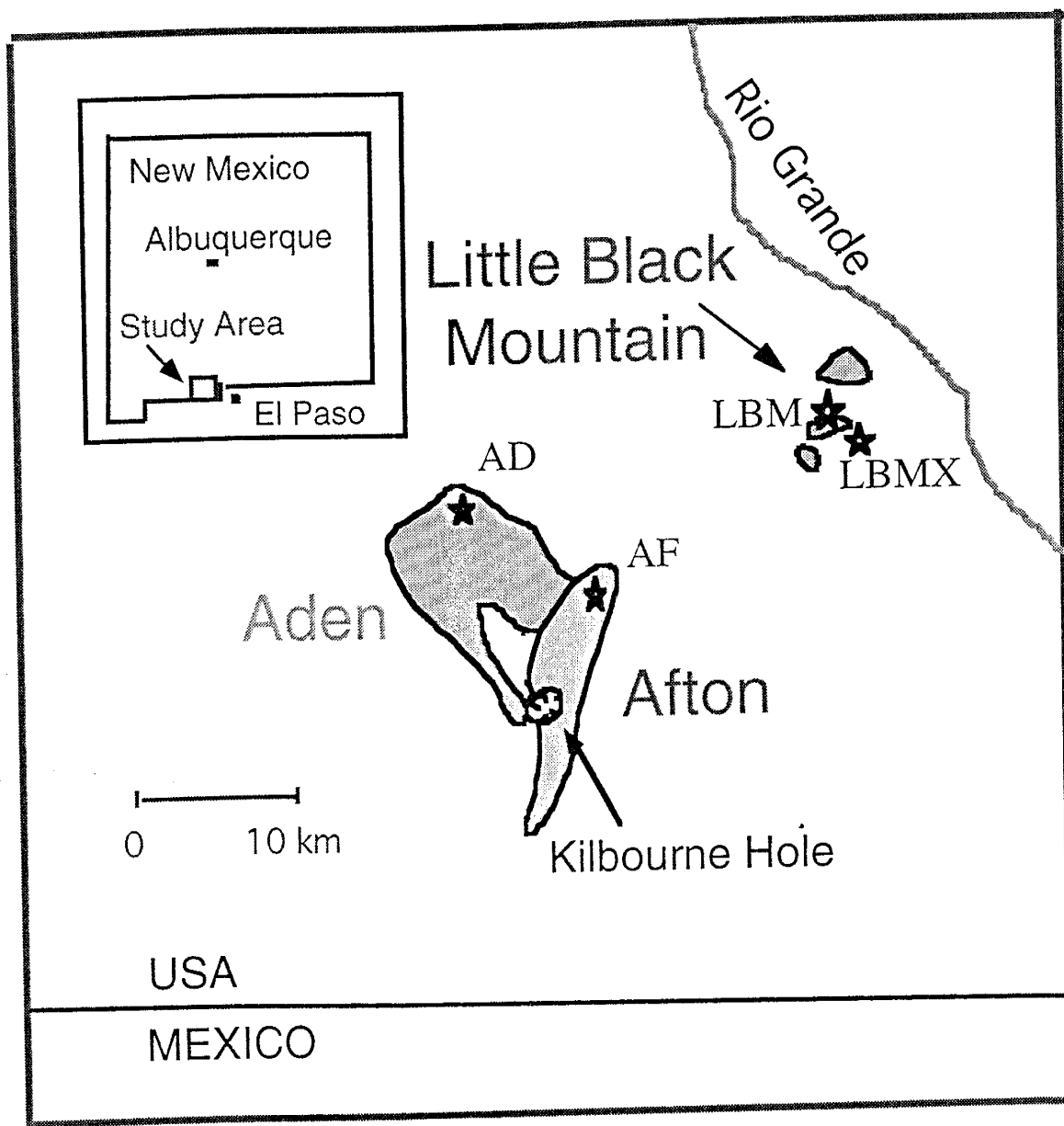
soils developing on basalt flows in the Potrillos, and determine the amount of random variability in the soils, and 3) determine which soils in the Potrillo volcanic field are most suitable for a chronosequence study.

## THE POTRILLO VOLCANIC FIELD

### *Geologic Setting*

The Potrillo volcanic field covers over 1000 square kilometers in southwestern Doña Ana County, New Mexico, in the axis of the Rio Grande rift, about 40 km southwest of Las Cruces (Fig. 1). This region is located in a major intermontane basin, and is considered to be a portion of the Mexico Highland section of the Basin and Range Province (Hoffer, 1976). The floor of the basin, the La Mesa surface, is ~500 ka in age (Gile et al., 1981). The La Mesa surface underlies all of the basalt flows of the Potrillo volcanic field. The numerous cinder cones and lava flows of the field are major topographic features in the area.

The climate of the Potrillo area is arid to semi-arid with ~30 cm/yr. precipitation (US Weather Service, 1996). Winds are strongest in the spring, and dust storms are common. All basalt flows in the Potrillos are vegetated with creosote, mesquite, and various cacti and grasses. Relative abundances of these plants differ depending on the age of the surface and topography. In general younger surfaces have greater diversity than older



★ Location of soil,  $^3\text{He}$ , and  $^{40}\text{Ar}/^{39}\text{Ar}$  sample sites

Figure 1: Location of study area, basalt flows, and sample sites in the Potrillo volcanic field.

surfaces, which are vegetated primarily with desert shrub species. There is a marked difference in vegetation between topographic highs and lows on all flows. In general, this difference is more dramatic on younger flows where topographic lows are vegetated with different species than topographic highs. On older surfaces, deposition of eolian material has masked the original topography, and the former lows appear to be marked not by different species, but rather by healthier plants.

All of the basalt flows in the Potrillo volcanic field are nepheline normative, their chemistry resembling other young alkaline lavas within the Basin and Range Province (Anthony et al., 1992). Individual flows show little geochemical variation relative to the field as a whole. The lavas are vesicular, and pahoehoe structures are visible on many flows. The field can be divided into three areas: the older Western Potrillos, a large strip of overlapping fissure-fed flows and cinder cones; the center of the field, a broad area of two younger flow complexes (Aden and Afton); and the eastern portion of the field, an alignment of cinder cones and associated flows (Little Black Mountain area). Four flows that are easily distinguishable and have been dated were chosen for this study: Aden (AD), Afton (AF), and two flows from Little Black Mountain (LBM, and LBMX; Fig. 1).

### *Ages of Basalts*

$^{40}\text{Ar}/^{39}\text{Ar}$  and  $^3\text{He}$  surface exposure dates have been obtained for basalt flows, maars, and cinder cones in the Potrillo volcanic field (E. Anthony et al., unpublished data, W. McIntosh et al., unpublished data; Table 1).  $^{40}\text{Ar}/^{39}\text{Ar}$  and  $^3\text{He}$  ages agree within  $1\sigma$  for the AD surface and  $2\sigma$  for the AF surface.  $1\sigma$  represents approximately 15% of the age of younger surfaces and ~10% of that of older surfaces. Averages of this age data are used for calculations in this study (Table 1).

Table 1:  $^{40}\text{Ar}/^{39}\text{Ar}$  and  $^3\text{He}$  dates obtained for the AD, AF, LBM, and LBMX flows in the Potrillo volcanic field.

Surface	$^{40}\text{Ar}/^{39}\text{Ar}$ dates (ka)	$^3\text{He}$ dates (ka)	Age of Surface (Avg. ka)
AD	$13 \pm 11^*$	$24 \pm 3.5^\bullet$	$19 \pm 8$
AF	$70 \pm 14^*$	$103 \pm 5^\bullet$ $110 \pm 7^\bullet$ $94 \pm 15^\bullet$	$94 \pm 17$
LBM	$188 \pm 9^*$	-----	$184 \pm 5$
"	$167 \pm 21^*$		
"	$186 \pm 9^*$		
"	$179 \pm 17^*$		
LBMX	$263 \pm 19^*$	-----	$263 \pm 19$

\* W. McIntosh et al., unpublished data

• E. Anthony et al., unpublished data

### *Geomorphology of Basalt Flows*

A transformation of basalt flow surface morphology similar to that observed by Wells et al. (1985) on younger surfaces in the Cima is evident in the Potrillo volcanic field. Flows evaluated for this study, however, are younger than ~300 ka and are all in the accretionary stage of the cycle described by Wells et al. (1985). Depressions on flows vary in size and number with increasing age. Topographic lows on the AD surface range in size but are often deep and interconnected (Fig. 2). Small topographic lows on the AF surface have been completely filled, although very large ( $>500 \text{ m}^2$ ), relatively shallow depressions are found locally. The LBM and LBMX surfaces are almost entirely covered by eolian deposits, so the size and locations of depressions in original basalt topography on these flows can only be estimated using changes in vegetation and desert pavements. Former depressions are marked by healthier vegetation and lack of desert pavement.



Figure 2: Photograph of the AD basalt flow (~20 ka) in the Potrillo volcanic field.

## FIELD AND LABORATORY METHODS

Soils were sampled over both original topographic highs (O.T.H. soils) and lows (O.T.L. soils) in flow topography. O.T.H. soils were sampled on all four surfaces, however O.T.L. trenches were not dug on the LBMX surface. Each pit was assigned a unique number (AD1, AD2; AF1, AF2 etc.). As catchment area size and shape could influence runoff and consequently soil development for individual depressions, the surface areas of the catchments in which the O.T.L. pits were dug were estimated as well as surficial relief and total depth of the depression (as measured from the bottom of the soil pit). The volume of dust filling the depressions was also estimated from surface area and depth to bedrock measurements. O.T.H. pits were shallow and were dug by hand or with a jackhammer. O.T.L. pits were dug with a backhoe with the exception of AF3 for which we were unable to use the backhoe. All pits were dug to depths of 10-40 cm into a coarse rubble zone that was assumed to be the top of the flow. This rubble zone was not reached in AF3, although basalt clasts were present in the bottom 20 cm of the pit. Rates of soil development may vary as a function of distance from the perimeters of the flow (Slate et al., 1991). Pits were therefore located within 0.5 km of flow perimeters for this study. All pits were described using methods summarized by the Soil Survey staff (1951,



1975) and sampled for laboratory analyses. Average carbonate rind thickness and volume percent of gravels was estimated for each horizon in all profiles. Soil analyses for all profiles included: bulk density, pH, soluble salts (by electrical conductivity), particle size, and  $\text{CaCO}_3$  of the <2mm portion. Standard procedures were used for all analyses (Singer and Janitzky, 1986).

Soil-water chloride concentrations were measured for O.T.L. soils, again with the exception of AF3. Chloride is hydrologically mobile and chemically inert making it a useful tracer for water movement through soils (Phillips, 1994, Liu et al., 1995). Gravimetric water contents were also determined for these samples in order to calculate soil-water chloride concentrations.

#### *Calculation of Profile Mass of Carbonate*

The profile mass of carbonate of a soil is usually calculated using the fine earth portion of a sample (e.g., Gile et al., 1981, Machette, 1985, Slate et al., 1991). However, in coarse deposits a significant amount of carbonate is found in clast coatings, and estimates of this volume of  $\text{CaCO}_3$  are required to quantitatively determine the profile mass of carbonate in a soil (McDonald, 1994). The following equation was used to calculate the total mass of  $\text{CaCO}_3$  in each sample:

$$\{BDs * \%Cs * (1 - \%G) + (GR - RT) * \%R * BDc\} * HT$$

BDs = Bulk density of the < 2mm portion of sample  
 %Cs = weight percent of  $\text{CaCO}_3$  in the <2mm portion of sample  
 %G = volume percent of gravels in each horizon  
 GR = average total clast volume in each horizon  
 RT = average horizon clast volume excluding the  $\text{CaCO}_3$  rind thickness  
 %R = volume percent of  $\text{CaCO}_3$  rind in each horizon  
 Bdc = average bulk density of  $\text{CaCO}_3$  rinds  
 HT = horizon thickness

The horizon mass of  $\text{CaCO}_3$  in the < 2mm portion of the sample was also calculated using bulk density and horizon thickness. These values were then summed for each profile to obtain profile mass of carbonate for the entire soil. (Similarly a profile sum of conductivity was also calculated for all soils.) To aid in comparing soils of different depths, the thickness of all bottom horizons was normalized to a height of 10 cm in O.T.H. soils, and 20 cm in O.T.L. soils. It should be noted that the loss of  $\text{CaCO}_3$  out through the bottom of these soils was not accounted for by the profile mass of carbonate calculations (see discussion).

#### *Total Element Analysis: E-I coefficients*

Total element analysis (TEA), though typically used for evaluating degree of weathering in soils, can also be used for examining hydrologic characteristics of a soil profile. By comparing the chemistry of horizons with the chemistry of the assumed parent material, relative gains and losses of major elements can be calculated. These gains or losses can then be used

to describe the leaching and accumulation characteristics of the soil profile in question.

Eluvial/Illuvial (E-I) coefficients (Muir and Logan, 1982) are used to calculate relative gains and losses of a chosen element in the soil. They are calculated using the major element composition of a sample, an assumed parent material, and an internal standard (assumed to be immobile and inert). The E-I coefficient is a percentage, where a negative coefficient will indicate a relative loss, and a positive coefficient a relative gain in an element. E-I coefficients thus measure the intensity of the elluviation/illuviation processes within a soil and provide for comparisons of soils with possible differing original chemical composition.

For this study, TEA was performed by the XRF laboratory of New Mexico Tech, Socorro, New Mexico, for AD5, AF2, and LBM4. Relative percentages of the following oxides were measured:  $\text{SiO}_2$ ,  $\text{Cr}_2\text{O}_3$ ,  $\text{BaO}$ ,  $\text{CaO}$ ,  $\text{Al}_2\text{O}_3$ ,  $\text{Na}_2\text{O}$ ,  $\text{Fe}_2\text{O}_3$ ,  $\text{K}_2\text{O}$ ,  $\text{MnO}$ ,  $\text{P}_2\text{O}_5$ , and  $\text{MgO}$ . E-I coefficients were calculated for all of these major elements using the A horizon of each profile as parent material, and Ti as the internal standard:

$$\text{E-I coefficient (\%)} = [((\text{Sh} * \text{Xpm}/\text{Xh})/\text{Spm}) - 1] * 100$$

Sh = concentration of element S in horizon h

Xpm = concentration of internal standard in parent material

Xh = concentration of internal standard in horizon h

Spm = concentration of element S in parent material

In order to more easily compare gains and losses for the entire profiles, E-I coefficients for each horizon were weighted by horizon thickness and bulk density and then summed to obtain a profile E-I coefficient for each element.

Assumptions involved these calculations are that 1) the composition of eolian dust in the Potrillo volcanic field has remained constant, 2) that the A horizons of these profiles are unaltered, and 3) that the internal standard chosen for the E-I calculation is immobile and inert. It is likely that none of these assumptions are *absolutely* valid for the soils in the Potrillos. However, for the purposes of this study E-I coefficients will be used as a tool to make relative observations of leaching and accumulation rather than to describe exact changes in chemistry of soil profiles. Even if dust composition has slightly changed, A horizons have been slightly altered, or if Ti has been somewhat mobile, major trends in leaching or accumulation should still be apparent. Therefore E-I coefficient data should still be useful to describe trends in elluvial/illuvial activity for soils developing in the Potrillo volcanic field.

Table 2: Soil Field Descriptions

Soil	Age (-ka)	Hor.	Depth (cm)	Structure	Texture	Consistence		Color		roots; boundaries	gravel % pores	Carbonates	
						moist	dry	moist	dry				
AD1	19	A	0-4	1 f sbk	L	sa pa	sh	7.5yr 3/3	10yr 5/4	2c 2m 2f; a s	<1; 2f/m	no evident	
		B	4-29	1 m sbk	SC	sa pa	b-vh	7.5yr 3/3	10yr 5/4	1c 1m 1f 1vf; c/l	<1; 1m	no evident	
		Bt	29-60	2 m sbk	C	s p	vh	7.5yr 4/4	8.75yr 5/4	5c 5m 1f; c/g s	<1; 1m	no evident	
		Bt2	60-135	3 m sbk	C	s p	vh-ch	7.5yr 4/4	8.75yr 5/4	1vc 1m 1f; g s	<1 1m 2f	no evident	
		2Bt2	135-160	2 m sbk	C	s p	h	7.5yr 4/4	8.75yr 5/4	1f 1vf; ---	30; 1f	rare coatings on basalt, <1mm	
		Surface Area: 900 m <sup>2</sup>				Total Depth: 1.8 m							
AD2	19	A	0-3	3 m sbk	SIL	sa pa	sh	7.5yr 4/3	8.75yr 5/4	2vf; c s	40; 2vf, 1f	no evident	
		B	3-9	2 f-m sbk	SIL	sa pa	sh	8.75yr 3/3	10yr 5/3	2f; c i	10; 1f	slight fix	
		Bk	9-23	3 f sbk	SL	sa pa	sh	7.5yr 3/2	7.5yr 5/3	0; a s	70; 0	coats fractures	
AD3	19	A	0-4	2 m sbk	SIL	sa pa	sh	8.75yr 3/3	8.75yr 6/3	2vf; c s	60; 2f	no evident	
		B	4-11	1 m sbk	SIL	sa pa	sh	7.5yr 4/4	7.5yr 5/4	1vf, 1m, 1c; c i	20; 1f	slight fix	
		Bk	11-20	2 m sbk	SIL	sa pa	sh	7.5yr 3/4	7.5yr 5/4	2vf; c i	<5; 1f	coats fractures	
		Ck	23-34	1 m sbk	ShCL	s p	sh	7.5yr 3/3.5	7.5yr 5/5	1vf, 1f; 0	<10; 1f	strong fix	
AD4	19	A	0-5	1 m sbk	SIL	sa pa	sh	7.5yr 3/3.5	10yr 5/3	1vf; c s	60; 1f	no evident	
		B	5-15	1 m sbk	SIL	sa pa	sh	7.5yr 3/4	8.75yr 5/4	1f; c i	10; 1f	slight fix	
		Bk	15-28	2 f sbk	SIL	sa pa	sh	7.5yr 3/4	7.5yr 4/4	1f; c i	70; 1f	coats fractures	
		Ck	20-40	3 f sbk	ShCL	s p	sh	7.5yr 4/4	7.5yr 4/4	1f, 1m; 0	90; 1f	strong fix	
AD5	19	A	0-3	1 f sbk	L	sa pa	sh	8.75yr 3/3	10yr 5/4	1c 3m 1f 1vf; a s 0; 1f	no evident		
		Bt	3-20	1 m 1c sbk	L	sa pa	sh	8.75yr 3/3	8.75yr 5/4	1vc 1m 1f 1vf; c 0; 1c 1m	no evident		
		Bt2	20-63	2 m sbk	SC	s p	sh	7.5yr 4/4	8.75yr 5/4	1c 1m 1f 1vf; c s 0; 1c 1m 2f	no evident		
		Bt3	63-110	2 m sbk	C	s p	sh	7.5yr 4/4	8.75yr 5/4	1c 1m 1f 1vf; c s 0; 1c 1m 1f	no evident		
		Bt4	110-137	1c 1m sbk	C	s p	sh	7.5yr 4/4	8.75yr 5/4	1c 1m 1vf; c i	0; 2f	scarce on roots; no fix in matrix	
		2Bt4	137-160	1 m sbk	C	s p	sh	7.5yr 4/4	8.75yr 5/4	1m 1f 1vf; ---	20; 1f	scarce on roots; no fix in matrix; scarce slight coating on basalt	
Surface Area: 640 m <sup>2</sup>				Total Depth: 1.6 m									
AD6	19	A	0-2	1 f sbk	L	sa pa	sh	7.5yr 4/4	10yr 5/4	2c 1m 1f; a s	<1; 1m 1f	no evident	
		Bt	2-21	1 m sbk	CL	s p	sh	7.5yr 4/4	10yr 5/5	1f 1vf; c s	<1; 2f	no evident	
		Bt2	21-50	1m 2f sbk	C	s p	sh	7.5yr 4/4	8.75yr 5/4	2m 1f 1vf; g s	<1; 1f	no evident	
		2Bt3	50-85	1f 2f sbk	C	s p	sh	7.5yr 4/4	8.75yr 5/4	1m 1f 1vf; g s	<1; 1f	scarce coats on basalt, <1mm	
		C	85-130	1f sbk	C	s p	<sh	7.5yr 4/4	8.75yr 5/4	1m 1f 1vf; ---	<1; 1f	scarce coats on basalt, <1mm	
Surface Area: 130m <sup>2</sup>				Total Depth: 364									
AF1	94	Av	0-5		L	sa pa	sh	8.75yr 4/4	10yr 5/4	1vf; a s	<1; 1vf	no evident	
		Bt	5-20		CL	sa pa	sh-b	7.5yr 4/4	8yr 4/4	1m 1vf; c s	<1; 1f	very small specs; no matrix fix	
		Bt2	20-84		SC	s p	h	7.5yr 4/4	8yr 5/4	1m 1f 1vf; c s	<1; 5c 1f	very small specs; no matrix fix	
		Btk	84-102		SC	s p	sh-b	7.5yr 4/4	8yr 5/4	1f 1vf; a i	<1; 2f	filaments along roots; slight fix on ped faces	
		2Btkb	102-117		SC	s p	sh	7.5yr 4/6	8yr 5/4	1m 1vf; c s	40; 1f	filaments along roots; slight fix on ped faces	
		Kb	117-170		SC	s p	b-vh	7.5yr 4/6	8yr 5/4	1c 1vf; c i	55-60; 1f	Stage 2; abundant filaments; complete cover on pf; strong matrix fix	
		Kb2	170-195		SC	s p	sh-b	7.5yr 4/6	8yr 5/4	1vf; ---	35; 5 vf	Stage 1+; fewer visible carbs	
		Surface Area: 12800 m <sup>2</sup>				Total Depth: 2.8 m							
AF2	94	A	0-4	2 m sbk	L	sa pa	sh	5yr 3/2	10 yr 5/4	0; c s	<5; 0	no evident	
		B	4-25	2.5 m sbk	SIL	sa p	vh	6.75yr 3/3	7.5yr 4/4	2vf, 1m; c s	<5; 2f	slight fix in roots	
		B2	25-48	2 m sbk	SL	s p	h	7.5yr 3/4	8.75yr 4/4	1vf, 1m, 1c; c s	<5; 1f	no evident	
		Bk	48-77	2 m sbk	SC	sa p	h	7.5yr 3/4	7.5yr 5/6	1f; c s	<5; 1m	on roots and peds	
		Btkb	77-120	2 f sbk	ShCL	sa p	sh	7.5yr 4/3	7.5yr 5/4	1m; c s	<5; 1f	Stage 1	
		K2	120-170	1 m sbk	ShCL	sa pa	sh	7.5yr 4/3	7.5yr 5/4	1f; c s	<5; 1f	Stage 1	
		Ck	170-240	1 m sbk	CL	sa pa	sh	7.5yr 4/4	7.5yr 6/4	1f; 0	<5; 1f	strong fix	
Surface Area: 2700 m <sup>2</sup>				Total Depth: 3.2									
AF3	94	A	0-4	1 f sbk	LS	sa po	so	7.5yr 4/6	7.5yr 4/3	1vf; a s	<5 2.5f	slight fix	
		B	4-40	2 m sbk	SL	sa p	sh	5yr 3/3	7.5yr 4/4	1f; c s	<5; 1m	coats on some clasts	
		B2	40-63	2 m sbk	SC	sa pa	sh	7.5yr 3/4	5yr 4/6	1vf; c s	<5; 1m	coats on some clasts	
		K	63-165	1 m sbk	L	sa pa	vh	7.5yr 4/3	10yr 5/4	1f; 0	<5; 0	coats on all clasts	
Surface Area: 1020 m <sup>2</sup>				Total Depth: 2.2									
AF4	94	A	0-3	1 m sbk	SL	sa po	sh	7.5yr 3/3	7.5yr 5/4	2vf; c s	45; 1f	no evident	
		B	3-10	2 m sbk	SIL	sa po	sh	7.5yr 4/4	7.5yr 5/4	2vf; c i	10; 1f	slight fix	
		BK	10-46	1 f sbk	SIL	sa pa	sh	7.5yr 4/4	7.5yr 5/4	1vf; g i	75; 0	coats fractures	
		Ck	46-55	1 m sbk	ShCL	sa p	sh	7.5yr 4/4	7.5yr 5/4	1vf; 0	70; 0	along vert. fractures	
AF5	94	A	0-1	3 vf sbk	SL	sa po	so	7.5yr 4/4	7.5yr 5/4	1vf; a s	>75; 1f	no evident	
		B	1-9	2.5 m sbk	CL	s p	sh-b	5yr 4/4	7.5yr 5/4	2vf, 1f, 1c; c s	25; 1f	coats on bottoms of some clasts; no matrix fix	
		K	9-18	3 f sbk	CL	sa-p so	so-sh	7.5yr 3/4	7.5yr 5/6	1m; g i	75; 0	Stage 1+; carbs go deeper along fractures;	
		Rk	18-28							0; 0		coats entire clasts; in all pores	
AF6	94	A	0-1	1 f sbk	LS	sa po	sh	7.5yr 3/3.5	7.5yr 4/6	1vf; a s	20; 1f	no evident	
		Bt	1-15	1.5 f-m sbk	L	sa pa	sh-b	5yr 4/4	5yr 4/6	1vf, 1f, 1c; c s	15; 1f	no evident	
		Ck	15-21	1 f sbk	SIL	sa pa	sh	6.75yr 4/4	5yr 4/6	0; g i	75	carbs in pores only	
		R	21-31										
LBM1	184	A	0-3	sg	LS	sa pa	so	7.5yr 4/3	7.5yr 6/4	0; a s	10	slight fix	
		B	3-11	2 m sbk	LS	sa pa	sh	7.5yr 4/4	7.5yr 6/4	2f; c s	<5	under clasts	
		Bk	11-26	1 f sbk	LS	sa po	sh	7.5yr 4/3	7.5yr 6/4	1f, 1m; c s	10	coats clasts	
		K	26-48	3 f sbk	SL	sa pa	sh	7.5yr 4/3	7.5yr 6/4	2f; c w	70	Stage II	
LBM2	184	A	0-2	sg	S	sa po	so	7.5yr 4/4	7.5yr 6/4	0; c s	10	coats small clasts	
		Bk	2-25	1 f sbk	LS	sa po	sh	7.5yr 5/4	7.5yr 6/4	3vf; g w	<10	coats all clasts	
		K	25-40	3 f sbk	LS	sa po	sh	7.5yr 5/4	7.5yr 6/3	0; c w	75	Stage II	
		Rk	40-53+										
LBM31	184	A	0-4	1.5 f-m sbk	LS	sa po	so-sh	7.5yr 4/3	7.5yr 5/4	1vf; c s	10	moderate fix in matrix; visible on clasts at surface	
		Bk	4-12	2 m-c sbk	LS-SL	sa po	sh	7.5yr 5/3.5	7.5yr 5/4	1vf, 1f, 1c; c/g s	<5	strong fix; visible on ped faces, along roots; slight coat on clasts	
		Bk2	12-25	1.5 m-c sbk	LS	sa po	so-sh	7.5yr 4/4	7.5yr 5/4	0; c s	5	coatings on entire clasts, 1-3 mm; carbonate granules in matrix	
		K	25-40	3 f sbk	L	sa po	so	8.75yr 5/4	7.5yr 6/4	2.5 f, 2.5m	75	Stage 2+; 2.5mm coats on clasts, laminar in areas	

Table 2 cont.: Soil Field Descriptions

Soil	Age (-ka)	Hor.	Depth (cm)	Structure	Texture	Consistence	Color	roots; boundaries	gravel %; pores	Carbonates
LBM32	184	A	0-5	1 f sbk	S	moist dry so po so	7.5yr 4/4 7.5yr 6/6	1vf; c s	<5	no fix
		Bk	5-18	2 m sbk	LS	so po sh	7.5yr 4/4 7.5yr 4.5/6	1f; 1c; c-s	10	no fix; slight (<1mm) coat on clasts
		K	18-47	sg	LS	so-sa pt lo	7.5yr 4/6 7.5yr 5/4	1vf, 1f, 2m; g l	30	stage 2+ in areas where there are smaller clasts; 2-5 mm coats
		Rk	47-58					0;0		Carbonate along fractures 1-2 mm coatings
LBM4	184	Av	0-4	2 m p	L	sa sp sh	8.75yr 4/3 10-yr 5/4		<1	slight fix
		Bw	4-10	2 m/c sbk	L	sa sp sh	8.75yr 4/3 10-yr 5/4		<1	spare filaments along roots
		B	10-25	1 m sbk	LS	so po sh	7/5yr 4/4 8.75yr 5/4		<1	strong fix throughout; some filaments
		Bk	25-86	1 m sbk	SL	sa sp sh	7/5yr 4/4 8.75yr 5/4		<1	strong fix, filaments
		Kib	86-110	1 f/m sbk	SCL	s p b	7/5yr 4/8 7.5yr 5/5		5-10	small nodules; carbonates on top of clay films, thin coatings on clasts, carbs on ped faces
		Kib2	110-230	2 f/m sbk	SCL	s p b-vh	7/5yr 4/8 7.5yr 5/6		20	thicker carbs on ped faces; abundant 2mm+ nodules, abundant carbs along roots; carbs dispersed through matrix; stage II
		Bkb	230-270	1 f sbk	SCL	s p w-sh	7/5yr 4/8 7.5yr 5/6		20	slight fix, occasional specs of carbonate
		Bkbb	270-290	2 f sbk	SCL	s p sb-b	7/5yr 4/8 7.5yr 5/6		20	slight fix, occasional filaments and specs
		Bkb2	290-330	1 f sbk	SL	sa sp sh	7/5yr 4/5 7.5yr 5/5		20	v. slight fix
				Surface Area 1125 m <sup>2</sup>	Total Depth: 3.43 m					

\*Area estimated by observing extent of healthy vegetation and lack of desert pavement.

LBMX-1	263	A	0-5	sg	S	so po lo	7.5yr 4/4 7.5yr 7/6	0; a w	<5	coats small clasts
		Bj	5-25	2 m sbk	LS	so po sh	10yr 4/4 10yr 6/5	1f; a w	<5	slight fix
		K	25-70	1 f gr	LS	so po	7.5yr 4/4 7.5yr 6/4	0; g l	75	Stage II
		K	70-90	1 f gr	S	so po	10yr 6/3 10yr 7/3	0; -	80	Stage III
LBMX-2	263	A	0-5	1 f sbk	S	so po so	7.5yr 4/6 7.5yr 6/4	1vf; c s	10	coats bottoms of clasts at surface; fix throughout
		B	5-18	2 m sbk	S	so po sh	7.5yr 4/5 7.5yr 6/5	1.5m, 2vf, 1f; a s	<10	fix throughout; filaments and flakes
		K2	18-58	5 vf sbk	LS	so-sa pt so	7.5yr 5/4 7.5yr 5.5/4	2f, 1c; c s	75	Stage 3; coats all clasts 2-5 mm
		K2	58-102	sg	LS	so-sa pt lo	7.5yr 5/3 7.5yr 7/4	1f, 1m; c s	75	Stage 2; not as indurated as K; 1-2 mm coats on clasts
		CK	102-116	sg	LS	so-sa pt lo	7.5yr 6/3 7.5yr 7/3	0;0	60	Coatings on most clasts (1-<1mm); less carbs in matrix.

ABBREVIATIONS	STRUCTURE	TEXTURE	CONSISTENCE	ROOTS/BOUNDARIES
	sg = single grain	S = sand	se = non sticky	vf = very fine
	f = fine	C = clay	sa = slightly sticky	f = fine
	m = medium	L = loam	s = sticky	m = medium
	c = coarse	SL = sandy loam	pe = non plastic	co = coarse
	gr = granular	LS = loamy sand	pe = slightly plastic	a = abrupt
	sbk = subangular/blocky	SL = Silty loam	p = plastic	c = clear
		SCL = Sandy clay loam	sh = slightly hard	g = gradual
		SC = Sandy clay	h = hard	s = smooth
		SCL = Silty clay	vh = very hard	w = wavy
				l = irregular

Table 3: Soil Analyses

Soil	Age (-ka)	Hor.	Depth (cm)	conductivity (decisiemens/m)	Clay ( weight %)	Silt ( weight %)	Sand ( weight %)	pH (H2O)	pH (CaCl2)	Soil Water Chloride (g/ml)	CaCO3 ( weight %)	horizon mass of carbonate (g/cm2/horizon)		
AD1	19	A	0-4	285.01	4.32	55.91	39.77	6.9	7.5	2634.58	negligible	negligible		
		B	4-29	121.13	13.46	57.10	29.44	7.2	7.6	290.03	negligible	negligible		
		Bt	29-60	111.15	19.16	64.87	15.97	7.3	6.7	127.95	negligible	negligible		
		Bt2	60-80	149.63	22.52	64.77	12.70	7.4	6.9	271.00	negligible	negligible		
			80-100	122.56	22.38	67.50	10.12	7.4	7.0	232.28	negligible	negligible		
			100-120	78.38	20.81	71.37	7.83	7.5	6.8	104.52	negligible	negligible		
		2Bt2	120-135	91.20	19.12	71.23	9.65	7.8	6.9	118.15	negligible	negligible		
			135-150	95.48	16.73	72.16	11.11	7.8	6.9	73.09	negligible	negligible		
			150-170	82.65	12.71	79.12	8.17	7.9	6.9	92.30	negligible	negligible		
170-190	64.13	13.94	77.24	8.82	8.1	7.1	83.23	negligible	2.925					
	AD2	19	A	0-3	85.50	13.14	33.20	53.66	6.6	6.3	N/A	0.423	0.010	
			B	3-9	101.18	13.34	26.25	60.41	7.1	6.4	N/A	0.275	0.019	
Bk			9-23	148.21	13.75	26.37	59.88	8.0	7.2	N/A	1.181	14.320		
AD3	19	A	0-4	64.13	10.09	33.59	56.32	7.5	6.3	N/A	0.166	0.004		
		B	4-11	82.70	8.83	31.72	59.45	7.9	6.4	N/A	0.398	0.024		
		Bk	11-20	51.30	15.66	30.14	53.99	7.3	6.6	N/A	0.419	12.859		
		Ck	23-34	49.88	19.66	31.06	49.28	7.4	6.5	N/A	0.347	0.008		
AD4	19	A	0-5	69.83	12.26	27.05	60.69	8.0	6.1	N/A	3.582	0.100		
		B	5-15	92.63	13.43	29.40	57.17	7.2	6.3	N/A	1.040	0.097		
		Bk	15-28	68.40	17.75	41.09	41.16	7.3	6.5	N/A	0.682	18.583		
		Ck	20-40	122.56	15.94	52.84	31.22	7.6	6.8	N/A	0.295	0.003		
AD5	19	A	0-3	171.01	17.54	47.22	35.24	6.5	5.8	5693.90	negligible	negligible		
		Bt	3-20	88.35	12.55	46.32	41.13	7.3	6.3	428.71	negligible	negligible		
		Bt2	20-40	78.38	21.21	45.22	33.57	7.4	6.7	119.59	negligible	negligible		
			40-63	65.55	20.95	50.93	28.12	7.5	6.9	197.50	negligible	negligible		
		Bt3	63-83	74.10	21.45	55.16	23.39	7.6	6.9	64.06	negligible	negligible		
			83-110	66.98	19.11	58.33	22.56	7.9	7.1	69.65	negligible	negligible		
		Bt4	110-130	75.53	18.51	72.65	8.84	7.7	6.8	62.60	negligible	negligible		
			130-137	76.95	17.29	55.41	27.30	7.8	7.1	68.25	negligible	3.279		
		2Bt4	137-160	88.35	9.61	71.81	18.58	8.1	7.2	51.83	negligible	3.279		
AD6	19	A	0-2	142.51	16.10	40.23	43.67	6.8	5.9	2655.98	negligible	negligible		
		Bt	2-21	71.25	19.79	39.58	40.63	7.2	6.2	528.75	negligible	negligible		
		Bt2	21-50	62.83	39.09	43.25	17.67	7.5	6.7	131.54	negligible	negligible		
		2Bt3	50-70	86.93	21.20	57.78	21.03	7.8	6.8	240.55	negligible	negligible		
			70-85	109.73	22.13	59.02	18.84	7.8	6.9	278.83	negligible	2.951		
		C	85-110	156.76	23.58	57.27	19.15	7.9	7.1	490.67	negligible	3.279		
	110-130	185.28	24.35	59.73	15.91	7.9	7.2	684.03	negligible	3.279				
AF1	94	Av	0-5	75.53	12.26	25.22	62.52	6.8	6.3	1836.67	0.061	0.020		
		Bt	5-20	128.26	24.51	26.03	49.46	7.6	7.1	1170.50	0.081	0.027		
		Bt2	20-40	121.13	23.85	35.86	40.29	8.1	7.2	473.06	0.106	0.035		
			40-60	109.73	25.31	45.31	29.38	8.2	7.5	103.50	0.139	0.048		
			60-84	129.68	19.79	53.63	26.58	8.3	7.7	273.89	0.189	0.062		
		Btkb	84-102	159.61	20.76	46.54	32.70	8.4	7.7	191.24	0.376	25.425		
		2Btkb	102-117	153.91	16.46	43.80	39.74	8.6	7.7	55.76	0.408	25.433		
		Kb	117-137	152.48	19.32	41.84	38.83	8.6	7.9	104.16	0.614	18.936		
			137-157	178.13	23.09	35.25	41.66	8.5	7.8	92.50	5.552	74.267		
			157-170	185.26	18.86	45.37	35.77	8.6	7.9	119.93	5.809	74.308		
		Kb2	170-195	185.26	20.45	43.98	35.57	8.6	7.9	110.70	3.164	73.893		
			195-220	188.11	18.68	37.73	43.60	8.6	7.9	67.79	0.809	73.523		
		Ck	220-240	178.13	20.17	36.54	43.29	8.6	7.8	134.87	3.261	73.908		
			240-260	185.58	16.33	35.90	47.77	8.6	7.9	94.33	3.724	109.335		
		AF2*	94	A	0-4	71.06	26.54	27.87	45.59	6.9	6.9	2100.88	0.300	0.019
				B	4-25	73.19	33.93	21.72	44.36	7.2	6.7	155.75	0.420	0.154
B2	25-48			82.43	39.02	34.99	25.99	7.8	7.2	172.30	0.260	0.104		
Bk	48-77			187.05	26.17	24.95	48.87	8.8	7.2	359.90	0.840	9.338		
K	77-120			258.62	27.85	60.82	11.32	9.2	7.7	178.45	1.470	15.651		
K2	120-170			252.83	21.24	45.44	33.32	9.3	7.9	1951.41	3.510	18.431		
Ck	170-240			332.59	24.89	45.56	29.55	8.5	7.8	5582.05	4.030	25.817		
	240-260			370.52	12.58	28.71	58.71	8.2	7.6	5617.71	3.677	7.431		
	260-280			412.77	8.93	42.89	48.18	8.5	7.6	2850.99	4.759	161.104		
	280-300			470.27	12.59	44.40	43.01	9.0	7.6	427.15	1.958	160.126		
	300-320			531.40	11.09	48.57	40.34	8.6	7.7	517.14	2.285	160.241		
										1496.68				
										1129.00				
* Chloride concentrations for AF2 were measured every 20 cm after the A horizon														

\* Chloride concentrations for AF2 were measured every 20 cm after the A horizon

Table 3 cont.: Soil Analyses

Soil	Age (-ka)	Hor.	Depth (cm)	conductivity (decisiemens/m)	Clay (weight %)	Silt (weight %)	Sand (weight %)	pH (H <sub>2</sub> O)	pH (CaCl <sub>2</sub> )	Soil Water Chloride (g/ml)	CaCO <sub>3</sub> (weight %)	horizon mass of carbonate (g/cm <sup>2</sup> /horizon)
AF3	94	A	0-4	82.43	11.58	13.43	74.99	6.9	6.3	N/A	0.480	0.030
		B	4-40	85.27	21.85	15.92	62.24	7.5	6.8	N/A	0.390	71.341
		B2	40-63	135.02	31.33	23.51	45.16	7.7	7.3	N/A	0.320	45.551
		K	63-110	144.97	28.81	29.60	41.59	7.5	7.5	N/A	2.690	115.245
			110-165	255.82	20.18	43.10	36.72	7.4	7.5	N/A	3.430	439.381
AF4	94	A	0-3	84.08	8.24	18.12	73.64	7.0	6.9	N/A	0.342	0.008
		B	3-10	81.23	9.48	18.34	72.18	7.7	6.8	N/A	0.207	0.016
		Bk	10-46	142.51	18.68	20.31	61.00	8.0	7.2	N/A	0.948	24.225
		Ck	46-55	138.23	27.47	18.64	53.89	8.4	7.5	N/A	2.711	43.343
AF5	94	A	0-1	148.21	8.21	14.85	76.94	7.3	7.3	N/A	0.057	0.000
		B	1-9	136.81	34.66	7.59	57.75	8.0	6.8	N/A	0.167	9.332
		K	9-18	313.51	22.31	24.12	53.57	8.3	7.8	N/A	4.023	30.972
AF6	94	A	0-1	88.35	5.69	18.08	78.23	8.4	7.5	N/A	0.133	0.002
		Bi	1-15	101.18	12.68	19.98	67.35	8.3	7.3	N/A	0.119	0.017
		Ck	15-21	199.51	16.78	25.75	57.47	8.2	7.5	N/A	0.303	23.917
LBM1	184	A	0-3	211.40	9.68	10.96	79.36	8.4	7.8	N/A	0.900	0.045
		B	3-11	177.35	9.68	10.96	79.36	8.6	7.9	N/A	2.950	5.653
		Bk	11-26	163.16	12.56	8.25	79.18	8.6	7.6	N/A	3.750	79.707
		K	26-48	181.61	10.77	7.68	81.57	8.6	7.9	N/A	6.980	41.313
LBM2	184	A	0-2	177.35	7.84	11.02	81.34	8.4	7.7	N/A	0.950	0.602
		Bk	2-25	174.51	8.85	5.39	85.76	8.6	7.8	N/A	3.820	125.482
		K	25-40	170.28	10.90	7.50	81.61	8.4	7.8	N/A	9.310	37.125
LBM31	184	A	0-4	185.26	9.23	11.97	78.79	8.5	7.8	N/A	1.122	1.214
		Bk	4-12	208.63	10.75	5.74	83.51	8.8	7.9	N/A	1.646	5.257
		Bk2	12-25	199.51	9.48	7.96	82.56	8.9	8.0	N/A	3.334	72.216
		K	25-40	213.76	9.82	12.46	77.73	8.6	7.9	N/A	13.500	37.262
LBM32	184	A	0-5	182.41	6.73	5.41	87.86	8.5	8.0	N/A	0.596	0.046
		Bk	5-18	105.45	10.69	8.88	80.43	8.5	7.8	N/A	1.027	44.696
		K	18-47	205.21	11.80	5.05	83.15	8.6	8.0	N/A	3.021	27.897
LBM4	184	Av	0-4	213.76	10.55	17.26	72.19	8.0	7.3	8435.66	0.446	0.032
		Bw	4-10	128.28	9.44	10.45	80.11	8.1	7.2	388.44	0.297	0.108
		B	10-25	92.63	7.09	13.83	79.07	8.0	7.4	388.44	0.536	0.192
		Bk	25-86	128.26	9.36	11.15	79.49	8.3	7.4	184.69	1.539	0.551
		Kib	86-110	133.96	10.33	13.53	76.15	8.3	7.3	163.91	1.520	0.544
		Kib2	110-130	121.13	10.77	11.88	77.36	8.3	7.4	218.61	0.867	75.042
			130-150	141.08	15.59	18.37	66.04	8.2	7.4	123.82	1.782	132.861
			150-170	156.76	19.43	15.95	64.62	8.2	7.4	217.23	5.285	133.876
			170-190	148.63	14.04	15.72	70.24	8.3	7.3	144.33	2.196	132.986
			190-210	142.51	13.32	17.45	69.24	8.3	7.3	144.33	2.323	133.023
			210-230	131.11	13.86	2.63	83.51	8.3	7.3	224.45	1.932	132.910
		Bkb	230-250	156.76	12.50	15.56	71.95	8.4	7.3	741.32	2.350	133.030
			250-270	139.66	12.28	30.20	57.53	8.3	7.3	234.80	0.812	132.588
		Bkb	270-290	111.15	12.26	30.20	57.53	8.2	7.2	169.03	0.162	132.400
		Bkb2	290-310	105.45	11.34	18.87	69.78	8.3	7.2	134.17	0.109	132.365
		C	310-330	111.15	11.34	18.87	69.78	8.2	7.2	241.22	0.035	132.364
			330-350	125.41	10.44	19.56	70.00	8.2	7.3	274.79	0.173	132.404
			350-370	136.81	11.35	17.37	71.29	8.1	7.2	353.32	0.145	132.396
LBMX-1263		A	0-5	171.67	4.72	2.69	92.59	8.3	7.7	N/A	0.550	3.554
		Bj	5-25	141.88	7.59	3.68	88.73	8.5	7.7	N/A	0.630	14.253
		K1	25-50	146.14	7.81	5.18	87.01	8.6	7.7	N/A	1.190	107.283
			50-70	153.23	8.81	6.25	84.95	8.6	7.8	N/A	5.710	107.428
		K2	70-80	156.07	12.63	11.30	76.07	8.5	7.8	N/A	18.100	65.694
			80-90	187.28	14.84	18.15	69.01	8.5	7.9	N/A	34.240	66.178
LBMX-2263		A	0-5	116.85	3.48	4.38	91.65	8.9	8.0	N/A	0.296	3.304
		B	5-18	131.11	6.12	5.92	87.95	8.9	8.0	N/A	0.790	8.666
		K2	18-58	175.28	9.57	7.02	83.41	8.5	8.1	N/A	9.187	229.224
		K2	58-102	242.26	14.45	12.46	72.09	8.8	8.1	N/A	24.210	158.461
		CK	102-116	223.73	13.14	12.03	68.83	8.8	8.3	N/A	28.623	23.359



## RESULTS AND DISCUSSION

### *Variability Between O.T.L. and O.T.H. Soils*

#### Morphology differences between O.T.L. and O.T.H. soils

There is a marked difference between soils developing over original highs and lows of basalt topography in the Potrillo volcanic field. This overall variability is similar to that observed on terrace treads in the Cajon Pass chronosequence, where soils developing in swales are distinct from soils developing on bars (Harrison et al., 1990). In the Potrillos, O.T.L. soils are thick and fine textured with carbonates dispersed throughout the profile (Fig. 3). Clasts near the bottom of these soil profiles have thin carbonate coatings which increase in thickness with age (Table 2). O.T.H. soils on the AD surface develop primarily in eolian material found in fractures in the basalt. A thin band of carbonate precipitates at a shallow depth on basalt faces in these soils. O.T.H. soils for all other surfaces are generally characterized by a thin veneer of dust overlying a carbonate horizon which continues into the basalt for unknown distances. Like in the O.T.L. soils, the thickness of clast coatings increases significantly with the age of the surface. Soils developing in topographic lows have overall finer textures than soils developing on topographic highs (Table 3). Higher proportions of clay and silt in the O.T.L. soils are likely a result of the addition of fine material from the sides of depressions by runoff.

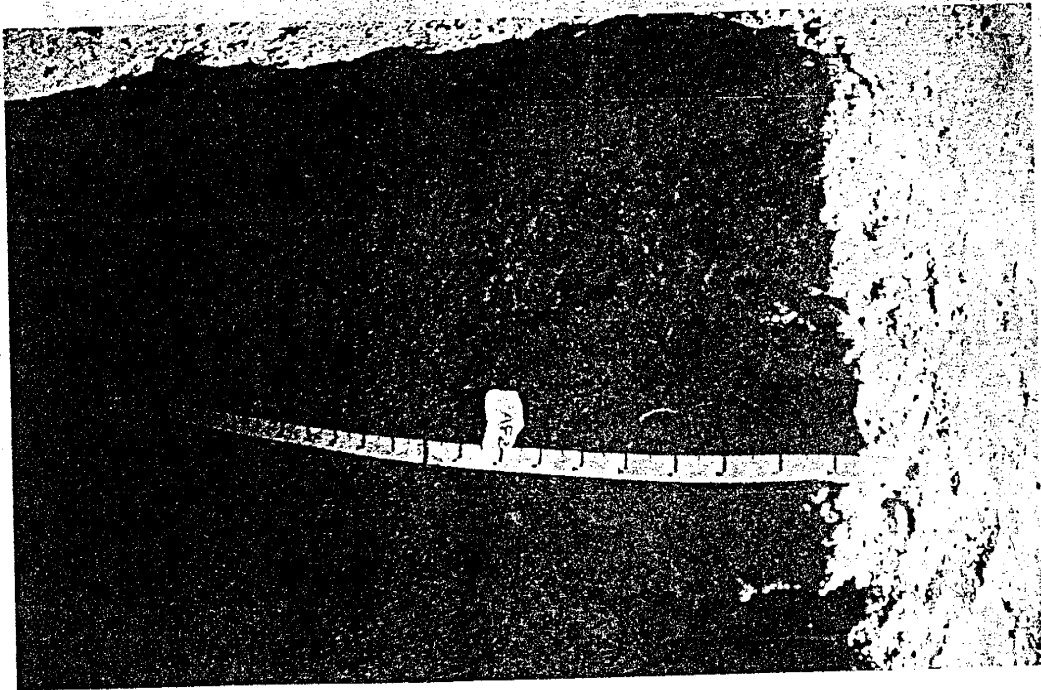
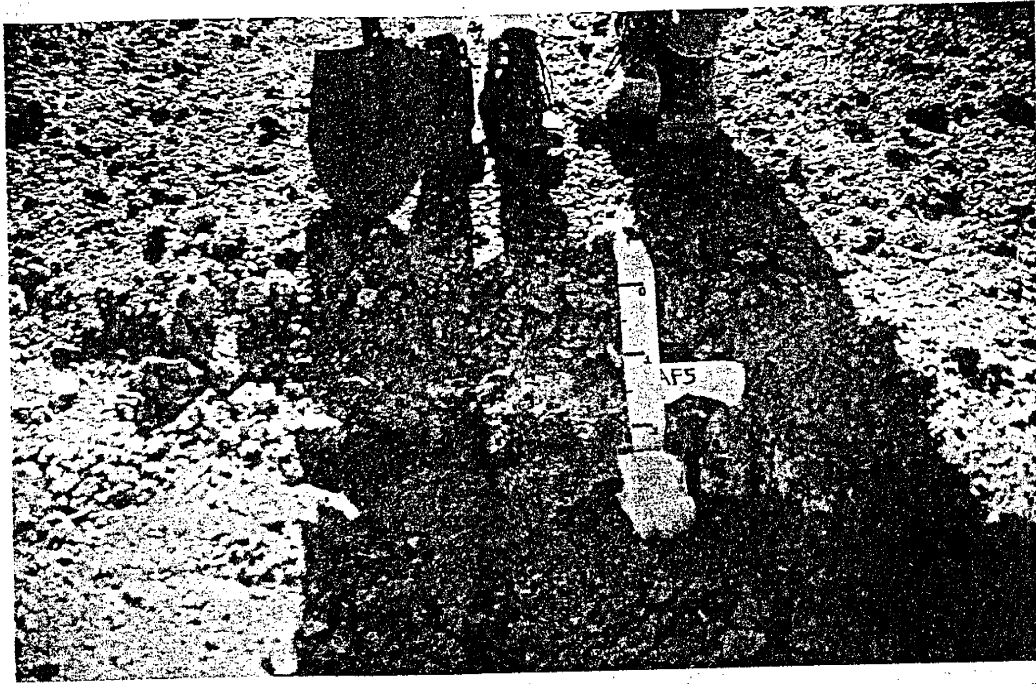


Figure 3: Photographs of O.T.H. and O.T.L. soils in the Potrillo volcanic field.

Buried soils were found in O.T.L. profiles on the AF and LBM surfaces. One buried soil is found in AF profiles and two in the LBM profile. As buried soils represent periods of relative stability in the landscape, their presence in the soils in the Potrillos provides evidence for at least two changes in the regional dust flux since ~90 ka. In general, buried soil horizons are characterized by sharp increases in clay and/or carbonate content below upper Bt and K horizons (Table 2). In AF2, manganese coatings are present on ped faces in the uppermost buried soil. No evidence of buried soils was found in any O.T.H. soil profile.

#### Soil chemistry differences between O.T.L. and O.T.H. soils

With the exception of AD soils, profile mass of carbonate and sum of profile conductivity are significantly greater in O.T.L. soils (Figs. 4&5). Given that soils developing in depressions contain greater volumes of dust from which carbonates and salts can be leached, it was expected that overall carbonate and soluble salt content would be greater in these soils than in those developing on topographic highs. Also, the presence of carbonate coatings along fractures and in vesicles at the base of O.T.H. soil pits on the AF, LBM, and LBMX surfaces suggests that carbonate is being lost through the underlying bedrock. The large difference between O.T.L. and O.T.H. soils in the total amount of carbonates and sum of conductivity could also be attributable to this leaching along fractures to unknown

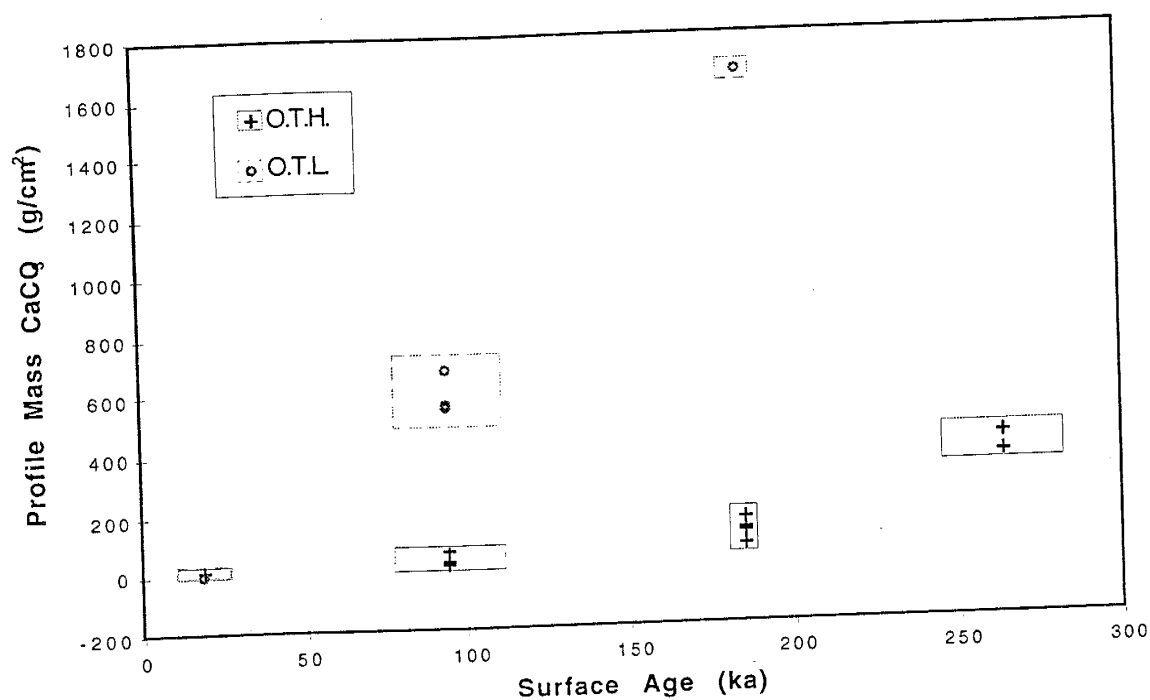


Figure 4: Graph of profile sum of CaCO<sub>3</sub> for both O.T.H. and O.T.L. soils developing on basalt flows of varying ages in the Potrillo volcanic field. Boxes represent analytical error for single points and 1σ error for multiple points.

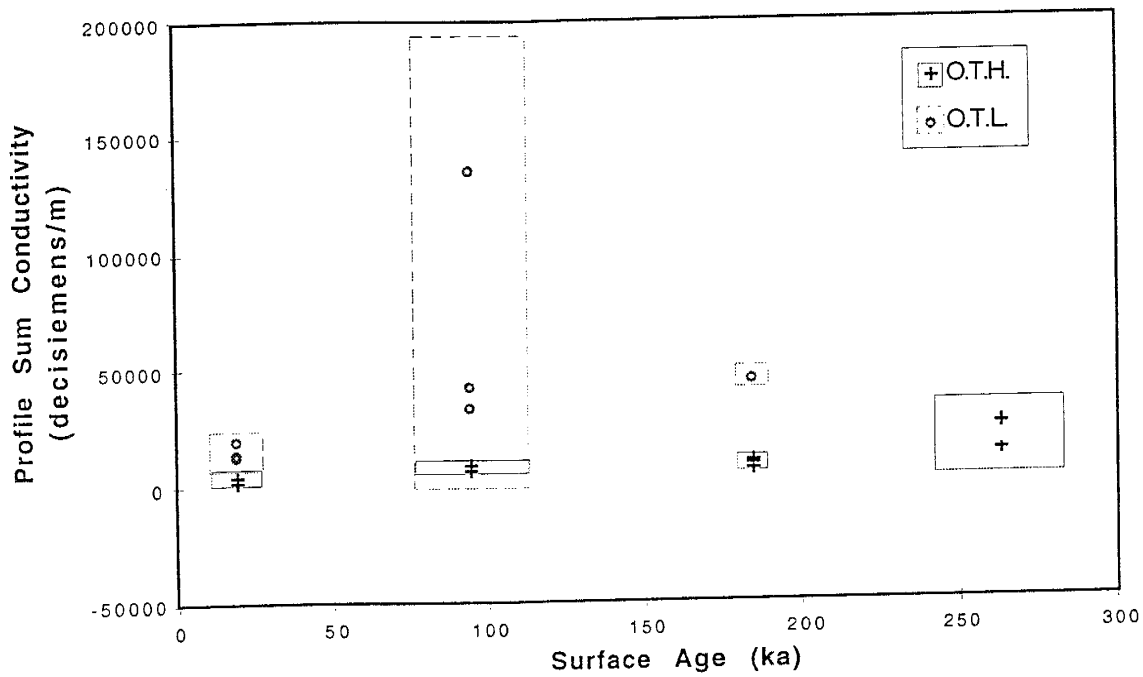


Figure 5: Graph of profile sum of conductivity for both O.T.H. and O.T.L. soils developing on basalt flows of varying ages in the Potrillo volcanic field. Boxes represent analytical error for single points and  $1\sigma$  error for multiple points.

depths in the O.T.H. soils. One other possible cause for the higher carbonate content in O.T.L. soils could be that topographic lows in the Potrillos have generally higher amounts of vegetative cover than do topographic highs. As carbonate precipitates readily along root pathways, this could also cause an increase in the carbonate content of soils. However, no significant amount of carbonate is evident along roots in O.T.L. soils, and the majority of carbonate in O.T.L. soils appears to be tied up in clast coatings. Furthermore, percentages of  $\text{CaCO}_3$  in the  $< 2\text{mm}$  portion are similar for both O.T.H. and O.T.L. soils suggesting that precipitation of carbonate along plant roots is not significant.

#### Soils developing on topographic highs: A preference for soil chronosequence study

In general, O.T.L. soils have overall greater variability than O.T.H. soils, with larger standard deviations for soil properties such as profile mass of carbonate and conductivity (Figs. 4&5). Similarly, in the Cajon Pass chronosequence, soils developing in swales are found to be more variable than soils developing on bars (Harrison et al., 1990). O.T.H. soils in the Potrillos have been developing in a more stable environment through time than have the O.T.L. soils. Desert pavements are more developed, and soils are not subject to runoff from topographic highs. Overall variability of O.T.H. soils is low, though variability increases slightly with age for profile mass of carbonate and for conductivity (Figs. 4&5). Given

UNIVERSITY  
OF ARIZONA  
LIBRARY

33  
100-443887-100

33  
100-443887-100

33  
100-443887-100

33  
100-443887-100

33  
100-443887-100

concentrations in AD6 and AF2 suggest that the moisture flux through these soils is currently significantly lower than other soils on the same aged surfaces. Given the evidence for lower moisture flux, it would be expected that leaching in these soils is minimal. The overall positive E-I coefficient values for AF2 suggest that leaching is in fact minimal for this profile (Fig. 7). (E-I data is only available for one soil per surface.) E-I data for AD5 and LBM4, soils with relatively high water flux as evidenced by chloride data, are negative suggesting overall leaching of these profiles.

Given the range of water flux affecting O.T.L. soils, and that soil chemistry and morphology will be greatly affected by water, it is likely that much of the spatial variability observed in O.T.L. soils is a function of differences in leaching characteristics of their profiles. The question arises, therefore, as to the cause of the differences in water flux through these soil profiles in the Potrillo volcanic field.



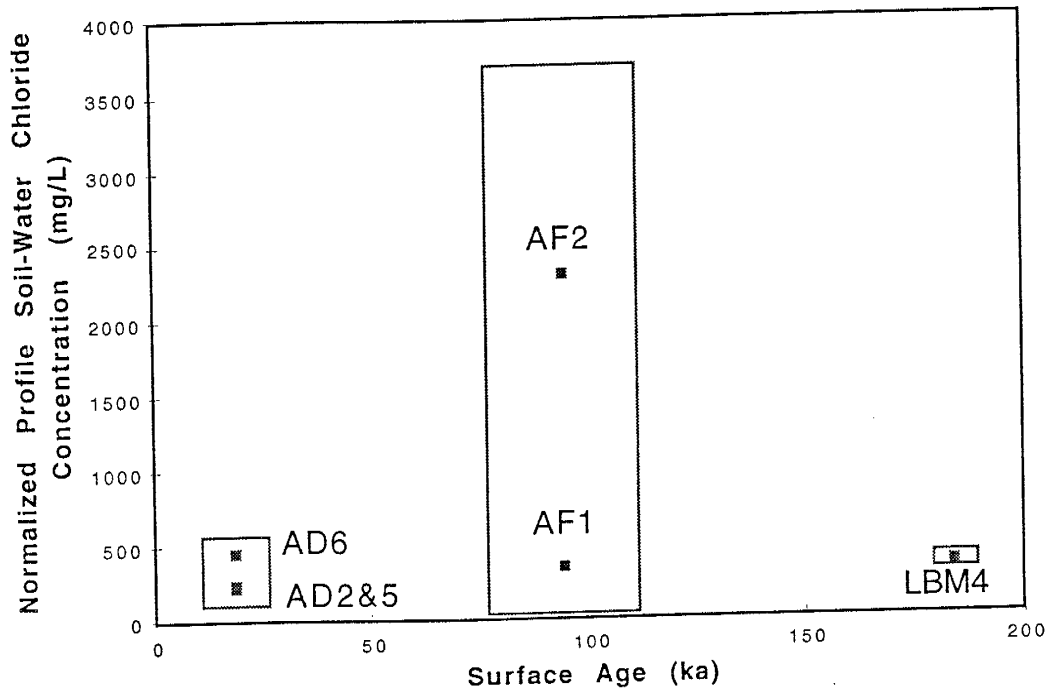


Figure 6: Graph of profile normalized soil-water chloride concentrations vs surface age for O.T.L. soils. Boxes represent analytical error for single points and  $1\sigma$  error for multiple points.

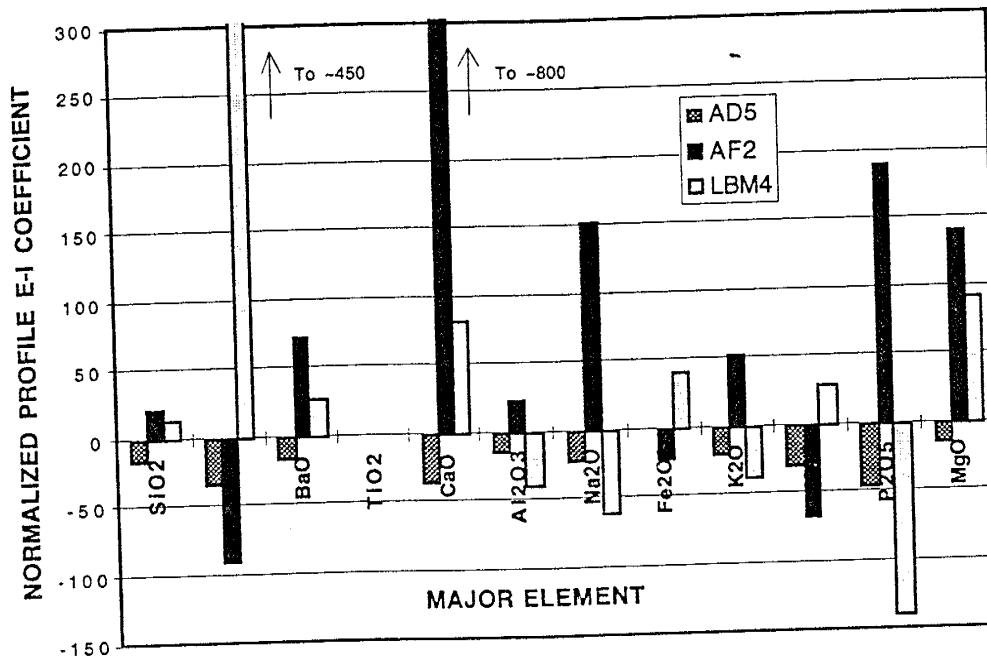


Figure 7: Overall profile E-I coefficients for AD5, AF2, and LBM4.

## Effects of infilling depressions with different sizes and shapes on water flux in soil profiles: Depositionally induced aridity

In general, soils developing in depressions with large surface areas have overall lower concentrations of soil-water chloride than smaller depressions on that same surface (Fig. 8). These data suggest that for the AD and AF surfaces, moisture flux is higher in the larger depressions of those surfaces. This trend does not hold true, however, between surfaces of different ages. AD1&5 are similar in size to AF2, but have dramatically lower water flux characteristics. However, there is a decrease in soil water chloride concentrations with depth in the AF2 profile (Fig. 9). No other soils examined for this study had a similar bulge, though it is a common feature of desert soils (Scanlon, 1991, Phillips, 1994). This decrease suggests that water flux in this soil was higher at some time in the past (Phillips, 1994). Furthermore the presence of manganese coatings on ped faces in the buried soil on AF2 also provides evidence that moisture conditions were higher in this profile at some time in the past. (The presence of manganese coatings in desert soils is thought to represent partial reducing conditions (Weitkamp et al., 1996).) These data suggest that depression size as well as changing environmental conditions through time are responsible for the variation seen in O.T.L. soils in the Potrillos.

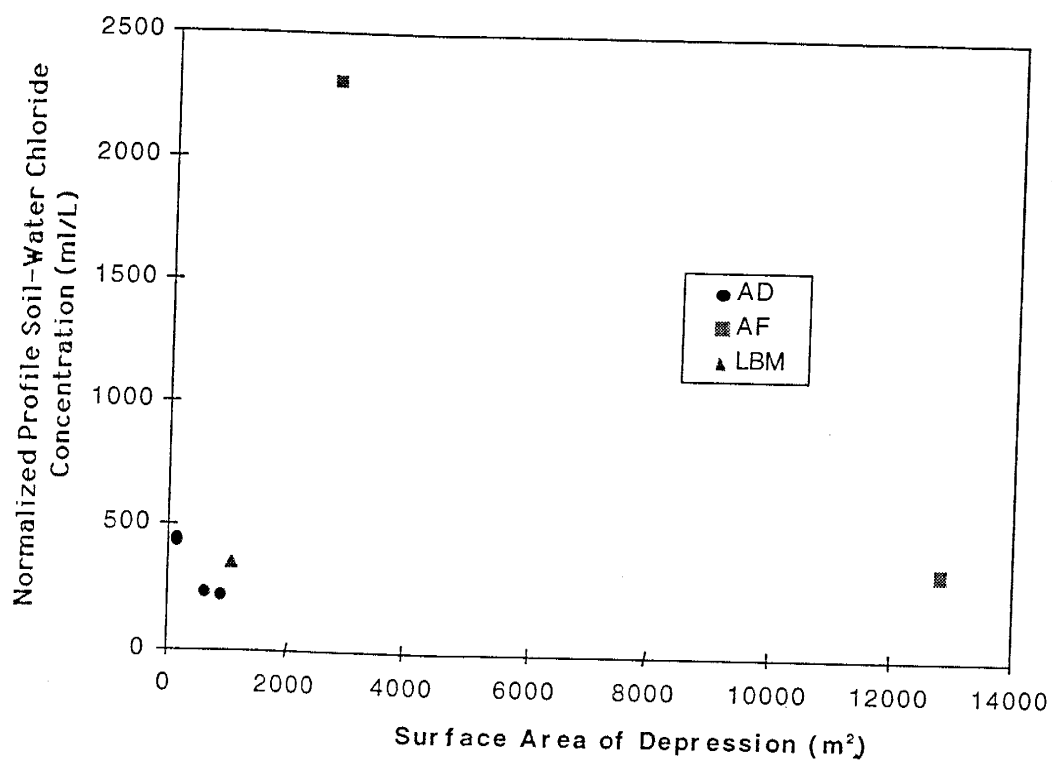


Figure 8: Graph of depression surface area vs normalized profile soil-water chloride concentrations.

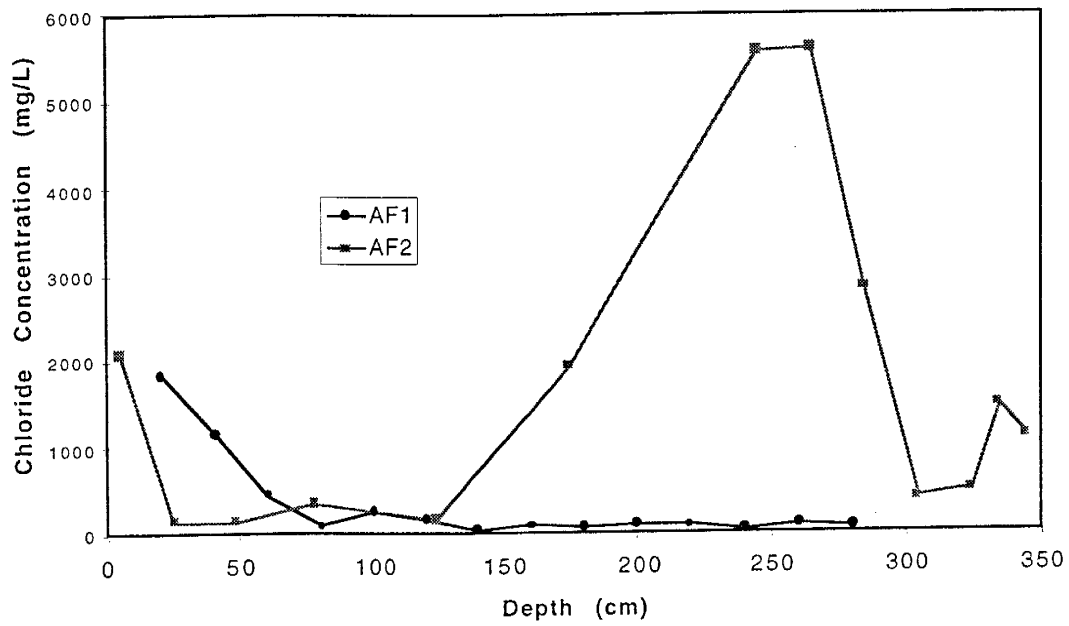


Figure 9: Soil water chloride depth profiles for the AF1 and AF2 soils.

Depressions in basalt flows serve as miniature catchment basins for both dust and water. Precipitation drains off basalt surfaces into depressions, washing with it fine material. This water then filters down through whatever eolian mantle has accumulated in the bottom of topographic lows. Leaching potential of soils developing in depressions, therefore, is a function of 1) catchment area size (which controls the amount of runoff) and 2) the amount of eolian material which has accumulated in that depression (Fig. 10). When this mantle is thin, water can completely wash through the soil. This will result in low chloride concentrations (AF1, AD1&5). With time, however, the thickness of the eolian mantle increases, and the leaching of the profile is effectively reduced resulting in the depositionally induced aridity of a soil which was once developing with high moisture flux conditions (AF2, AD6; Fig. 10).

The two properties, catchment area and thickness of eolian mantle, however, themselves vary as a function of a number of variables from depression to depression. The catchment area of individual depressions varies as a function of the total surface area of the depression, as well as of how much of that area is covered with eolian mantle (Fig. 10). A larger catchment area will result in greater runoff. Accumulation of a thick eolian mantle, however, will results in a *loss* of catchment area, reducing water flux through soils. Such is the case in AD6, and AF2 where the current ratio of exposed basalt to eolian mantle is small.

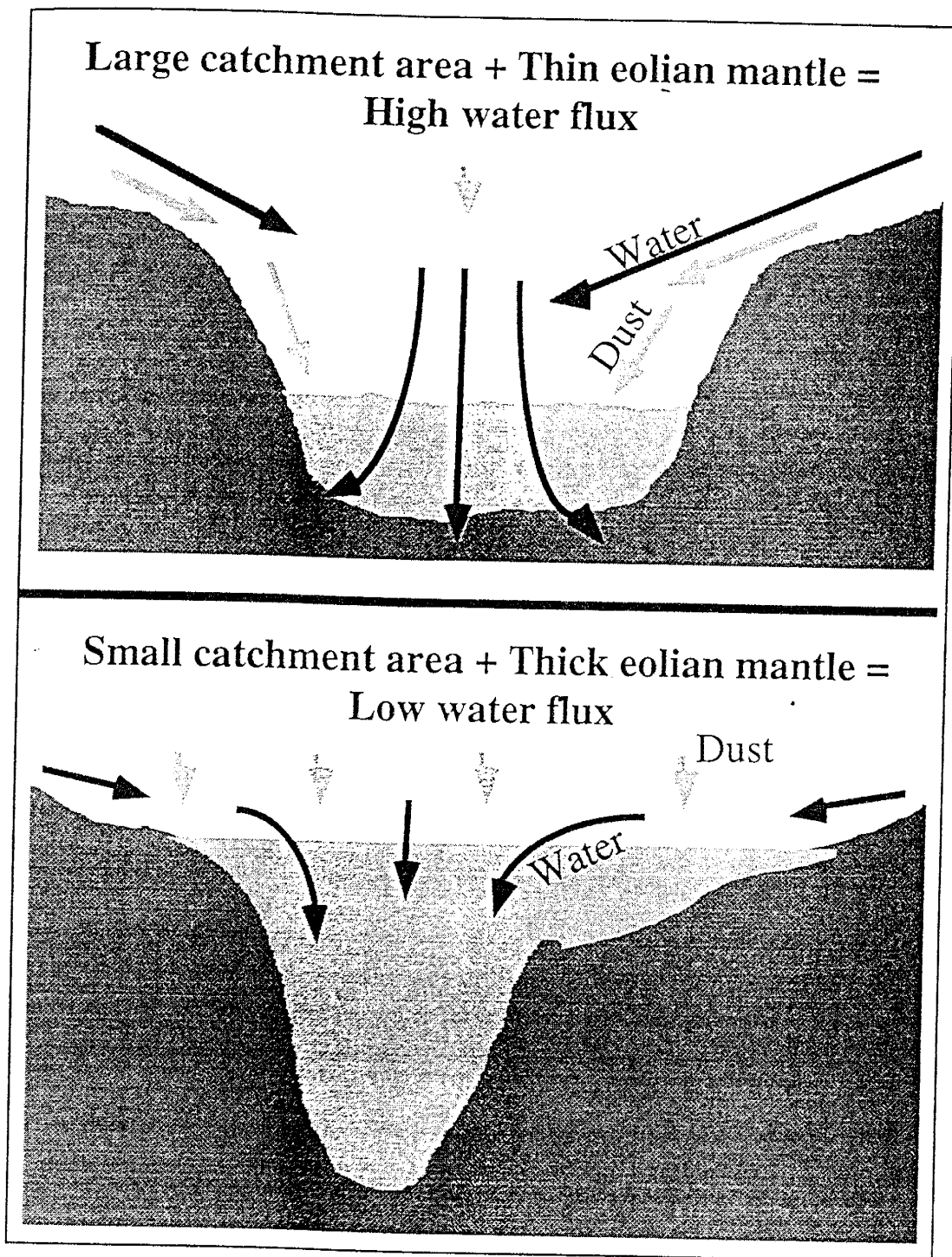


Figure 10: Effects of catchment area and thickness of eolian mantle on water flux through O.T.L. soils.

The thickness of eolian mantle in individual depressions varies as a function of not only the amount of time that it has been filling and the surface area of the depression, but also as a function of the shape of the depression (Fig. 11). It is logical that two depressions with similar shapes but different surface areas will accumulate different thicknesses of eolian material in a given time period given similar catchment areas and dust flux. However, three depressions with equal surface areas will accumulate dramatically different thicknesses of eolian material depending on the shape of the depression. Evidence for this variable rate of infilling of depressions is found in buried soils on the AF surface. The uppermost buried soil in AF2, a small relatively narrow depression, is found at a depth of around 1 m. The uppermost buried soil in the AF1 profile is found at a depth of approximately 2 m, suggesting that vertical deposition in this depression is significantly lower than that of AF2.

#### Effects of infilling depressions with different sizes and shapes on water flux in soil profiles: Depositionally induced stability

The differences in the rate of infilling of soils on basalt surfaces not only affect soil development in terms of leaching, but also in terms of surface stability. The depression size of AF3 is somewhat smaller than AF2 (Table 2). The carbonate content in this soil is significantly higher than AF2 (Table 3, Fig. 4). It has been noted that topographic highs are



the most stable geomorphic surfaces on basalt flows in the Potrillo volcanic field. However, as depressions become completely filled through time, they too become stable geomorphic surfaces no longer subject to the changing environmental conditions described above. Small depressions on basalt flows will be the first to fill and stabilize (Fig. 11). Consequently soils on these surfaces will become more strongly developed than those that are still being affected by processes of aggradation and leaching.

As more depressions fill through time, on each isochronous basalt surface, many geomorphic surfaces of varying age will be formed. Soils on each of these surfaces will vary depending on the time at which the surface became relatively stable (Fig. 12). This change from time-transgressive soils to stable soils further adds to the complexity of variability of the O.T.L. soil profiles on basalt flows in the Potrillo volcanic field. While the three studied O.T.H. soils on the AF surface have been stable for equal periods of time, AF3 is the only O.T.L. soil that has reached stability and consequently has a greater degree of soil development than AF2, which is in turn more stable than AF1.

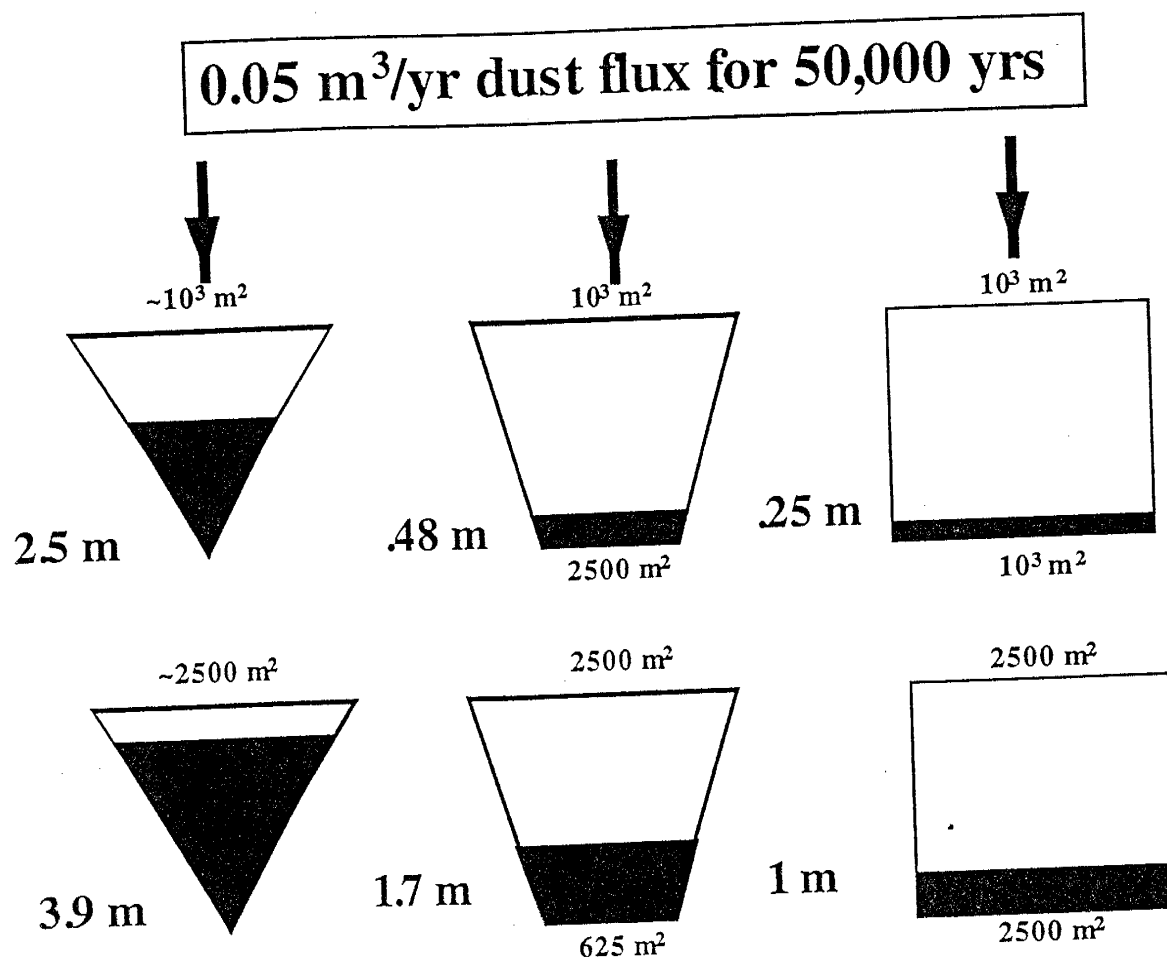


Figure 11: Differences in the depth of eolian mantle accumulated in depressions with different surface areas and shapes. Rate of dust accumulation is assumed constant at  $0.05 \text{ m}^3$  over a period of 50,000 years. Catchment area for all depressions is equal.

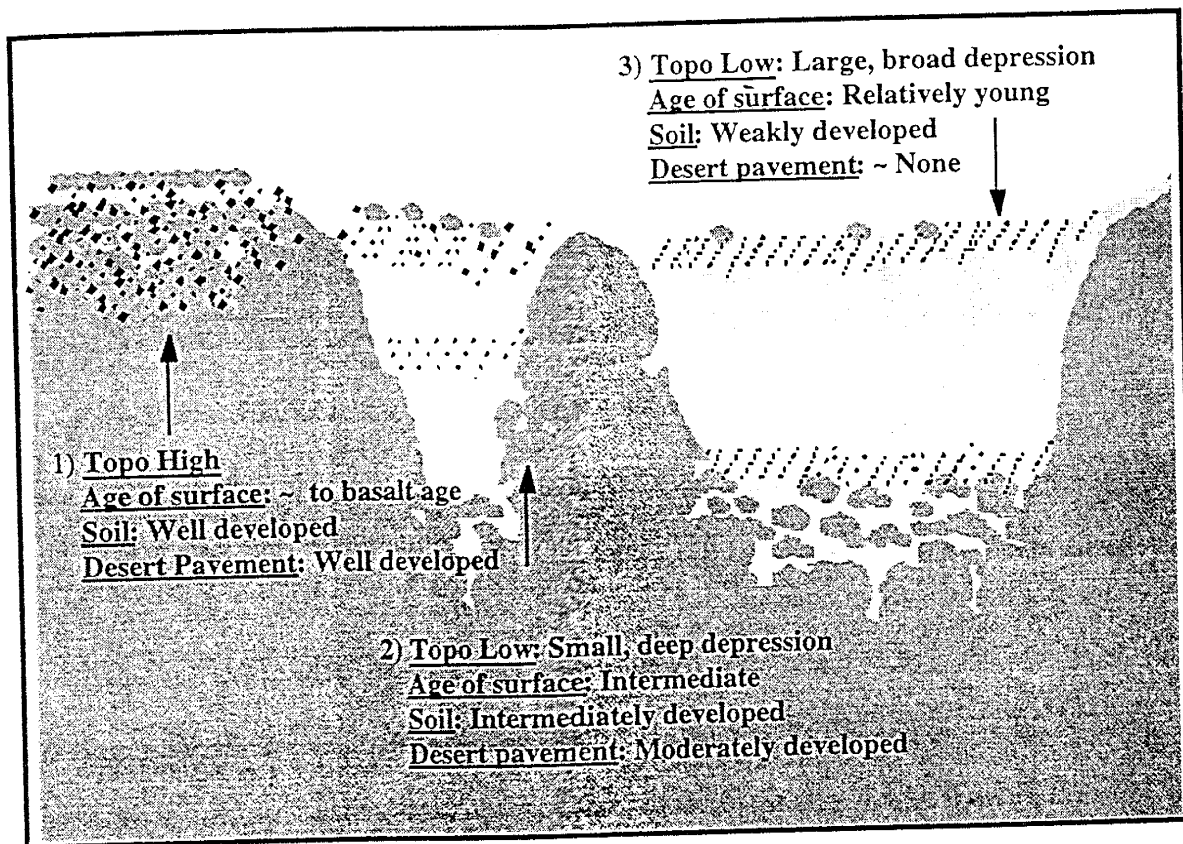


Figure 12: Three geomorphic surfaces on an isochronous basalt flow. The timing of the stability of the surface is a function of the size and shape of the depression in which eolian material is accumulating. Topographic highs become stable essentially at the time of basalt deposition.

*Implications for Aquifer Recharge*

Though soils developing in depressions are of little use for soil chronosequence study because of their variability, the high moisture flux conditions of those areas have implications for local aquifer recharge in the Potrillo volcanic field. The low soil water chloride concentrations in O.T.L. soils provide strong evidence of high water fluxes through these soils. Furthermore, E-I coefficients for the AD and LBM soils are predominately negative providing evidence that leaching is affecting these profiles and further suggesting that water fluxes are high (Fig. 7).

These high water fluxes are probably the result of an increased effective precipitation at the bottom of depressions. When a young cone-shaped depression receives precipitation, the actual amount of precipitation that the eolian mantle receives is extremely large as a result of runoff from the basalt. Through time, as depressions fill, the amount of precipitation affecting the mantle reduces to the actual regional precipitation. Figure 13 shows the maximum amount of precipitation affecting the mantle at any given time for a cone, trapezoid, and rectangle shaped depression. It is obvious that, especially on young flows, large amounts of water are being

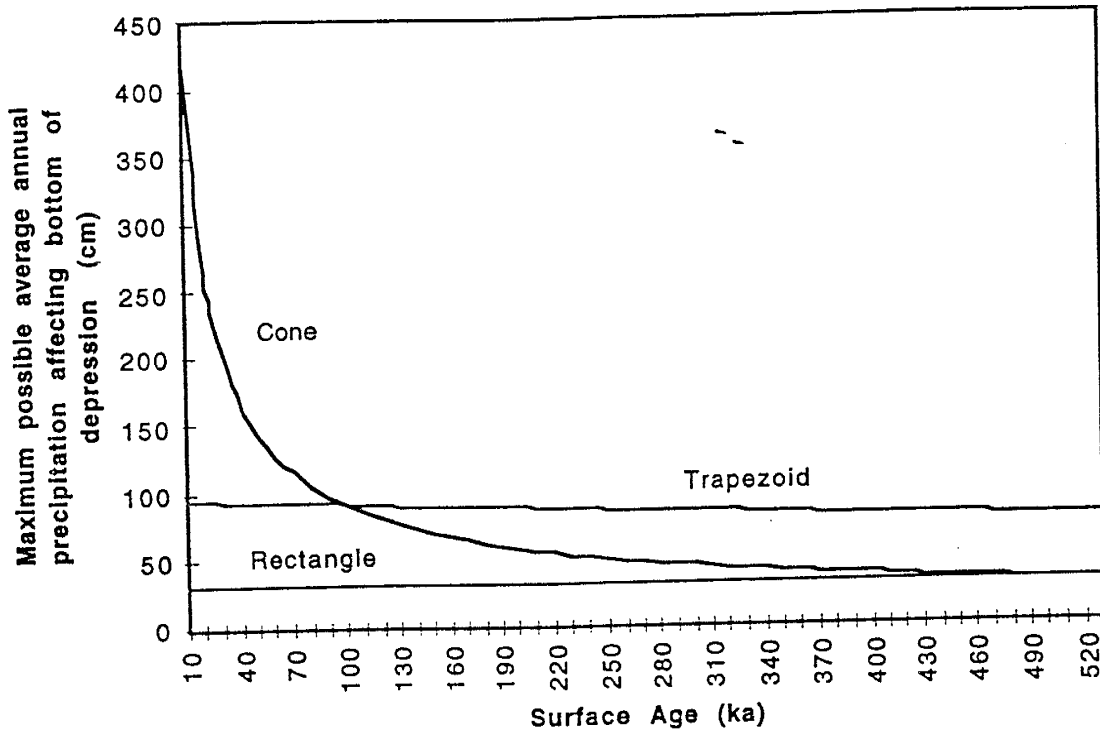


Figure 13: A graph of the maximum amount of precipitation affecting the bottom of depressions with similar surface areas but different shapes. Graph assumes 100% runoff with a constant dust accumulation rate of  $0.05 \text{ m}^3/\text{yr}$ . As the area of the bottom of the depression approaches the surface area of the depression itself, effective precipitation approaches the average precipitation of the region.

funneled down through cone and trapezoid shaped depressions. Therefore a vadose zone in a conical shaped depression, while once receiving large amounts of effective precipitation, eventually aridifies. This aridification would explain the bulge and then drop in chloride concentrations with depth in the AF2 soil (Fig. 8).

There are two schools of thought concerning aquifer recharge from desert vadose zones. One suggests that desert soils are stable environments characterized by minimal water and solute flux as evidenced by bulges in soil water chloride concentrations (Phillips, 1994). However, a drop in chloride concentrations below this bulge has been widely documented in desert soils. In keeping with the idea of hydrologically stable vadose zone, the generally accepted interpretation for this drop is that it is a result of paleoclimate variations (Scanlon, 1991). However, studies have shown that preferential flow of water through desert vadose zones is common (Hendrickx and Dekker, 1991, Spikers, 1994), and it is suggested that changes with depth in soil water chloride concentrations could be a result of short term temporal and spatial variability at the soil surface. The implication in this theory of changing moisture flux with changing surface conditions is that, at least on short term time scales, desert vadose zones have potential to be significant contributors to local aquifer recharge. Data from the Potrillo volcanic field support this latter theory where moisture

Furthermore, maximum chloride concentrations in depressions in the Potrillo volcanic field are generally around 300 mg/L below upper horizons (Table 3). Maximum concentrations reported by Scanlon (1991) for an area just south of the Potrillos are between 2000 and 3000 mg/L and by Phillips (1994) for a similar area are around 3000 mg/L. The difference in these data suggest water flux through soils developing in depressions on basalt flows is significantly larger than that of other soils in the region. Given that basalt flows in the Potrillo volcanic field occupy over 200 km<sup>2</sup>, these larger moisture fluxes could be major contributors to aquifer recharge in the area.

## CONCLUSIONS

Soils in the Potrillo volcanic field vary according to whether they are developing on high or low points in flow topography. Soils developing in depressions are forming primarily in eolian dust with carbonates precipitating on occasional clasts found in the profiles. O.T.H. soils are developing primarily in the basalt rubble zone overlying the flow. The amount of carbonate tied up in clast coatings is the significant contributor to profile carbonate mass of O.T.L. soils.

O.T.L. soils show significantly more variability in morphology and chemistry than O.T.H. soils. This variability appears to be a function of not only time, but also of the influence of the size and shape of depressions on changing environmental conditions through time. Chloride concentrations indicate that water flux has decreased significantly in small depressions that have been completely filled with eolian mantle. Also, small depressions become stable sooner than large depressions, allowing soil development rates to increase, and adding further to soil spatial variability. High water flux through large depressions suggests that these sites may be important areas of aquifer recharge and deserve further investigation.

Variability in soils developing on isochronous basalt flows in the Potrillo volcanic field has implications for chronosequence studies as well



as for soil-paleoclimate studies. Given that variability of O.T.L. soils is being influenced by a number of complex factors other than time, and that variability of the O.T.H. soils is minimal, O.T.H. soils should be the primary basis for chronosequence studies in this area. Buried soils found on the AF and LBM surfaces provide evidence that there have been changes in the dust flux in the Potrillos. However, O.T.H. soils in the Potrillo volcanic field do not show evidence for either the change in dust flux which occurred in the area, nor for the potential of aquifer recharge which these basalt surfaces represent. Without investigating many soils in the field, these important environmental conditions of the Potrillo volcanic field would have gone undocumented.

*Part 2*

EXAMINATION OF A SOIL CHRONOSEQUENCE IN LIGHT OF A  
PRIOR SPATIAL VARIABILITY STUDY:  
SOILS DEVELOPING ON WELL DATED BASALT FLOWS IN  
THE POTRILLO VOLCANIC FIELD, SOUTHERN NEW MEXICO

Martha Cary Eppes

Department of Earth and Environmental Science  
New Mexico Tech

## ABSTRACT

Soils developing on well dated basalt flows in the Potrillo volcanic field, southern New Mexico provide the means to place more accurate constraints on the rates of soil development in the desert southwest. Soils developing on high points in basalt flow topography are only slightly variable, and were therefore employed for the soil chronosequence study. Soils were described on four basalt flow surfaces which had been dated using  $^{40}\text{Ar}/^{39}\text{Ar}$  and  $^3\text{He}$  surface dating methods. Averages of their ages are: ~19 ka, ~94 ka, ~184 ka, and ~260 ka.

Profile mass of carbonate and normalized profile weight percent of carbonate in the < 2mm portion of the soils were found to have strong exponential relationships with time. The chronofunctions of these properties reveal higher rates of carbonate accumulation on older surfaces. These higher rates may represent an intrinsic threshold, where plugging of underlying basalts with silt and carbonate decreased infiltration capacities, causing an increase in the rate of carbonate accumulation in the overlying soil. Changes in the dust flux and/or composition, and differences in soil texture are considered and eliminated as other possible explanations for this difference. Overall rates of carbonate accumulation in soils <250 ka in the Potrillo volcanic field are comparable with those estimated in the Desert Project, and are probably more accurate estimates of the minimum rate of

carbonate accumulation in that area. The carbonate chronofunction for these soils appears to accurately predict surface age in the Potrillo volcanic field.

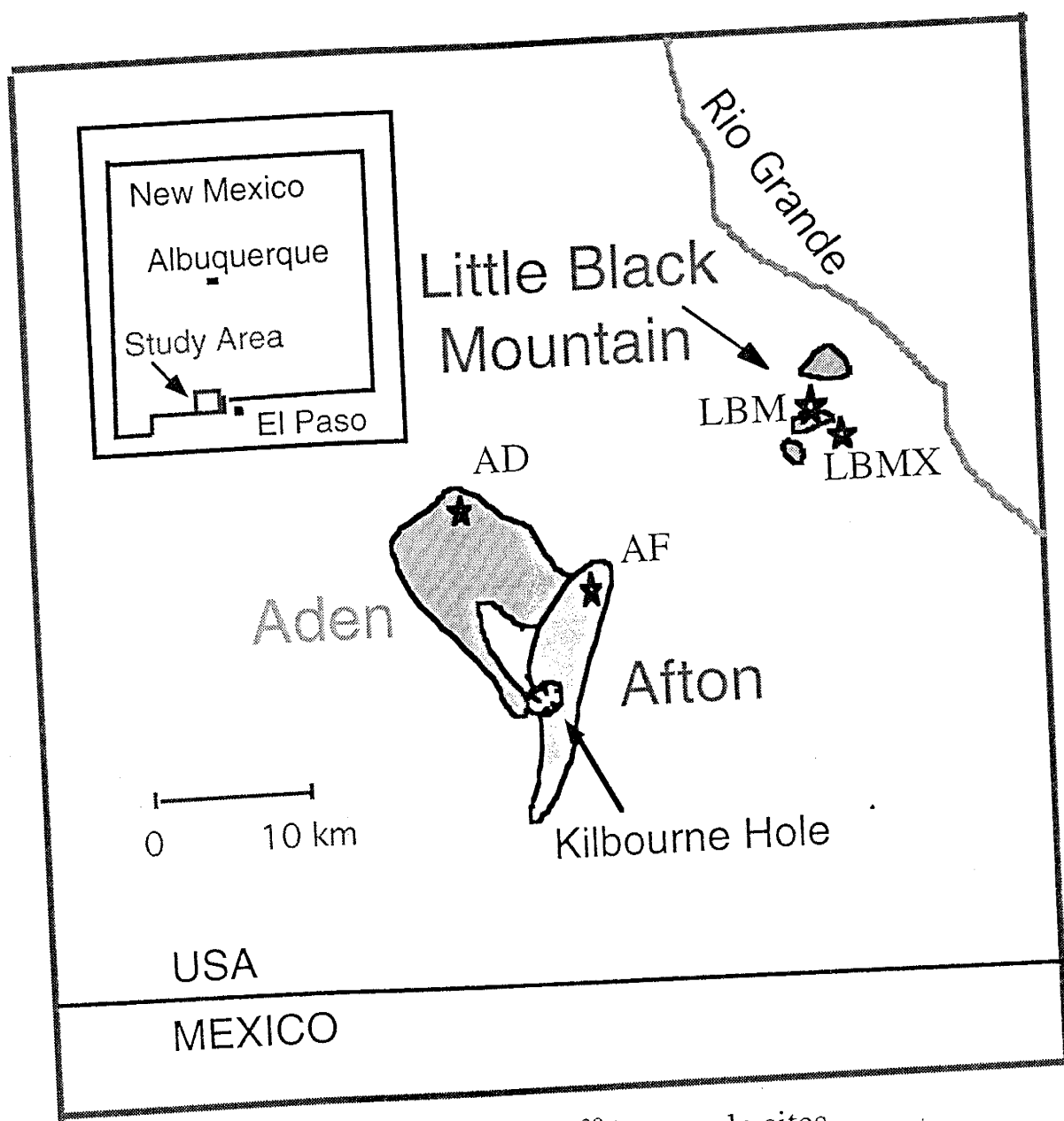
## INTRODUCTION

Soils are simple and effective tools for dating and correlating geomorphic surfaces. Use of soil chronosequences to accurately describe soil development has been limited, however, due to problems such as poor dating of geomorphic surfaces, too few soils on each surface, and spatial variability of soils on supposedly isochronous surfaces (Bockheim, 1980, Harrison et al., 1990, Harrison and Yaalon, 1992). Basalt flows in the Potrillo volcanic field have been well dated using  $^{40}\text{Ar}/^{39}\text{Ar}$  and cosmogenic  $^3\text{He}$  techniques. Furthermore, spatial variability of soils developing on basalt flows in the Potrillo volcanic field has been thoroughly described in a companion paper (Eppes and Harrison, 1996). Here, in hopes of more accurately describing rates of soil development in southern New Mexico, we discuss a soil chronosequence in which not only is good age control established, but also in which soil spatial variability is considered *before* the derivation of chronofunctions.

## THE POTRILLO VOLCANIC FIELD

*Geologic Setting*

The Potrillo volcanic field covers over 1000 square kilometers in southwestern Doña Ana County, New Mexico, in the axis of the Rio Grande rift, about 40 km southwest of Las Cruces (Fig. 1). The floor of the basin, the La Mesa surface, underlies the basalt flows of the Potrillo volcanic field and is ~500 ka in age (Gile et al., 1981). The climate of the Potrillo volcanic field is arid to semi-arid with an average precipitation of ~30 cm/yr (US Weather Service, 1996). Basalt flows in the Potrillo Volcanic field show little geochemical variation relative to the field as a whole. The field can be divided into three areas: the older Western Potrillos, a large strip of overlapping fissure-fed flows and cinder cones; the center of the field consisting of two younger flow complexes, Aden and Afton; and the eastern portion of the field, an alignment of cinder cones and associated flows including the Little Black Mountain area. Four well dated and clearly distinguishable flows were chosen for this study: Aden (AD), Afton (AF), and two flows from Little Black Mountain (LBM, and LBMX; Fig. 1).



★ Location of soil,  $^3\text{He}$ , and  $^{40}\text{Ar}/^{39}\text{Ar}$  sample sites

Figure 1: Location of study area, basalt flows, and sample sites in the Potrillo volcanic field.

Table 1: Summary of  $^{40}\text{Ar}/^{39}\text{Ar}$  and  $^3\text{He}$  age data for the AD, AF, LBM, and LBMX surfaces in the Potrillo volcanic field.

Sample #	Surface	Lat. and Long.	$^{40}\text{Ar}/^{39}\text{Ar}$ dates (ka)	$^3\text{He}$ dates (ka)	Age of Surface Avg. (ka)
-----	AD	-----	$13 \pm 11^*$	$24 \pm 3.5^\bullet$	$19 \pm 8$
-----	AF	-----	$70 \pm 14^*$	$103 \pm 5^\bullet$ $110 \pm 7^\bullet$ $94 \pm 15^\bullet$	$94 \pm 17$
-----	LBM	-----	$188 \pm 9^*$	-----	$184 \pm 5$
-----	"	-----	$167 \pm 21^*$		
nm1331	"	N 32 07 23.2	$186 \pm 9$		
nm1332	"	W 106 47 22.9	$179 \pm 17$		
nm1333	LBMX	N 32 07 23.2 W 106 47 22.9	$263 \pm 19$	-----	$263 \pm 19$

\* W. McIntosh et al., unpublished data

• E. Anthony et al., unpublished data

*Ages of Basalt Flows*

$^{40}\text{Ar}/^{39}\text{Ar}$  and  $^3\text{He}$  surface exposure dates have been obtained for basalt flows, maars, and cinder cones in the Potrillo volcanic field (E. Anthony et al., unpublished data; W. McIntosh et al., unpublished data). All age data are summarized in Table 1.  $^{40}\text{Ar}/^{39}\text{Ar}$  and  $^3\text{He}$  ages agree within  $1\sigma$  for the AD surface and  $2\sigma$  for the AF surface.  $1\sigma$  error represents approximately 15% of the age of younger surfaces and ~10% for older surfaces. Averages of age data are used for this study (Table 1).

Additional  $^{40}\text{Ar}/^{39}\text{Ar}$  ages for the LBM and LBMX flows were obtained for this study in the New Mexico Geochronological Research Lab (Table 1). Methods followed are those specified in McIntosh and Cather (1994). Three of the six samples yielded disturbed age spectra and large uncertainties on individual heating steps. They do not provide reliable eruption ages. The remaining three samples yielded good precision on individual steps and relatively flat spectra that met age plateau (Appendix 2). Furthermore, the ages obtained for the LBM flow in this study all agree within  $1\sigma$  with previous ages obtained for the same flows. Analytical methods and data for these six samples are summarized in Appendix 3.



## SPATIAL VARIABILITY OF SOILS

The relief of basalt flow topography in the Potrillo volcanic field is reduced with time. Young basalt surfaces (AD and AF) are extremely irregular with high relief. The older LBM and LBMX surfaces, however, are almost entirely covered in eolian deposits and are indistinguishable at the surface. Regardless of age, however, spatial variability of soils is significant depending on their position with respect to original flow topography. There is a dramatic contrast between soils developing on high points in original basalt flow topography (O.T.H. soils) and those soils developing on original topographic lows (O.T.L. soils) which are being filled or have been buried by eolian dust (Eppes and Harrison, 1996). This variability is similar to that observed on terrace treads in the Cajon Pass chronosequence, where soils developing in swales are distinct from soils developing on bars (Harrison et al., 1990).

Eppes and Harrison (1996) found that while O.T.L. soils in the Potrillos are developing primarily in a thick mantle of eolian material, O.T.H. soils are developing in the rubble zone overlying the basalt flow. Many O.T.L. soils contain one or more buried soils signifying that there have been changes in the regional dust flux. O.T.H. soils in the Potrillos are much less variable than O.T.L. soils. Similarly, in the Cajon Pass Chronosequence, bar soils are found to be less variable than soils

developing in swales (Harrison et al., 1990). While variation of O.T.H. soils is minimal, the variation of soils developing on low points in original basalt flow topography is large and complex. The size and shape of depressions was found to strongly influence hydrologic characteristics as well as the timing of surface stability resulting in much of the variability observed in the soils.

In terms of this chronosequence study, two important conclusions were made from the spatial variability study of soils in the Potrillo volcanic field: 1) There have been at least two changes in the dust flux in this area since ~90 ka, and 2) Given the complex variables affecting the development of the O.T.L. soils, O.T.H. soils should be employed for a soil chronosequence study of these surfaces (Eppes and Harrison, 1996).

## FIELD AND LABORATORY METHODS

Soils were examined on topographic highs for all four surfaces. Sites were assigned a unique designation (AD1, AD2, etc.). Sites were selected by the degree of desert pavement development. As soils may vary as a function of their distance from the boundary of flow (Slate et al., 1991), all sites were located within 0.5 km of the perimeter of flows. The bottom of all pits is a very coarse interlocking basalt rubble, assumed to be the top of the flow. All pits were described using methods summarized by the Soil Survey Staff (1951, 1975) and then sampled for laboratory analyses.

Average carbonate rind thickness and volume percent of gravels was estimated for each horizon. The following analyses were performed on each sample: bulk density, pH, soluble salts (by electrical conductivity), particle size, and  $\text{CaCO}_3$  of the  $<2\text{mm}$  portion. Standard procedures were used in all of these analyses (Singer and Janitzky, 1986). Normalized profile percents of  $<2\text{mm}$   $\text{CaCO}_3$ , and the profile mass of carbonate were calculated.

### *Calculation of profile mass of carbonate*

The profile mass of carbonate of a soil is usually calculated using the fine earth portion of a sample (e.g., Gile et al., 1981, Machette, 1985, Slate et al., 1991). However, in coarse deposits a significant amount of carbonate is found in clast coatings, and estimates of this volume of  $\text{CaCO}_3$  are required to quantitatively determine the profile mass of carbonate in a soil (McDonald, 1994). The following equation was used to calculate the total mass of  $\text{CaCO}_3$  in each sample:

$$\{BD_s * \%C_s * (1 - \%G) + (GR - RT) * \%R * BDC\} * HT$$

$BD_s$  = Bulk density of the < 2mm portion of sample

$\%C_s$  = weight percent of  $\text{CaCO}_3$  in the <2mm portion of sample

$\%G$  = volume percent of gravels in each horizon

$GR$  = average total clast volume in each horizon

$RT$  = average horizon clast volume excluding the  $\text{CaCO}_3$  rind thickness.

$\%R$  = volume percent of  $\text{CaCO}_3$  rind in each horizon

$BDC$  = average bulk density of  $\text{CaCO}_3$  rinds

$HT$  = horizon thickness

The horizon mass of  $\text{CaCO}_3$  in the < 2mm portion of the sample was also calculated using bulk density and horizon thickness. These values were then summed for each profile to obtain profile mass of carbonate for the entire soil. To aid in comparing soils of different depths, the thickness of

all bottom horizons was normalized to a height of 10 cm in O.T.H. soils, and 20 cm in O.T.L. soils. It should be noted that the loss of  $\text{CaCO}_3$  out through the bottom of these soils was not accounted for by the profile mass of carbonate calculations (see discussion).

Table 2: Soil Field Descriptions

Soil	Age (-ka)	Hor.	Depth (cm)	Structure, Texture	Consistence moist dry	Color moist dry	roots, boundaries	gravel %; pores	Carbonates
AD2	19	A B Bk	0-3 3-9 9-23	3 m sbk SIL 2 f-m sbk SIL .5 f sbk SL	so ps sh ss ps sh so ps sh	7.5yr 4/3 8.75yr 3/3 7.5yr 3/2	2vf, c s 2f, ci 0, a s	40; 2vf, 1f 10; 1f 70; 0	no evident slight fiz coats fractures
AD3	19	A B Bk Ck	0-4 4-11 11-20 23-34	2 m sbk SIL 1 m sbk SIL 2 m sbk SIL 1 m sbk SICL	so ps sh ss ps sh ss ps sh s p sh	8.75yr 3/3 7.5yr 4/4 7.5yr 3/4 7.5yr 3/3.5	2vf, c s 1vf, 1m, 1c, ci 2vf, ci 1vf, 1f, 0	60; 2f 20; 1f <5; 1f <10; 1f	no evident slight fiz coats fractures strong fiz
AD4	19	A B Bk Ck	0-5 5-15 15-28 20-40	1 m sbk SIL 1 m sbk SIL 2 f sbk SIL .5 f sbk SICL	so ps sh ss ps sh ss ps sh s p sh	7.5yr 3/3.5 7.5yr 3/4 7.5yr 3/4 7.5yr 4/4	1vf, c s 1f, ci 1f, ci 1f, 1m, 0	60; 1f 10; 1f 70; 1f 90; 1f	no evident slight fiz coats fractures strong fiz
AF4	94	A B Bk Ck	0-3 3-10 10-46 46-55	1 m sbk SL 2 m sbk SIL 1 f sbk SIL 1 m sbk SICL	so po sh so ps sh ss ps sh ss p sh	7.5yr 3/3 7.5yr 4/4 7.5yr 4/4 7.5yr 4/6	2vf, c s 2vf, ci 1vf, ci 1vf, 0	45; 1f 10; 1f 75; 0 70; 0	no evident slight fiz coats fractures along vert. fractures
AF5	94	A B K Rk	0-1 1-9 9-18 18-28	.5 vf sbk SL 2.5 m sbk CL .5 f sbk CL	so po so s p sh-h ss-s po so-sh	7.5yr 4/6 5yr 4/4 7.5yr 3/4	1vf, a s 2vf, 1f, 1c, c s 1m, 8 i 0, 0	>75; 1f 25; 1f 75; 0	no evident coats on bottoms of some clasts; no matrix fiz Stage 1+; clasts go deeper along fractures; coats entire clasts; in all pores
AF6	94	A Bt Ck R	0-1 1-15 15-21 21-31	1 f sbk LS 1.5 f-m sbk L 1 f sbk SIL	so po sh ss ps sh-h ss ps sh	7.5yr 3/3.5 5yr 4/4 6.75yr 4/4	1vf, a s 1vf, 1f, 1c, c s 0, g i	20; 1f 15; 1f 75	no evident no evident carbs in pores only
LBM1	184	A B Bk K	0-3 3-11 11-26 26-48	sg LS 2 m sbk LS 1 f sbk LS .5 f sbk SL	so ps lo so ps sh so po sh so ps sh	7.5yr 4/3 7.5yr 4/4 7.5yr 4/3 7.5yr 4/3	0, a s 2f, c s 1f, 1m, c s 2f, c w	10 <5 10 70	slight fiz under clasts covers clasts Stage II
LBM2	184	A Bk K Rk	0-2 2-25 25-40 40-53+	sg S 1 f sbk LS .5 f sbk LS	so po lo so po sh so po sh	7.5yr 4/4 7.5yr 5/4 7.5yr 5/4	0, c s 3vf, g w 0, c w	10 <10 75	coats small clasts coats all clasts Stage II
LBM31	184	A Bk Bk2	0-4 4-12 12-25	1.5 f-m sbk LS 2 m-c sbk LS-SL 1.5 m-c sbk LS	so po so-sh so po sh so po so-sh	7.5yr 4/3 7.5yr 5/3.5 7.5yr 4/4	1vf, c s 1vf, 1f, 1c; c/g s 0, c s	10 <5 5	moderate fiz in matrix; visible on clasts at surface strong fiz; visible on ped faces; along roots; slight coat on clasts coatings on entire clasts; 1-3 mm; carbonate granules in matrix

Table 2 cont.: Soil Field Descriptions

Soil	Age (-ka)	Hor.	Depth (cm)	Structure, Texture	Consistence	Color	roots; boundaries	gravel %; pores	Carbonates
LBM32 184		K	25--40	.5 f sbk	L so po so	moist 8.75yr 5/4 dry 7.5yr 6/4	2.5 f, 2.5m, 8.75yr 5/4	75	Stage 2+; 2-5mm coats on clasts, laminar in areas
		A	0--5	1 f sbk	S so po so	7.5yr 4/4 7.5yr 4/4 7.5yr 4.5/6	1vf; c s 1f; c s 1f, 1c; c s	<5 10	no fiz no fiz; slight (<1mm) coat on clasts
		Bk	5--18	2 m sbk	LS so po sh	7.5yr 4/4 7.5yr 4/4 7.5yr 4.5/6	1f, 1c; c s 1f, 1c; c s	30	stage 2+ in areas where there are smaller clasts; 2-5 mm coats
		K	18--47	sg	LS so-ss pc lo	7.5yr 4/6 7.5yr 5/4	8.75yr 5/4 8.75yr 5/4		
LBMX-1 263		Rk	47--58				8.75yr 5/4 8.75yr 5/4		Carbonate along fractures 1-2 mm coatings
		A	0--5	sg	S so po lo	7.5yr 4/4 7.5yr 4/4 7.5yr 7/6	0; a w 1f; a w	<5	coats small clasts
		Bj	5--25	2 m sbk	LS so po sh	10yr 4/4 10yr 6/5	1f; a w	<5	slight fiz
		K	25--70	1 f gr	LS so po	7.5yr 4/4 7.5yr 6/4	0; g i	75	Stage II
LBMX-2 263		K	70--90	1 f gr	S so po	10yr 6/3 10yr 7/3	0; -	80	Stage III
		A	0--5	1 f sbk	S so po so	7.5yr 4/6 7.5yr 6/4 7.5yr 6/5	1vf; c s 1.5m, 2vf,	10	coats bottoms of clasts at surface; fiz throughout
		B	5--18	2 m sbk	S so po sh	7.5yr 4/5 7.5yr 6/5	1f; a s	<10	fiz throughout, filaments and flakes
		K2	18--58	.5 vf sbk	LS so-ss pc so	7.5yr 5/4 7.5yr 5/4 7.5yr 5.5/4	2f; 1c; c s	75	Stage 3; coats all clasts 2-5 mm
I		K2	58--102	sg	LS so-ss pc lo	7.5yr 5/3 7.5yr 7/4	1f; 1m; c s	75	Stage 2; not as indurated as K; 1-2 mm coats on clasts
		CK	102--116	sg	LS so-ss pc lo	7.5yr 6/3 7.5yr 7/3	0; 0	60	Coatings on most clasts (1-<1mm); less carbs in matrix.

## ABBREVIATIONS STRUCTURE

sg = single grain

f = fine

m = medium

c = coarse

gr = granular

sbk = subangular/blocky

## TEXTURE

S = sand

C = clay

L = loam

SL = sandy loam

LS = loamy sand

SIL = silty loam

SCL = sandy clay loam

SC = sandy clay

SIC = silty clay

## CONSISTENCE

so = non sticky

ss = slightly sticky

s = sticky

po = non plastic

ps = slightly plastic

p = plastic

sh = slightly hard

h = hard

vh = very hard

## ROOTS/BOUNDARIES

vf = very fine

f = fine

m = medium

c = coarse

a = abrupt

c = clear

g = gradual

s = smooth

w = wavy

i = irregular

## RESULTS AND DISCUSSION

### *Rates of Carbonate Accumulation in the Potrillo Volcanic Field*

Examination of soil data in the Potrillo volcanic field revealed that most soil properties show some overall increase or decrease with time (Table 2). However, a strong exponential relationship exists between time and both profile mass of carbonate ( $r^2 = .94$ ) and normalized profile weight percent of  $\text{CaCO}_3$  ( $r^2 = .69$ ; Fig. 2). Plotting the same data as a linear/linear function more clearly reveals that the LBM and LBMX surfaces have significantly higher rates of carbonate accumulation than the AD and AF surfaces. A number of options exist as explanations for these differences in the rates of carbonate accumulation in Potrillo soils. Changes in the dust flux or composition, differences in soil texture, or the crossing of some type of intrinsic threshold in older soils, are considered here as possible explanations for the differences in carbonate accumulation in soils developing in the Potrillo volcanic field.

### **Intrinsic Thresholds**

Many workers have recognized both intrinsic and extrinsic thresholds in soils, where constant processes affecting soil profiles produce dramatic changes in the rates of soil development (e.g., Birkeland, 1984;



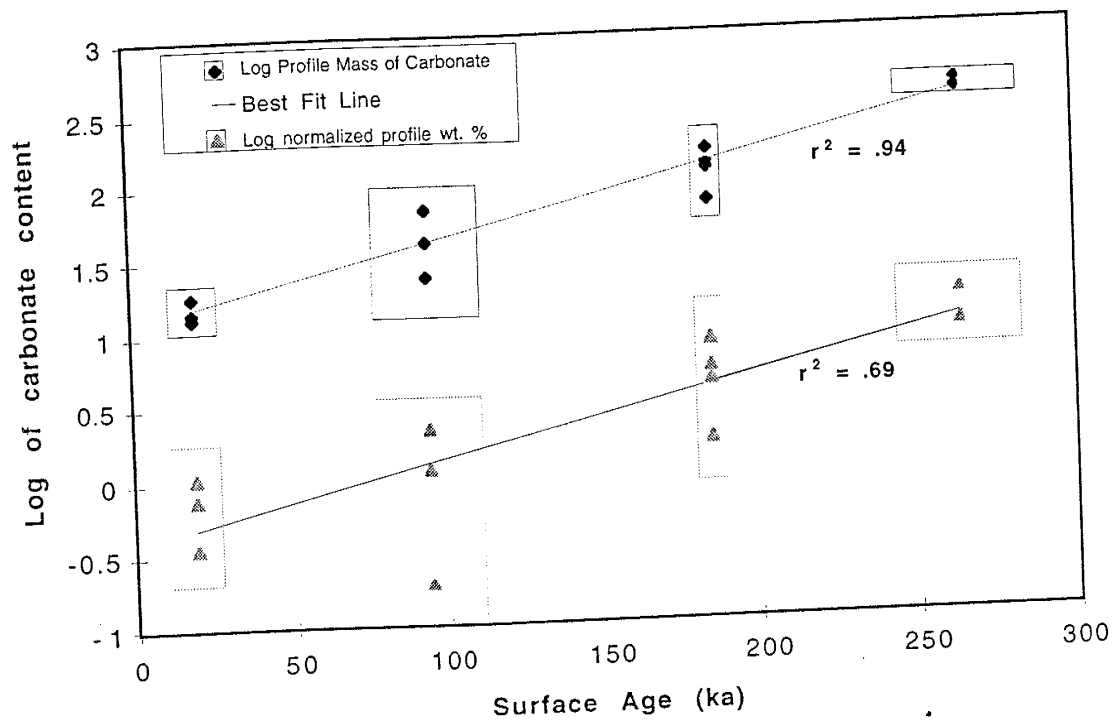


Figure 2: Chronofunctions of the log of carbonate content (profile mass and normalized profile weight percent of  $\text{CaCO}_3$ ). Boxes represent analytical error for single points and  $1\sigma$  error for multiple points.

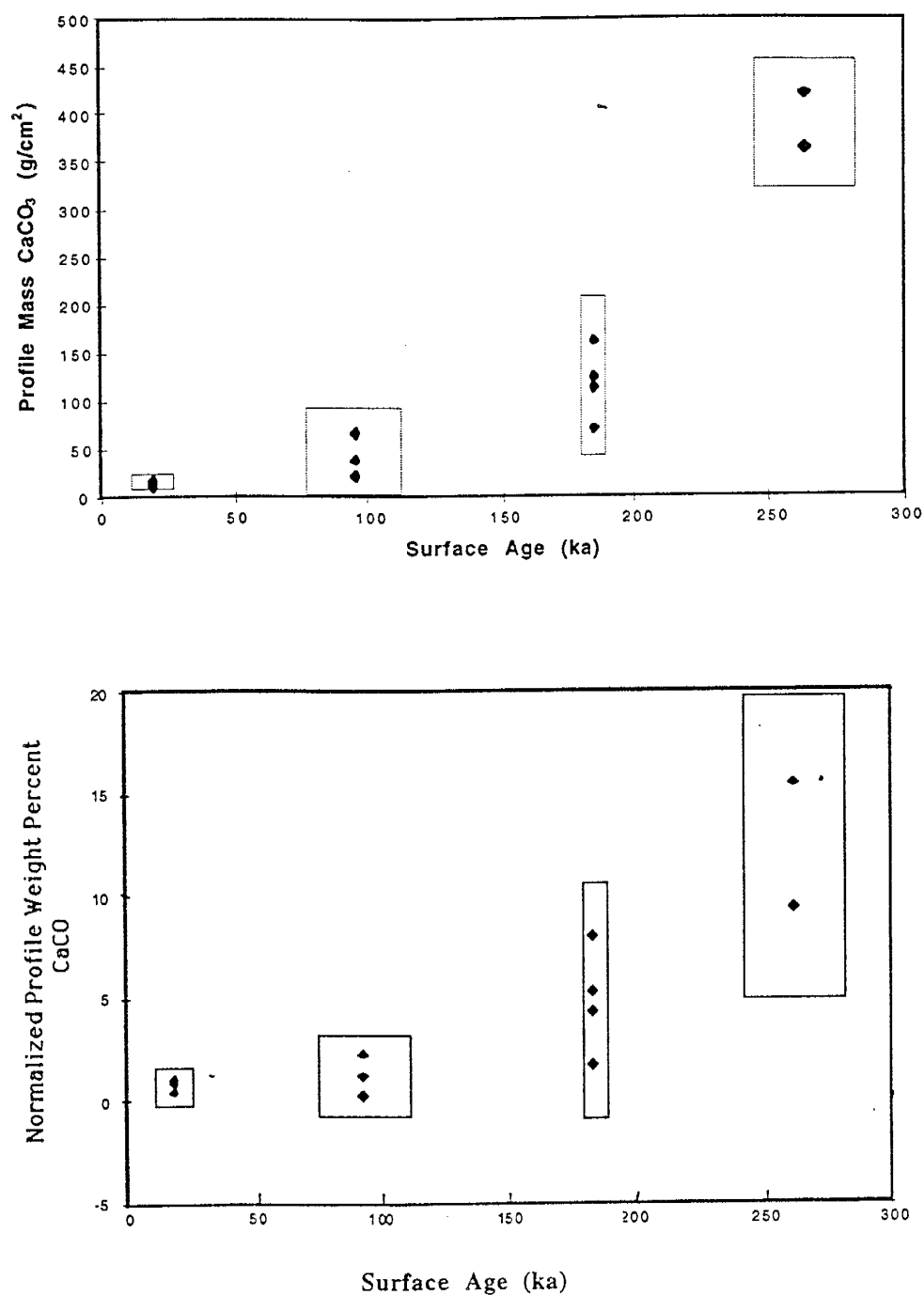


Figure 3: Graphs of profile mass of  $\text{CaCO}_3$  and normalized profile weight percent of  $\text{CaCO}_3$  in the <2mm portion of sample vs surface age for soils developing on basalt flows of different ages in the Potrillo volcanic field. Boxes represent analytical error for single points and  $1\sigma$  error for multiple points.

McFadden, 1987). McFadden et al. (1987) attributed an increase in rates of soil development in the Cajon Pass chronosequence to a change in soil infiltration capacities induced by plugging of horizons by silt. Additionally, Gile et al. (1966, 1981) recognized that infiltration capacities of soils can be greatly reduced by accumulation of carbonate in lower horizons. Vesicles and fractures in the basalt underlying soils on LBM and LBMX surfaces in the Potrillo volcanic field are completely filled with carbonate and eolian dust. It is possible that an intrinsic threshold, caused by a plugging of basalt flows, is crossed in the LBM and LBMX soils resulting in an increase in the rate of carbonate accumulation in these soils. Carbonate and eolian dust accumulating in the basalts of the Potrillos could have combined to produce a change in infiltration capacities similar to that seen by Gile et al. (1966, 1981) and McFadden et al. (1987). Chloride concentrations in O.T.L. soils on all surfaces provide evidence that water can flow out of these soils and down through the basalt (Eppes and Harrison, 1996). Eventually, however, in O.T.H. soils, these fractures and vesicles become plugged with loess and carbonate. It is likely that this plugging effectively reduces the infiltration capacity of the basalts. This change in infiltration capacity is evidenced by the presence of carbonate laminae on the top surface of basalt clasts in the bottom of pits, suggesting a lateral rather than vertical movement of water through the basalt. The water holding capacity of the overlying soil is thus increased, consequently

increasing carbonate accumulation in upper horizons. An intrinsic threshold is reached when this occurs, effectively increasing the rate of development of soils on the LBM and LBMX surfaces in the Potrillos and resulting in the higher rates of carbonate accumulation evident in the chronofunction.

#### A changing dust flux or composition

Though intrinsic thresholds provide one possible explanation for the higher rates of carbonate accumulation on the LBM and LBMX surfaces, other possible explanations are considered. Many workers have proposed that changes in the magnitude of dust flux affect soil development (e.g., Bockheim, 1980, Gile et al., 1981, Machette, 1985, McFadden and Tinsley, 1985). An abrupt shift in the rate of development of soils in the Cima volcanic field was found to be related to changes in the dust flux (McFadden, 1986). Carbonate in desert soils is introduced via eolian material. Were there higher rates of dust deposition in the past, it follows that rates of carbonate accumulation could also have been higher.

If the difference in  $\text{CaCO}_3$  accumulation rates in the Potrillos was a result of a change in dust flux, one would expect to see evidence of this influence in the soils. A buried soil found in O.T.L. profiles on the AF surface indicates that there has been at least two major changes in the dust flux in the Potrillo volcanic field since ~90 ka (Eppes and Harrison, 1996).

However, no change in dust flux appears to be morphologically recorded in any soils developing on topographic highs. Furthermore, the changes in dust flux recorded in the O.T.L. soils occurred after ~90 ka, while the higher rates of carbonate accumulation are found in surfaces older than 90 ka. If the change in dust flux which occurred after ~90 ka affected the rates of carbonate accumulation, we would expect to see higher rates in the AF surfaces as well. The fact that carbonate accumulation rates are not significantly high for the AF surface suggests that the dust flux is not the cause of higher carbonate accumulation rates on the LBM and LBMX surfaces.

It should be noted that though O.T.H. soils do not seem to be affected by a change in dust flux in the Potrillos, it is possible that changes through time in the dust composition with respect to carbonate could have resulted in differences in carbonate accumulation rates for surfaces of different ages. Such changes, however, could generally only be recognized by detailed geochemical study, and would be difficult if not impossible to recognize in the scope of this paper.

### Textural differences between surfaces

Another possible explanation for differing rates of carbonate accumulation between surfaces in the Potrillos might be found in textural

differences between the AD/AF soils and the LBM/LBMX soils. Sand content of LBM and LBMX soils is significantly higher than that of AD and AF soils (Table 2). Little Black Mountain is located in close proximity to the Rio Grande, a major potential source of sand in the area (Fig. 1). The sandier nature of these soils is probably a result of differences in parent material, where LBM and LBMX receive higher amounts of sand than do AD and AF due to their proximity to the Rio Grande. Although these older soils have different textures than younger soils, given that sandy soils are generally less likely to accumulate carbonates than clay rich soils, it is unlikely that the higher rates of carbonate in the LBM and LBMX soils are a function of their texture.

*Carbonate Accumulation Rates:  
Correlations With Other Chronosequence Studies*

Because the chronofunction derived for carbonate accumulation in the Potrillo volcanic field is more accurate than others derived in New Mexico and the desert southwest, it is likely that the rates of carbonate accumulation derived from this study will also be more accurate. Many workers have estimated rates of carbonate accumulation for soils in the desert southwest (e.g., Gile et al., 1981, Machette, et al., 1985, Harden et al., 1991, Reheis et al., 1995). The Desert Project (Gile et al., 1981) is the geographically closest of these studies. However, age constraints in the

Desert Project are poor with tens of thousands of years uncertainty for any one surface. Consequently, rates of carbonate accumulation calculated for the Desert Project range from 1-12 g/m<sup>2</sup>/yr. for soils younger than ~250 ka.

Average carbonate accumulation rates in the Potrillo volcanic field were calculated to be around  $6 \pm 2$  g/m<sup>2</sup>/yr. for surfaces that are less than ~260 ka in age. (The LBMX surface has rates of  $\sim 15 \pm 2$  g/m<sup>2</sup>/yr.) Given that some unknown amount of carbonate is lost into the basalt for the AF and LBM surfaces, it is likely that the average is an underestimation of the actual rate. However in AD soils, carbonate appears to be confined to a narrow strip within the rubble zone (Eppes and Harrison, 1996). Were carbonate being lost through the bottom of these soils, one would expect to see it deposited along the entire profile. This suggests that only minimal amounts, if any, are being lost through the bottom of the AD profiles. It is likely, therefore, that the actual rate of carbonate accumulation for surfaces younger than ~260 ka in the Potrillos is closer to that of the AD soils (i.e., 8 g/m<sup>2</sup>/yr.) than to the average of the rates for the three surfaces.

Rates of accumulation on younger surfaces calculated in this study fall within the range of those calculated in the Desert Project. Given that ages of surfaces in the Potrillos are much more accurate, these rates are a more accurate estimation of the minimum rate of carbonate accumulation

for soils in this area. There is a large discrepancy, however, between the rate of carbonate accumulation calculated for older soils in the Desert Project (~2-3 g/m<sup>2</sup>/yr.) and that of the LBMX soil of this study (~15 g/m<sup>2</sup>/yr.). Other studies, however, have found similar rates of carbonate accumulation in mid-late Pleistocene soils in New Mexico and southern Utah (Machette, 1985: 14-51 g/m<sup>2</sup>/yr.; Harden et. al., 1991: 14-26 g/m<sup>2</sup>/yr.) suggesting that rates calculated for older surfaces in the Desert Project are underestimated.

*Predicting Basalt Ages in the Potrillo Volcanic Field  
Using Carbonate Chronofunctions*

The ultimate goal in any chronosequence study is to be able to use the knowledge gained in that study to predict ages of undated surfaces using soil properties. Obtaining <sup>40</sup>Ar/<sup>39</sup>Ar or cosmogenic <sup>3</sup>He ages of basalts is an expensive and time consuming prospect. Soils, however, offer a relatively simple and inexpensive alternative to these geochemical methods. Given the relatively small amount of variability seen in the O.T.H. soils examined for this study, as well as the small error in the chronofunctions themselves, it is not unreasonable to assume surface ages for basalts in the Potrillo volcanic field can be accurately predicted using soils data.

Data for both the normalized profile percent of CaCO<sub>3</sub> in the fine portion of samples as well as the profile mass of carbonate chronofunctions



are relatively easy to obtain. However, calculations of profile mass of carbonate are considerably more complicated, making them a somewhat less attractive tool. Eppes and Harrison, (1995) used a chronofunction derived from preliminary data of normalized profile percent of carbonate and estimated an age for the LBMX surface of ~250 ka. This age falls within  $1\sigma$  of a later obtained  $^{40}\text{Ar}/^{39}\text{Ar}$  age of  $263 \pm 19$  ka for this surface.

## CONCLUSIONS

O.T.H. soils can be used with some confidence for soil chronosequence studies. The carbonate chronofunctions derived for O.T.H. soils in the Potrillos have an exponentially increasing trend through time with higher rates of carbonate accumulation for the LBM and LBMX surfaces. The higher rates of carbonate accumulation are possibly a result of the crossing of an intrinsic threshold within the soils. Underlying basalt became indurated with carbonate and silt decreasing the amount of carbonate flushed through the basalt and increasing the rate of carbonate accumulation in overlying horizons. Carbonate chronofunctions do not seem to reflect the changes in the dust flux which occurred sometime after ~90 ka. Accuracy of the chronofunction produced was greatly increased by first understanding the spatial variability of soils. Despite the changes in rates of carbonate accumulation, soil  $\text{CaCO}_3$  appears to be a relatively accurate predictor of the age of basalt surfaces in the Potrillo volcanic field.

## REFERENCES

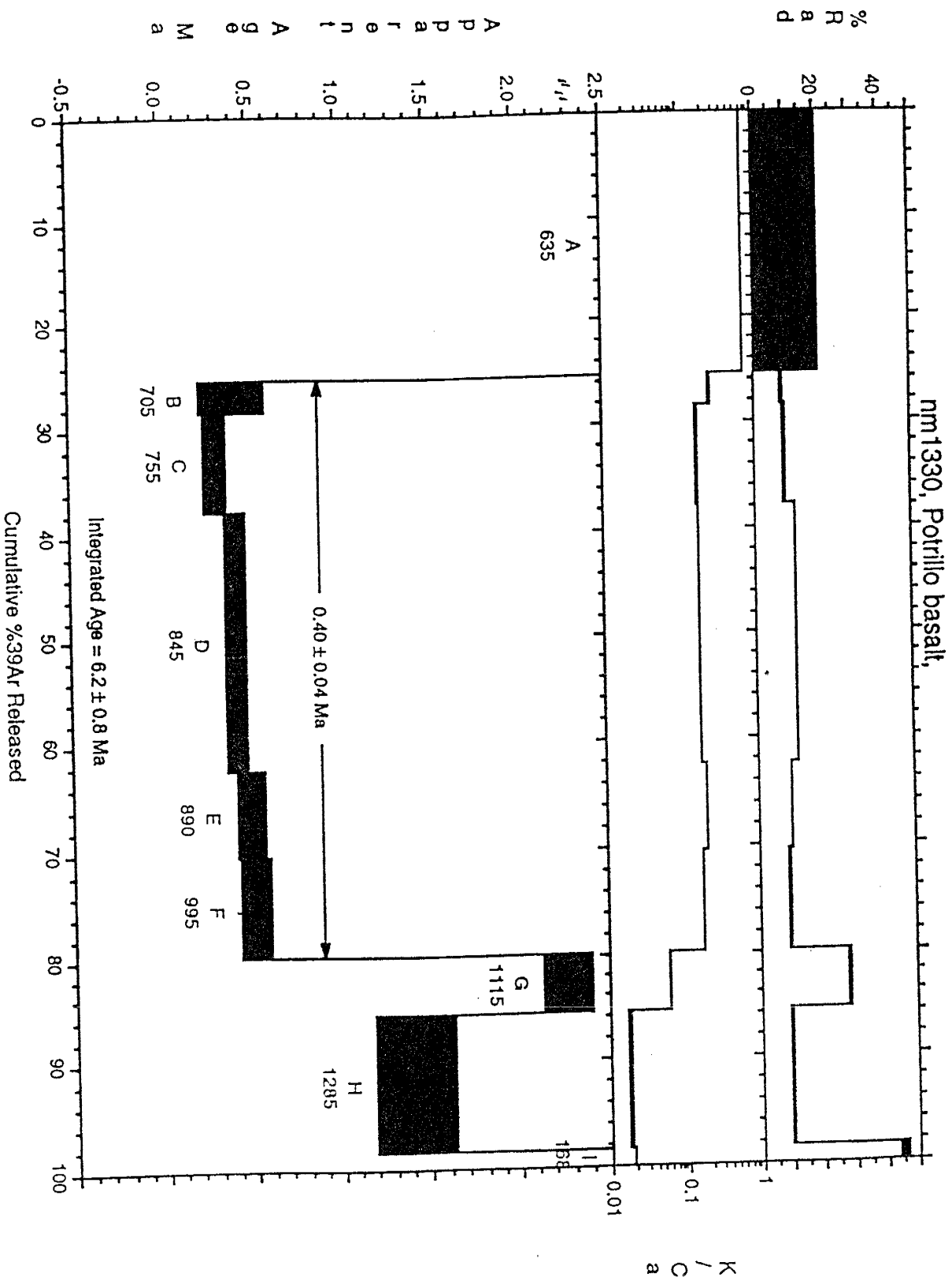
- Anthony, L., Poths, J., 1992.  $^3\text{He}$  surface dating and its implications for magma evolution in the Potrillo volcanic field, Rio Grande Rift, New Mexico, USA. *Geochimica et Cosmochimica*, 56: 4105-4108.
- Birkeland, P., 1984. *Soils and Geomorphology*. Oxford University Press, New York.
- Bockheim, J., 1980. Solution and use of chronofunctions in studying soil development. *Geoderma*, 24: 71-85.
- Cerling, T., 1990. Dating Geomorphologic Surfaces Using Cosmogenic  $^3\text{He}$ . *Quaternary Research*, 33: 148-156.
- Eppes, M., Harrison, B., 1996. A chronosequence study of soils developing on basalt flows in an arid environment; the Potrillo volcanic field, Dona Ana County, New Mexico. Geological Society of America 1995 Annual Meeting, Abstracts with Programs, 27: 57.
- Eppes, M., Harrison, B., 1996. Spatial variability of soils developing on basalt flows in the Potrillo volcanic field, southern New Mexico: Prelude to a chronosequence study. Unpublished.
- Gile, L., Peterson, F., Grossman, R., 1966. Morphological and genetic sequences of carbonate accumulation in desert soils. *Soil science*, 101: 347-360.
- Gile, L., Hawley, L., Grossman, R., 1981. Soils and geomorphology in the Basin and Range area of southern New Mexico-Guidebook to the Desert Project. New Mexico Bureau of Mines and Mineral Resources Memoir 39.
- Harden, J., Taylor, E., Hill, C., Mark, R., McFadden, L., Reheis, M., Sowers, J., Wells, S., 1991. Rates of soil development from four soil chronosequences in the southern Great Basin. *Quat. Res.*, 35: 383-399.
- Harrison, J., McFadden, L., Weldon, R., 1990. Spatial soil variability in the Cajon Pass chronosequence: implications for the use of soils as a geochronological tool. *Geomorphology*, 3: 399-416.
- Hoffer, J., 1976. Geology of Potrillo basalt field, south-central New Mexico. New Mexico Bureau of Mines and Mineral Resources Circular 149.
- Liu, B., Phillips, F., Hoines, S., Campbell, A., Sharma, P., 1994. Water movement in desert soil traced by hydrogen and oxygen isotopes, chloride, and chlorine-36, southern Arizona. *Journal of Hydrology*, 168: 91-110.

- Machette, M., 1985. Calcic soils of the southwestern United States, in Weide, D., ed., *Soils and Quaternary Geomorphology of the Southwestern United States: Geological Society of America Special Paper 203*: 1-21.
- McDonald, E., 1994. The relative influences of climatic change, desert dust, and lithologic control on soil-geomorphic processes and hydrology of calcic soils formed on Quaternary alluvial-fan deposits in the Mojave Desert, California. Ph.D. Dissertation, University of New Mexico, 383 pp., unpublished.
- McDougall, I., Harrison, M., 1988. *Geochronology and Thermochronology by the  $^{40}\text{Ar}/^{39}\text{Ar}$  Method*. Oxford University Press, New York.
- McFadden, L., Tinsley, J., 1985. The rate and depth of pedogenic carbonate accumulation in soils: Formation and testing of a compartment model.
- McFadden, L., Wells, S., Dohrenwend, J., 1986. Influences of Quaternary climatic changes on processes of soil development on desert loess deposits of the Cima volcanic field, California. *Catena*, 13: 361-389.
- McFadden, L., Weldon, R., 1987. Rates and processes of soil development on Quaternary terraces in Cajon Pass, California. *Geo. Soc. Am. Bull.*, 98: 280-293.
- McIntosh, W., Cather, S., 1994.  $^{40}\text{Ar}/^{39}\text{Ar}$  Geochronology of basaltic rocks and constraints on late Cenozoic stratigraphy and landscape development in the Red Hill-Quemado area, New Mexico. *New Mexico Geological Society Guidebook, 45th Field Conference, West-Central New Mexico and East-Central Arizona*.
- Muir, J., Logan, J., 1982. Eluvial/illuvial coefficients of major elements and the corresponding losses and gains in three soil profiles. *Jour. Soil Sci.*, 33: 295-308.
- Murphy, E., Ginn, T., Phillips, J., 1996. Geochemical estimates of paleorecharge in the Pasco Basin: Evaluation of the chloride mass balance technique. *Water resources research*, 32-9: 2853-2868.
- Phillips, F., 1994. Environmental Tracers for Water Movement in Desert Soils of the American Southwest. *Soil Sci. Soc. Am. Jour.*, 58-1: 15-24.
- Reheis, M., Sowers, J., Taylor, E., McFadden, L., Harden, J., 1992. Morphology and genesis of carbonate soils on the Kyle Canyon fan, Nevada, U.S.A. *Geoderma*, 52: 303-342.
- Scanlon, B., 1991. Evaluation of moisture flux from chloride data in desert soils. *Journal of Hydrology*, 28: 137-156.

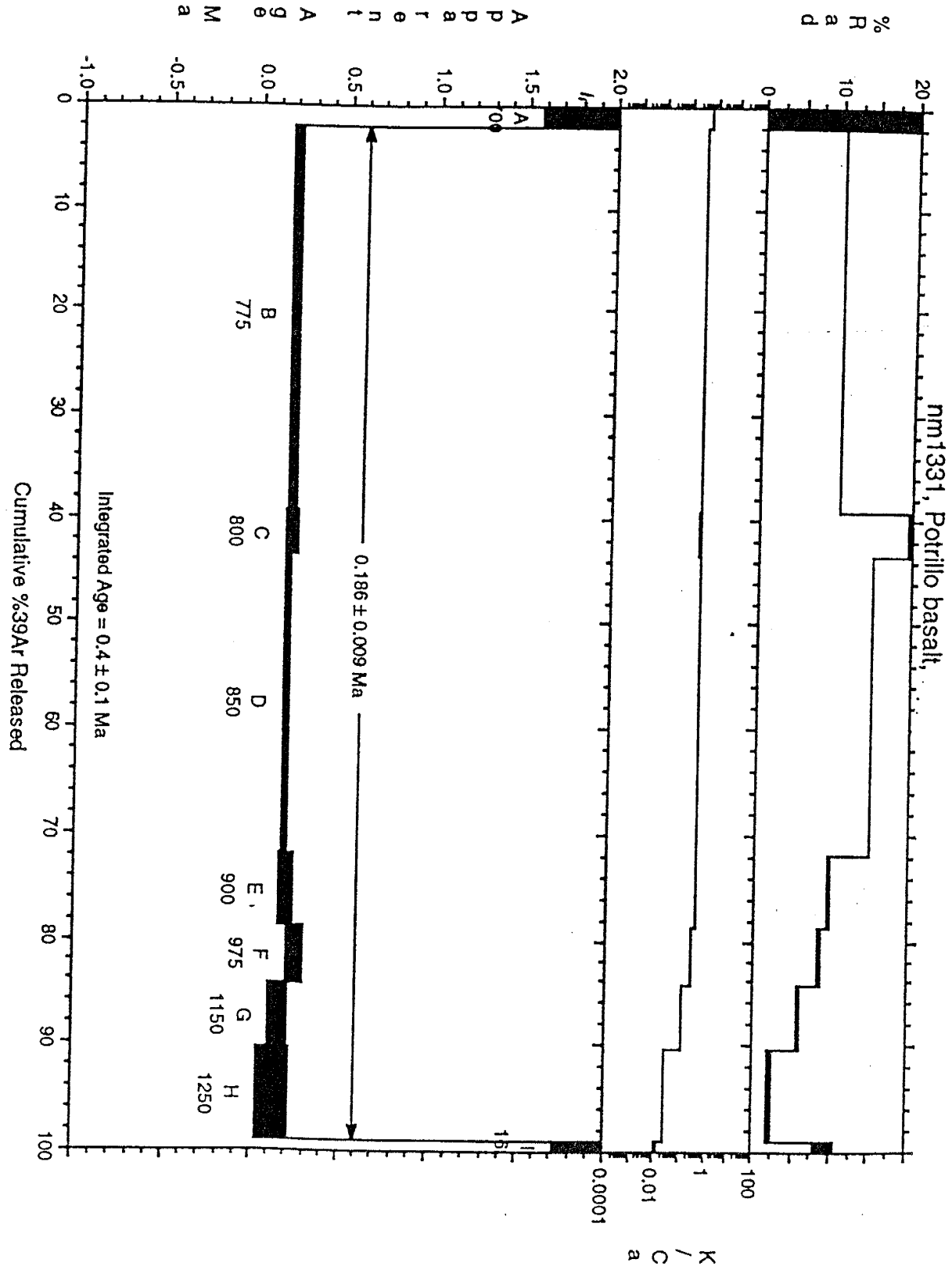
- Singer, M, Janitzky, P., (Eds.) 1986. Field and laboratory procedures used in a soil chronosequence study. Bulletin 1648. U.S. Geological Survey, Denver, CO.
- Slate, J., Bull, W., Ku, T., Shafiqullah, M., Lynch, D., Huang, Y., 1991. Soil-Carbonate genesis in the Pinacate volcanic field, northwestern Sonora, Mexico. *Quat. Res.*, 35: 400-416.
- Soil Survey Staff, 1951. Soil survey manual: Washington, D.C., U.S. Department of Agriculture and U.S. Government Printing Office, Agricultural Handbook 18.
- Soil Survey Staff, 1975. Soil taxonomy: Washington, D.C., W.S. Department of Agriculture and U.S. Government Printing Office, Agriculture Handbook 436.
- Switzer, P., Harden, J., Mark, R., 1988. A statistical method for estimating rates of soil development and ages of geological deposits: A design for soil chronological studies. *Math. Geol.*, 20: 49-61.
- United States Weather Bureau, Climatological summary for Las Cruces, New Mexico: Albuquerque, U.S. Department of Commerce.
- Weitkamp, W., Graham, R., Anderson, M., Amrhein, C., 1996. Pedogenesis of a Vernal Pool Entisol-Afisol-Vertisol Catena in Southern California. *Soil Sci. Soc. Am. Jour.*, 60-1: 323.
- Wells, S., Dohrenwend, J., McFadden, L., Turrin, B., Mahrer, K., 1985. Late Cenozoic landscape evolution on lava flow surfaces of the Cima volcanic field, Mojave Desert, California. *Geo. Soc. Am. Bull.*, 96: 1518-1529.

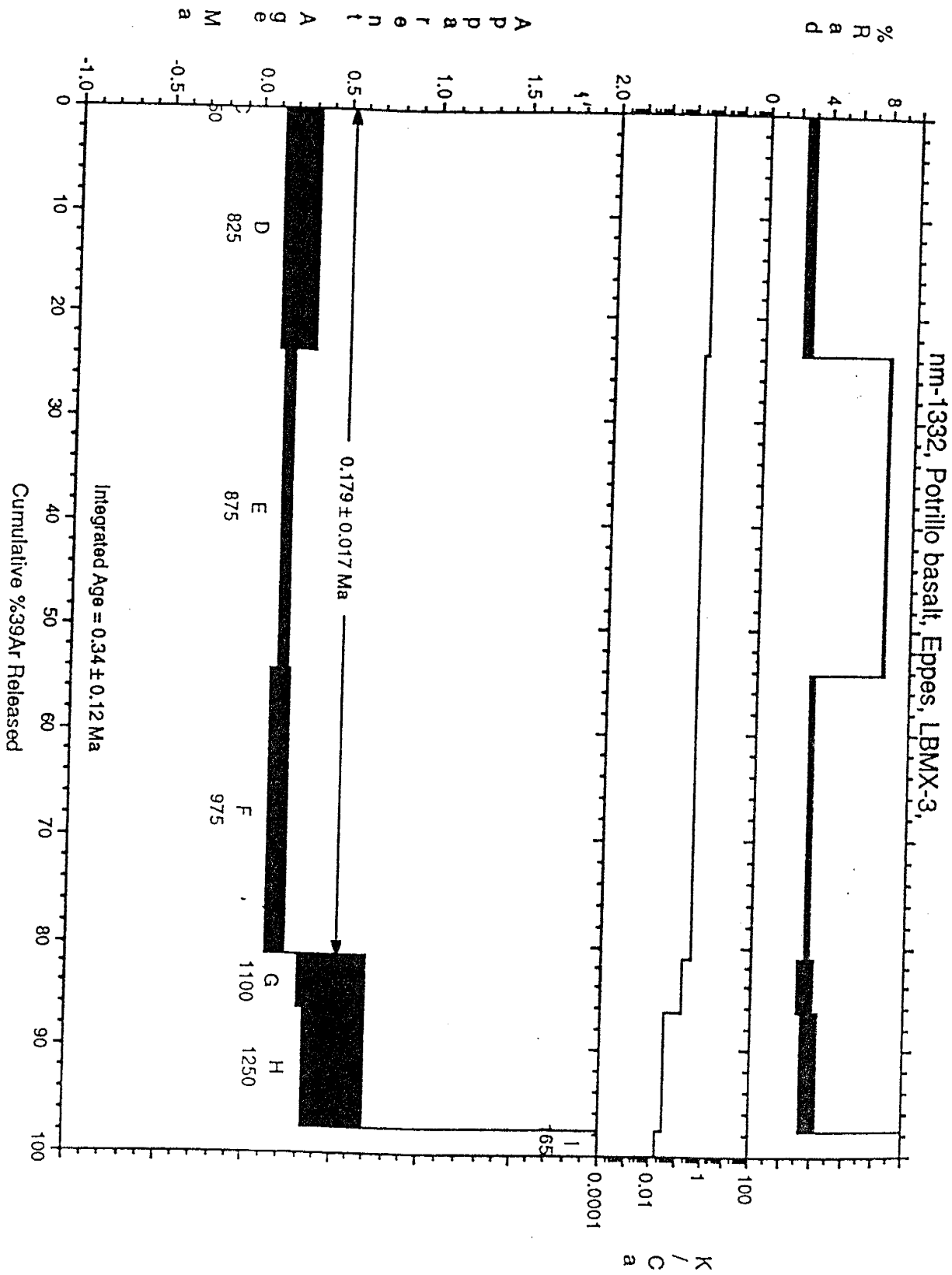
APPENDICES

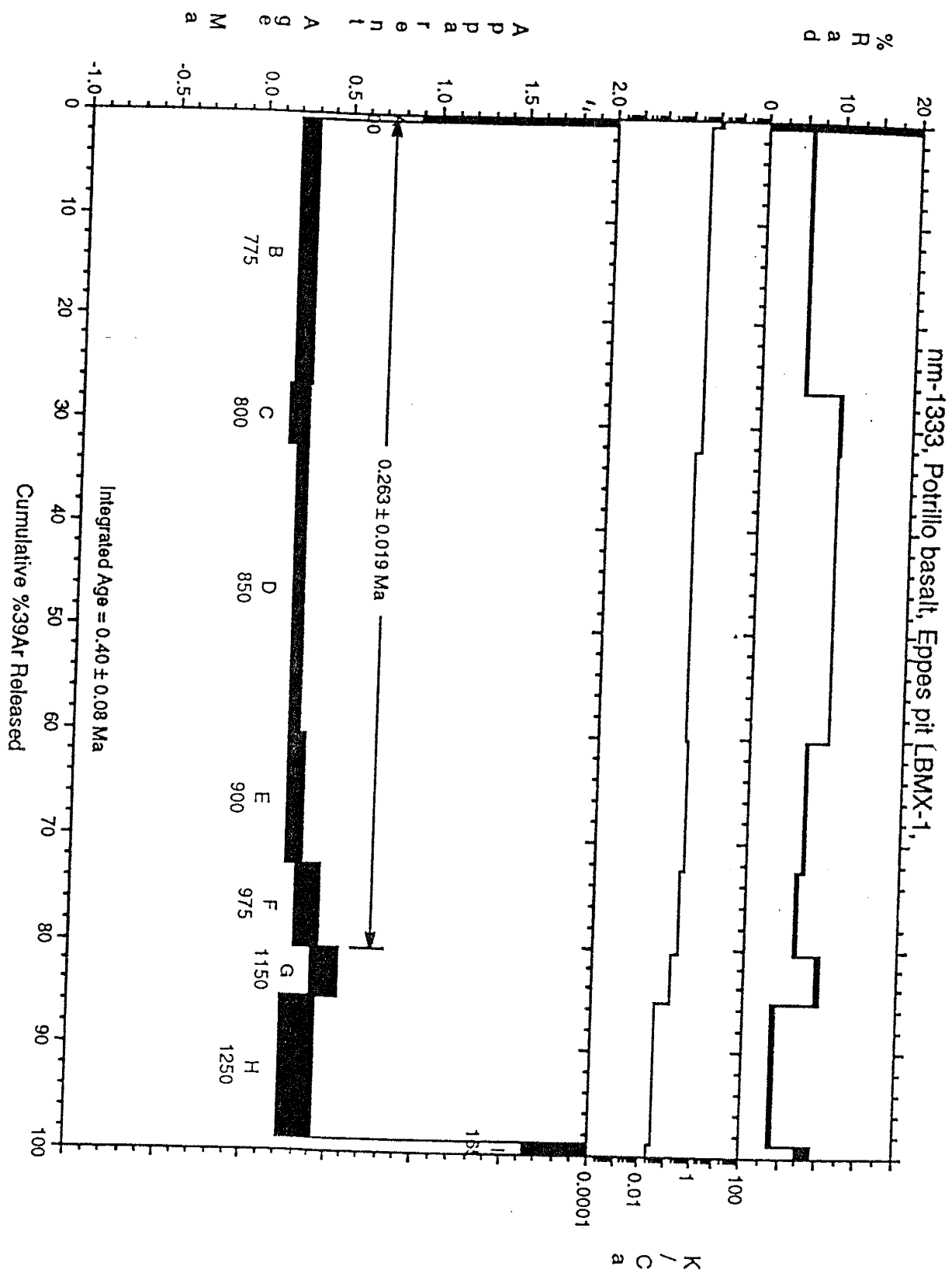
APPENDIX A:  $^{40}\text{Ar}/^{39}\text{Ar}$  Age Spectra for 6 Samples from the LBM and  
LBMX flows

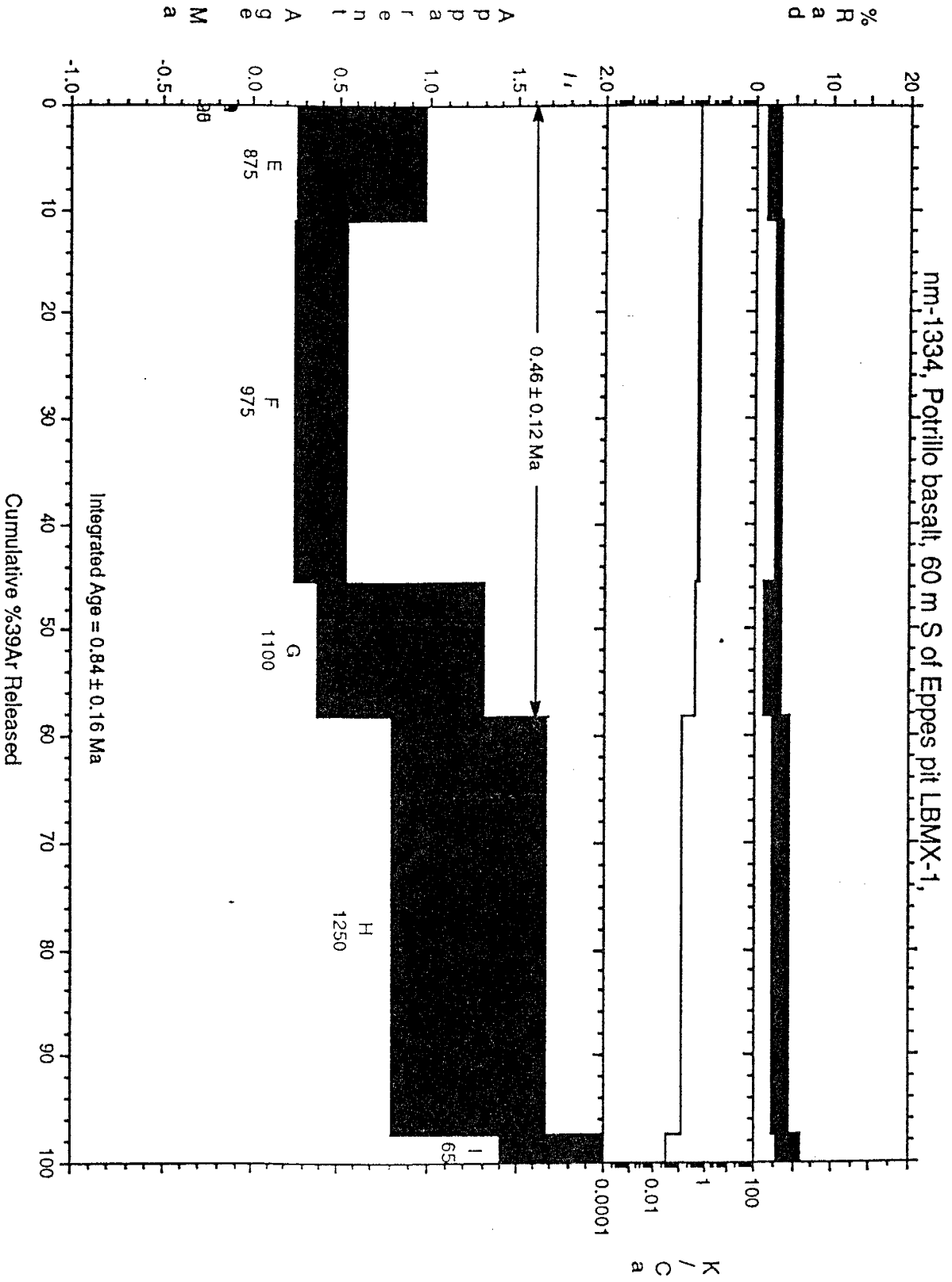




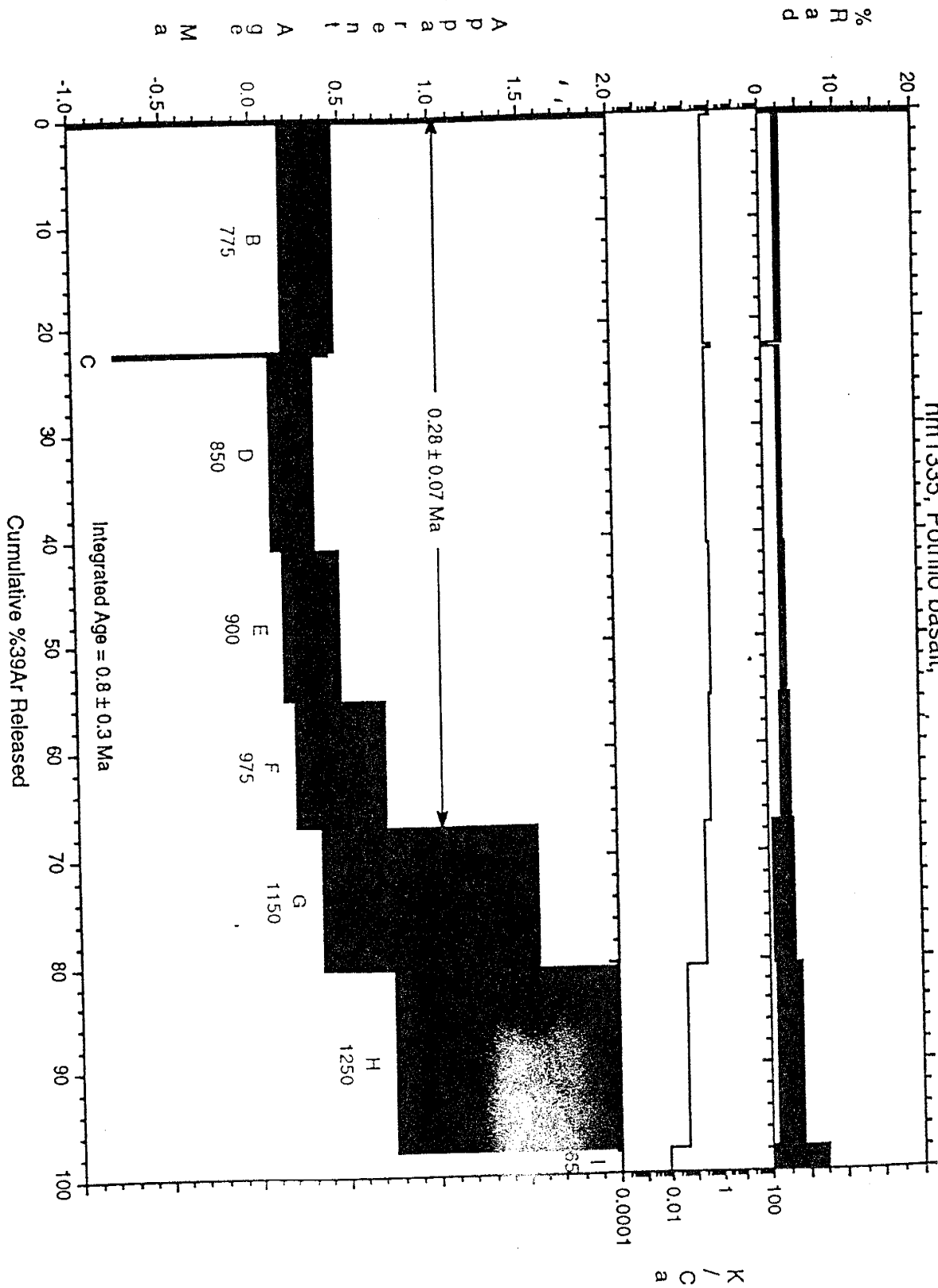








nm1335, Potrillo basalt,



APPENDIX B: Analytical Techniques and Data for 6 Samples from the  
LBM and LBMX flows

## Analytical Techniques

A total of six 2-6 kg basalt samples were collected from localities adjacent to or in studied soil pits in the Potrillo volcanic field. Where possible, fresh, non-vesicular, holocrystalline flow interiors were sampled. However, at some localities, only vesicular flow tops were exposed.

Laboratory preparations of dating samples were designed to produce a homogeneous groundmass sample free of possible contaminants. Approximately 1 kg each sample was mechanically crushed and sieved to 200-800  $\mu\text{m}$  grain size. Samples were rinsed in a 10% HCl solution for 5 minutes and ultrasonically cleaned in deionized water. With the aid of a binocular microscope, holocrystalline groundmass concentrates were hand-picked and separated from potential extraneous argon contaminants, including xenocrysts or xenoliths that might contain inherited  $^{40}\text{Ar}$ , phenocrysts of olivine that might contain excess  $^{40}\text{Ar}$ , and weathered material that might have lost or gained K or Ar.

100-150 mg of groundmass concentrate from each sample was placed in machined Al discs and sealed in an evacuated Pyrex tube along with interlaboratory standard Fish Canyon Tuff sanidine (FCT-1 with an age of 27.84 Ma relative to Mmhb-1 age of 520.4 (Samson and Alexander, 1987). Samples were irradiated for 2 hours in the boron-shielded D-3 position of the reactor at the Nuclear Science Center, College Station, TX.

$^{40}\text{Ar}/^{39}\text{Ar}$  analyses were performed at the New Mexico Geochronology Research Laboratory at New Mexico Tech, Socorro New Mexico. This facility includes an MAP 215-50 mass spectrometer operated in electron multiplier mode with an overall sensitivity of  $2.2 \times 10^{-17}$  moles Ar/pA. The mass spectrometer is attached to a computer-automated all-metal argon extraction line equipped with a 10 watt  $\text{CO}_2$  laser and a low-blank double-vacuum resistance furnace. Monitor sanidine grains were fused by  $\text{CO}_2$  laser for 15 seconds, then reactive gases were removed using a SAES GP-50 prior to expansion into the mass spectrometer. Extraction line blanks during these laser analyses ranged from 5

$\times 10^{-17}$  to  $2 \times 10^{-16}$  moles  $^{40}\text{Ar}$  and  $5 \times 10^{-19}$  to  $2 \times 10^{-18}$  moles  $^{36}\text{Ar}$ . The pooled results of four subsamples (3-4 crystals, approximately 1 mg) of each monitor allowed the neutron flux (J-values) within the irradiation package to be determined to a precision of  $\pm 0.25\%$ . Groundmass concentrate samples were incrementally heated steps within a double vacuum Mo resistance furnace in nine steps from  $700^\circ\text{C}$  to  $1650^\circ\text{C}$ . Heating times of eight to ten minutes were followed by five to ten minutes of cleanup with GP-50 getters. Data from each step were corrected for extraction line blank, which for furnace analyses ranged from  $3 \times 10^{-16}$  to  $3 \times 10^{-15}$  moles  $^{40}\text{Ar}$  and from  $2 \times 10^{-18}$  to  $9 \times 10^{-18}$  moles  $^{36}\text{Ar}$ . Mass discrimination measured before and after analyses averaged  $1.0082 \pm 0.00018$ . Correction for interfering reactions were determined using K glass and  $\text{CaF}_2$ . For samples irradiated at the Nuclear Science Center, College Station, TX, these values are:  $(^{40}\text{Ar}/^{39}\text{Ar})_k = 0.00020 \pm 0.0003$   $(^{36}\text{Ar}/^{37}\text{Ar})_{\text{Ca}} = 0.00026 \pm 0.00002$  and  $(^{39}\text{Ar}/^{37}\text{Ar})_{\text{Ca}} = 0.00070 \pm 0.00005$ . All errors are reported at the 1 sigma confidence level and the decay constant and isotopic abundances used in calculations are those suggested by Steiger and Jaeger (1977).

Total gas ages and associated uncertainties were calculated for each groundmass concentrate sample, using arithmetic means of the incremental ages and variances, each weighted by percent  $^{39}\text{Ar}$  in each increment. Three of the six samples yielded age plateaus defined by three or more contiguous incremental ages that comprise  $>50\%$  of total  $^{39}\text{Ar}$  released and agree within 2 standard deviations. Plateau ages were calculated by weighting these increments by the inverse of variance squared. Plateau age uncertainties representing standard weighted error of the mean were calculated using formula in Samson and Alexander (1987).



Run ID#	Temp.	40/39	37/38	36/35	39K moles	K/Ca	Cl/K	%40*	%39Ar	Age	± Err
NM-1330, 257.48 mg, J=0.000225748±0.000002											
6308-01A	625	7.64E+02	7.17E-01	2.44E+00	6.8E-15	7.1E-01	3.6E-03	5.7	25.41	17.506	2.707
6308-01B	700	1.11E+01	2.11E+00	3.52E-02	8.3E-16	2.4E-01	1.0E-03	7.7	28.52	0.350	0.091
6308-01C	750	7.73E+00	3.14E+00	2.47E-02	2.5E-15	1.6E-01	4.6E-04	8.5	37.94	0.269	0.029
6308-01D	825	7.58E+00	3.00E+00	2.34E-02	6.6E-15	1.7E-01	4.0E-04	12.0	62.59	0.371	0.025
6308-01E	875	1.09E+01	2.65E+00	3.40E-02	2.2E-15	1.9E-01	2.2E-04	9.7	70.71	0.432	0.037
6308-01F	975	1.27E+01	3.03E+00	4.02E-02	2.5E-15	1.7E-01	8.1E-04	8.4	80.12	0.438	0.040
6308-01G	1100	1.95E+01	8.65E+00	5.02E-02	1.5E-15	5.9E-02	1.5E-03	27.4	85.73	2.190	0.064
6308-01H	1250	3.49E+01	2.92E+01	1.16E-01	3.4E-15	1.7E-02	1.5E-03	8.6	98.40	1.242	0.102
6308-01I	1650	1.18E+02	2.67E+01	2.30E-01	4.3E-16	1.9E-02	1.6E-03	44.3	100.00	21.626	0.292
total gas age				n=9	2.7E-14	2.8E-01	2.1E-01			5.278	0.727
no plateau, discordant spectrum											
NM-1331, 124.87 mg, J=0.0002257454±0.000002											
6309-01A	700	1.30E+03	8.67E-01	4.33E+00	1.1E-15	5.9E-01	2.8E-03	1.8	2.02	9.268	3.847
6309-01B	775	4.52E+00	1.30E+00	1.41E-02	1.9E-14	3.9E-01	4.7E-04	10.3	39.27	0.190	0.012
6309-01C	800	2.49E+00	1.41E+00	7.14E-03	2.2E-15	3.6E-01	1.9E-04	19.5	43.49	0.198	0.017
6309-01D	850	2.95E+00	1.24E+00	8.80E-03	1.5E-14	4.1E-01	4.9E-04	14.9	71.93	0.179	0.009
6309-01E	900	4.93E+00	1.18E+00	1.54E-02	3.6E-15	4.3E-01	3.1E-04	9.6	78.79	0.192	0.020
6309-01F	975	7.11E+00	1.86E+00	2.26E-02	2.9E-15	2.7E-01	3.7E-04	8.3	84.34	0.242	0.026
6309-01G	1150	6.43E+00	4.42E+00	2.16E-02	3.2E-15	1.2E-01	1.2E-03	5.8	90.39	0.151	0.026
6309-01H	1250	1.35E+01	1.92E+01	4.96E-02	4.5E-15	2.7E-02	1.4E-03	2.4	98.97	0.132	0.045
6309-01I	1650	5.52E+01	4.05E+01	1.80E-01	5.4E-16	1.3E-02	5.3E-04	9.3	100.00	2.144	0.215
total gas age				n=9	5.2E-14	3.4E-01	2.0E-01			0.387	0.096
plateau age				n=7, steps B to H						0.186	0.009
NM-1332, 235.05 mg, J=0.0002257426±0.000002											
6310-01A	625	7.91E+03	2.46E-01	2.65E+01	1.8E-17	2.1E+00	2.1E-02	1.1	0.04	34.895	150.095
6310-01B	700	2.26E+03	3.21E-01	7.45E+00	1.4E-17	1.6E+00	1.9E-02	2.6	0.07	24.211	44.072
6310-01C	750	7.42E+02	6.29E+00	-1.19E+00	2.0E-19	8.1E-02	1.9E-01	147.6	0.07	400.262	595.050
6310-01D	825	2.04E+01	1.05E+00	6.76E-02	1.0E-14	4.9E-01	5.5E-04	2.7	23.59	0.225	0.054
6310-01E	875	5.36E+00	1.58E+00	1.70E-02	1.3E-14	3.2E-01	4.1E-04	8.2	54.24	0.180	0.016
6310-01F	975	1.13E+01	1.70E+00	3.74E-02	1.2E-14	3.0E-01	2.2E-04	3.5	81.34	0.163	0.029
6310-01G	1100	3.48E+01	3.16E+00	1.15E-01	2.2E-15	1.6E-01	5.9E-04	3.5	86.42	0.494	0.103

## APPENDIX C: Vegetation

Vegetation of the AD, AF, LBM, and LBMX surfaces differs only slightly. All flows are vegetated with creosote, mesquite, and various cacti and grasses though relative abundances of these plants between surfaces may vary. Typically there are a greater number of grasses and cacti on the younger flows (AD and AF), while the LBM and LBMX flows are vegetated primarily with creosote and mesquite. On all flows, however, there is a marked difference in vegetation between topographic highs and lows. In general this difference is more dramatic on the younger flows where topographic lows are vegetated with different species (primarily buffalo gourds, cacti, grasses) than topographic highs (primarily creosote and mesquite). Topographic lows (buried) on the LBM and LBMX appear to be marked not by different species, but rather by healthier plants. Mesquite and creosote over these lows are larger and bloom earlier than those growing over shallower basalt.

APPENDIX C cont.: Table of vegetative cover of surfaces in the Potrillo volcanic field

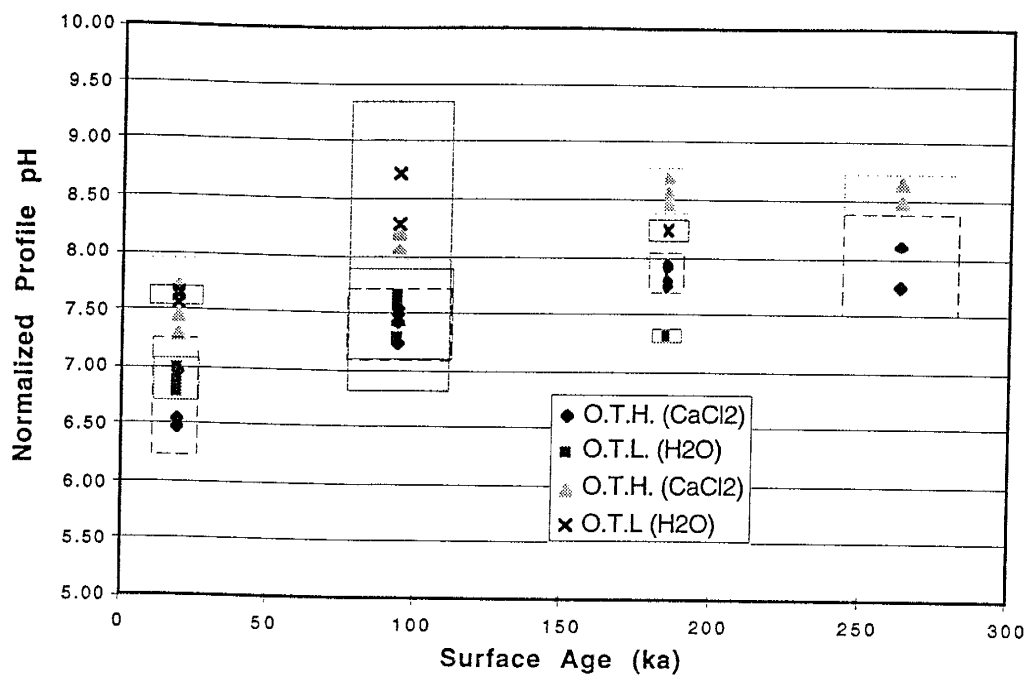
Surface	Grasses		Creosote &/or mesquite		Cacti		Other Vegetation	
	<u>% cover</u>		<u>% cover</u>		<u>% cover</u>		<u>% cover</u>	
	OTH	OTL	OTH	OTL	OTH	OTL	OTH	OTL
AD	30	70	10	<5	5	<5	<5	5
AF	5-20	30-50	10	<5	<5	<5	<5	<5
LBM	<5	<5	25	25	<5	<5	<5	<5
LBMX	<5	<5	25	25	<5	<5	<5	<5

## APPENDIX D: Profile Normalized Values of pH, Clay, Silt, and Sand

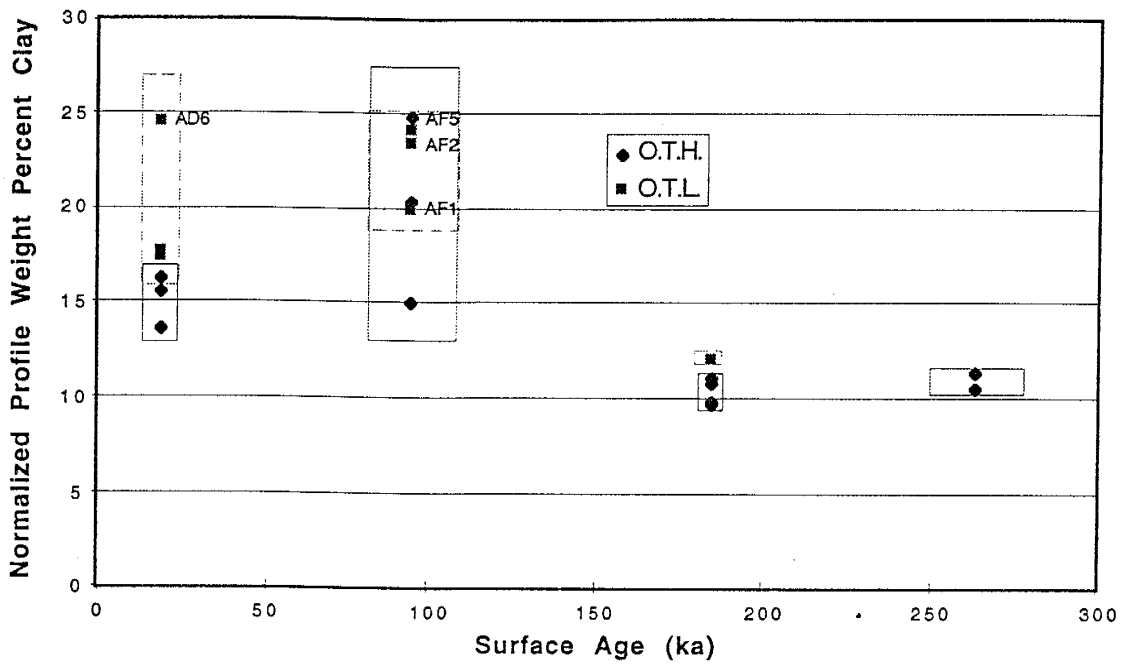
In order to more easily recognize trends in soil chemistry with age, normalized profile values of soil properties were calculated and plotted versus time. Those properties which were not addressed in Parts 1 or 2 are found below.

pH was measured in  $H_2O$  as well as in  $CaCl_2$ . Measuring the pH in a saline solution is more representative of soil water conditions. In general, values of pH increase with time. pH values average around 7.5 with those measured in  $CaCl_2$  being slightly higher. There is an overall increase of only about one from youngest to oldest surface for both measurements. Given that these soils are being buffered by a constant flux of incoming eolian material, these values of pH are not unusual.

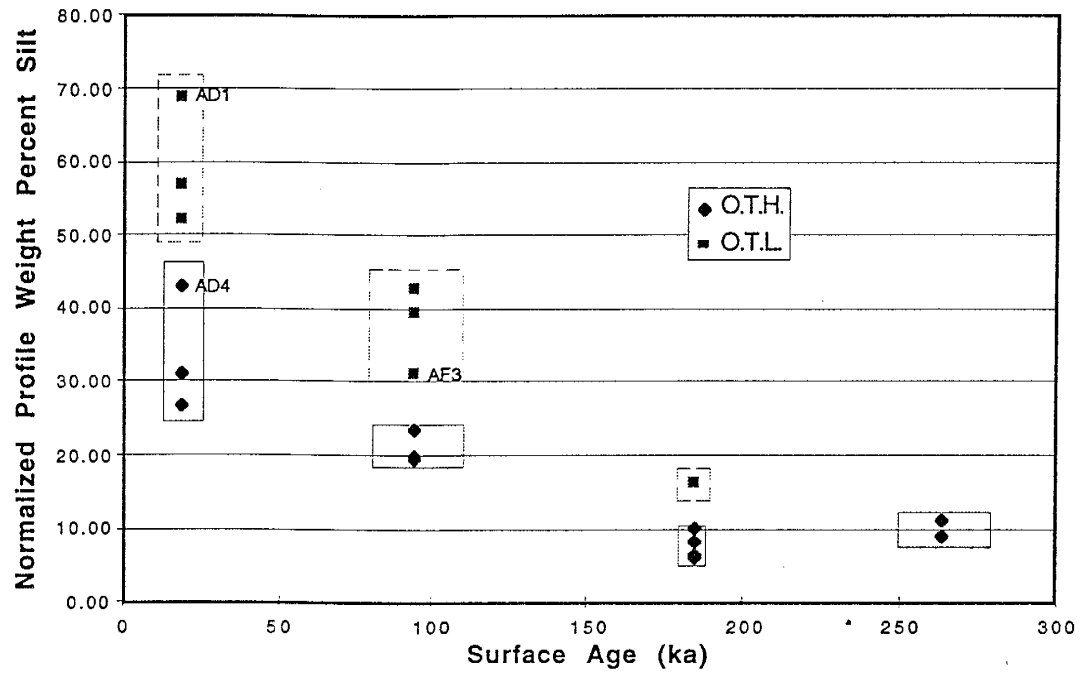
Overall values of clay and silt decrease with time, while that of sand increases. As texture values generally increase with age with respect to clay content, this trend is opposite of what is expected. However, as was mentioned in Part 2, the Little Black Mountain area is being affected by deposition of sands from the Rio Grande giving LBM and LBMX overall coarser textures than the AD and AF surfaces.



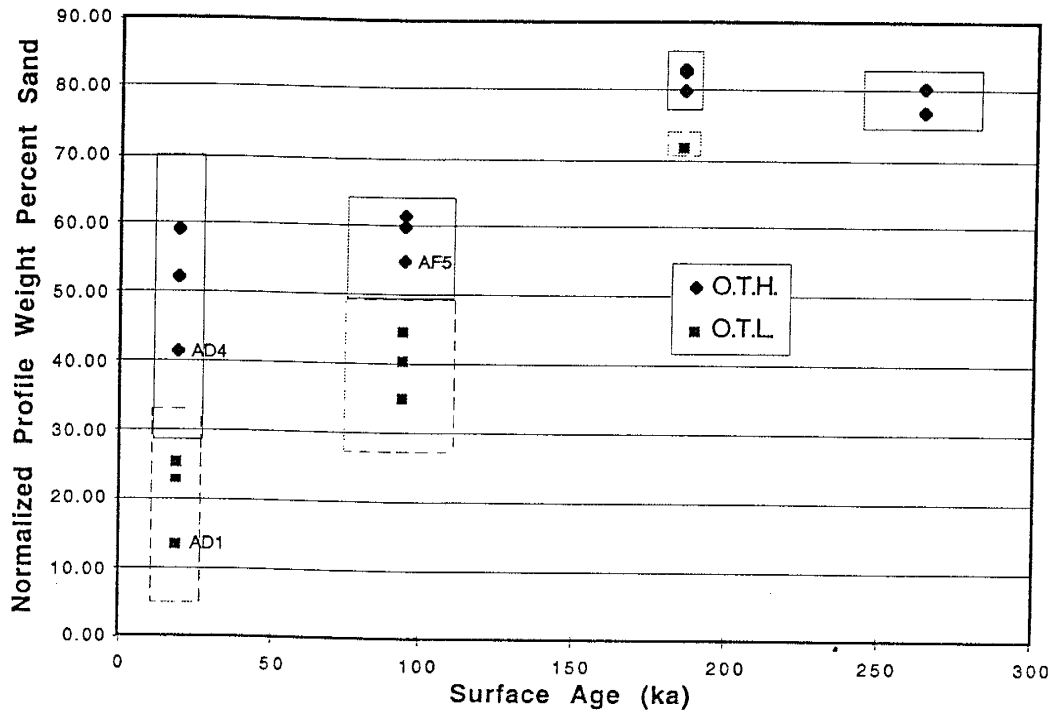
Appendix D-1: Plot of normalized profile pH vs time for soils developing on basalt surfaces in the Potrillo volcanic field.



Appendix D-2: Plot of normalized profile weight percent clay vs time for soils developing on basalt surfaces in the Potrillo volcanic field.



Appendix D-3: Plot of normalized profile weight percent silt vs time for soils developing on basalt surfaces in the Potrillo volcanic field.



Appendix D-4: Plot of normalized profile weight percent sand vs time for soils developing on basalt surfaces in the Potrillo volcanic field.



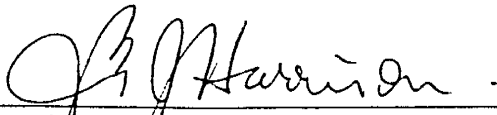
# APPENDIX E: Total Element Analysis: Major Element Sample Weight Percent

	% SiO <sub>2</sub>	% Cr <sub>2</sub> O <sub>3</sub>	% BaO	% TiO <sub>2</sub>	% CaO	% Al <sub>2</sub> O <sub>3</sub>	% Na <sub>2</sub> O	% Fe <sub>2</sub> O <sub>3</sub>	% K <sub>2</sub> O	% MnO	% P <sub>2</sub> O <sub>5</sub>	% MgO
ADS-1	65.404	0.006	0.064	0.607	1.244	11.774	1.663	3.355	2.875	0.07	0.167	0.9
ADS-2	70.585	0.005	0.07	0.642	1.179	12.392	1.833	3.492	3.091	0.069	0.128	0.866
ADS-3	70.11	0.006	0.072	0.653	1.165	12.737	1.777	3.721	3.137	0.07	0.139	0.927
ADS-4	68.98	0.006	0.067	0.683	1.201	12.835	1.706	3.927	3.083	0.073	0.155	1.086
ADS-5	70.35	0.006	0.069	0.701	1.272	12.838	1.734	3.891	3.067	0.07	0.182	0.992
ADS-6	70.503	0.006	0.066	0.701	1.25	12.748	1.735	3.874	3.025	0.068	0.157	1.001
ADS-7	69.459	0.006	0.07	0.703	1.232	12.536	1.695	3.836	2.937	0.07	0.159	0.971
ADS-8	70.343	0.006	0.066	0.716	1.215	12.661	1.705	3.881	2.956	0.069	0.152	0.961
ADS-9	70.405	0.006	0.067	0.742	1.231	12.705	1.677	3.972	2.916	0.071	0.173	0.953
AF2-1	69.61	0.007	0.071	0.656	1.047	12.616	1.478	4.082	2.969	0.089	0.128	1.13
AF2-2	69.202	0.007	0.071	0.646	1.035	12.971	1.397	4.23	3.003	0.086	0.119	1.227
AF1-2.5	70.219	0.006	0.07	0.634	1.13	12.513	1.502	3.867	3.042	0.081	0.145	1.002
AF2-3	66.503	0.007	0.072	0.689	1.068	13.168	1.394	4.57	2.904	0.082	0.123	1.342
AF2-4	70.058	0.007	0.086	0.762	1.229	12.722	1.649	4.108	3.011	0.125	0.085	0.932
AF2-5	63.504	0.008	0.068	0.751	1.888	14.029	1.523	5.006	2.856	0.091	0.184	1.737
AF2-6	67.49	0.005	0.082	0.612	2.885	12.235	1.865	3.646	3.074	0.08	0.163	1.347
AF2-7	69.042	0.005	0.075	0.565	2.979	11.747	1.857	3.167	3.124	0.06	0.157	1.276
AF2-8	69.711	0.004	0.075	0.527	3.18	11.681	1.863	3.075	3.135	0.055	0.195	1.282
AF2-10	70.2	0.004	0.08	0.601	2.221	12.133	1.991	3.3	3.221	0.065	0.178	1.237
AF2-11	69.221	0.005	0.073	0.626	2.367	12.187	1.979	3.418	3.192	0.066	0.171	1.394
AF2 80-100	61.856	0.009	0.069	0.731	1.665	14.676	1.403	5.258	2.877	0.095	0.151	1.826
LBMS	86.642	0.001	0.065	0.251	0.501	5.695	1.003	1.312	2.337	0.022	0.027	0.433
LBMA-1	74.491	0.003	0.063	0.469	1.437	9.584	1.354	2.753	2.665	0.045	0.135	1.074
LBMA-1.5	77.857	0.003	0.063	0.407	1.147	8.883	1.36	2.403	2.665	0.038	0.09	0.909
LBMA-2	78.697	0.003	0.064	0.38	1.239	8.245	1.186	2.352	2.527	0.037	0.07	0.927
LBMA-3	78.854	0.003	0.066	0.382	1.654	8.183	1.176	2.332	2.501	0.039	0.071	0.919
LBMA-4	78.074	0.004	0.065	0.41	1.685	8.512	1.195	2.527	2.518	0.042	0.075	0.919
LBMA-5	78.194	0.003	0.069	0.406	1.297	8.387	1.201	2.44	2.521	0.039	0.068	0.896
LBMA-6	76.046	0.005	0.067	0.5	1.795	9.233	1.133	3.246	2.496	0.054	0.102	1.118
LBMA-7	70.882	0.008	0.068	0.507	3.601	8.522	1.064	3.452	2.38	0.051	0.119	1.374
LBMA-8	74.757	0.006	0.062	0.487	2.128	8.314	1.187	3.273	2.507	0.048	0.109	1.385
LBMA-9	73.577	0.006	0.068	0.492	2.176	9.127	1.185	3.163	2.487	0.048	0.114	1.331
LBMA-10	75.285	0.007	0.068	0.54	2.133	9.076	1.222	3.335	2.43	0.052	0.149	1.762
LBMA-11	74.087	0.007	0.067	0.507	2.331	9.066	1.204	3.271	2.501	0.053	0.21	1.598
LBMA-12	73.793	0.006	0.066	0.552	1.724	9.791	1.265	3.434	2.552	0.051	0.097	1.427
LBMA-13	76.154	0.007	0.065	0.52	1.078	9.488	1.268	3.255	2.517	0.054	0.115	1.56
LBMA-14	76.613	0.006	0.065	0.51	1.079	9.332	1.266	3.255	2.504	0.051	0.109	1.283
LBMA-15	76.821	0.006	0.063	0.496	1.025	9.339	1.23	3.007	2.541	0.051	0.094	1.365
LBMA-16	77.665	0.006	0.067	0.507	1.043	9.034	1.302	3.034	2.541	0.051	0.094	1.365
LBMA-17	77.29	0.005	0.068	0.496	1.003	9.1	1.331	2.985	2.536	0.048	0.073	1.2

## APPENDIX F: Total Element Analysis: E-I Coefficients

	% SiO <sub>2</sub>	% Cr <sub>2</sub> O <sub>3</sub>	% BaO	% TiO <sub>2</sub>	% CaO	% Al <sub>2</sub> O <sub>3</sub>	% Na <sub>2</sub> O	% Fe <sub>2</sub> O <sub>3</sub>	% K <sub>2</sub> O	% MnO	% P <sub>2</sub> O <sub>5</sub>	% MgO
AD5-2	0.0204	-0.2121	0.0341	0.0000	-0.1039	-0.0049	0.0421	-0.0159	0.0165	-0.0680	-0.2753	-0.0902
AD5-3	-0.0036	-0.0704	0.0458	0.0000	-0.1295	0.0056	-0.0067	0.0310	0.0143	-0.0704	-0.2283	-0.0426
AD5-4	-0.0762	-0.1241	-0.0830	0.0000	-0.1544	-0.0452	-0.1015	0.0252	-0.0607	-0.0866	-0.1870	0.0569
AD5-5	-0.0686	-0.1341	-0.0664	0.0000	-0.1146	-0.0558	-0.0971	0.0042	-0.0763	-0.1341	-0.0563	-0.0456
AD5-6	-0.0666	-0.1341	-0.1070	0.0000	-0.1299	-0.0625	-0.0966	-0.0001	-0.0889	-0.1588	-0.1859	-0.0369
AD5-7	-0.0830	-0.1366	-0.0556	0.0000	-0.1449	-0.0807	-0.1199	-0.0128	-0.1179	-0.1366	-0.1779	-0.0684
AD5-8	-0.0882	-0.1522	-0.1257	0.0000	-0.1720	-0.0894	-0.1308	-0.0193	-0.1283	-0.1643	-0.2284	-0.0948
AD5-9	-0.1194	-0.1819	-0.1436	0.0000	-0.1805	-0.1173	-0.1751	-0.0315	-0.1703	-0.1703	-0.1525	-0.1338
AF2-2	0.0095	0.0155	0.0155	0.0000	0.0038	0.0441	-0.0402	0.0523	0.0271	-0.0187	-0.0559	0.1026
AF2-3	-0.0904	-0.0479	-0.0345	0.0000	-0.0288	-0.0062	-0.1020	0.0659	-0.0687	-0.1228	-0.0851	0.1307
AF2-4	-0.1336	-0.1391	0.0428	0.0000	0.0105	-0.1319	-0.0395	-0.1338	-0.1269	0.2091	-0.4283	-0.2900
AF2-5	-0.2031	-0.0017	-0.1634	0.0000	0.6586	-0.0287	-0.0989	0.0712	-0.1597	-0.1069	-0.2557	0.3427
AF2-6	0.0393	-0.2344	-0.2380	0.0000	1.9536	0.0395	0.3526	-0.0426	0.1098	-0.0365	0.3650	0.2777
AF2-7	0.1516	-0.1707	0.2265	0.0000	2.3035	0.0811	0.5373	-0.0982	0.2217	-0.2173	0.4241	0.3111
AF2-8	0.2466	-0.2887	0.3149	0.0000	2.7807	0.1525	0.5890	-0.0623	0.3144	-0.2308	0.8963	0.4122
AF2-10	0.1008	-0.3763	0.2299	0.0000	1.3154	0.0497	0.4704	-0.1176	0.1842	-0.2028	0.5179	0.1949
AF2-11	0.0421	-0.2515	0.0774	0.0000	1.3691	0.0123	0.4031	-0.1225	0.1266	-0.2229	0.4000	0.2927
# AF2 80-100	-0.2026	0.1538	-0.1279	0.0000	0.4271	0.0439	-0.1481	0.1559	-0.1304	-0.0421	0.0587	0.4501
LBM4-1.5	0.2044	0.1523	0.1523	0.0000	-0.0802	0.0680	0.1574	0.0058	0.1523	-0.0013	-0.2318	-0.0247
LBM4-2	0.3039	0.2342	0.2538	0.0000	0.0642	0.0618	0.0811	0.0544	0.1703	0.0148	-0.3600	0.0653
LBM4-3	0.2997	0.2277	0.2862	0.0000	0.4131	0.0483	0.0663	0.0400	0.1522	0.0640	-0.3543	0.0140
LBM4-4	0.1989	0.5252	0.1802	0.0000	0.3413	0.0160	0.0096	0.0500	0.0808	0.0676	-0.3645	-0.0212
LBM4-5	0.2126	0.1552	0.2652	0.0000	0.0428	0.0109	0.0246	0.0238	0.0928	0.0011	-0.4181	-0.0363
LBM4-6	-0.0424	0.5633	-0.0024	0.0000	0.1717	-0.0864	-0.2151	0.1060	-0.1215	0.1256	-0.2913	-0.0236
LBM4-7	-0.1198	1.4668	-0.0015	0.0000	0.3974	-0.0809	-0.2731	0.1509	-0.1739	0.0484	-0.1846	0.1834
LBM4-8	-0.0530	0.8873	-0.0713	0.0000	1.3181	-0.0829	-0.1727	0.1219	-0.1123	0.0066	-0.2381	0.2169
LBM4-9	-0.0584	0.9065	0.0289	0.0000	0.4435	-0.0922	-0.1657	0.0852	-0.1104	0.0168	-0.1050	0.1814
LBM4-10	-0.1222	1.0265	-0.0626	0.0000	0.2892	-0.1775	-0.2162	0.0521	-0.1590	0.1387	0.0744	0.3473
LBM4-11	-0.0800	1.1564	-0.0162	0.0000	0.5005	-0.1249	-0.2062	0.0598	-0.2026	0.0007	0.3217	0.2642
LBM4-12	-0.1583	0.6993	-0.1099	0.0000	0.0193	-0.1320	-0.1554	0.0664	-0.1363	0.0222	-0.3520	0.1984
LBM4-13	-0.0779	1.1045	-0.0684	0.0000	-0.3234	-0.1071	-0.1402	0.1107	-0.1410	0.0357	-0.2166	0.3367
LBM4-14	-0.0542	0.8392	-0.0512	0.0000	-0.3095	-0.1046	-0.1402	0.0328	-0.1116	0.0716	-0.2365	0.1296
LBM4-15	-0.0249	0.8911	-0.0544	0.0000	-0.3255	-0.0786	-0.1410	0.0328	-0.1116	0.0716	-0.2365	0.1296
LBM4-16	-0.0355	0.8501	-0.0162	0.0000	-0.3286	-0.1200	-0.1105	0.0105	-0.1180	0.0484	-0.3559	0.1757
LBM4-17	-0.0189	0.5759	0.0206	0.0000	-0.3400	-0.1022	-0.0705	0.0252	-0.1002	0.0086	-0.4887	0.0565

This thesis is accepted on behalf of the faculty  
of the institute by the following committee:

  
\_\_\_\_\_  
Advisor

  
\_\_\_\_\_

  
\_\_\_\_\_

\_\_\_\_\_  
Date